

# THE OPTIMIZATION OF THERAPEUTIC CANCER VACCINES

By

David Raynard Taylor

Dissertation

Submitted to the Faculty of the  
Graduate School of Vanderbilt University

in partial fulfillment of the requirements

for the degree of

DOCTOR OF PHILOSOPHY

in

Cancer Biology

December 17, 2022

Nashville, Tennessee

Approved:

Alissa Weaver, Ph.D.

Michael J. Korrer, Ph.D.

John T. Wilson, Ph.D.

Mary Phillips, MD/Ph.D.

Brent Ferrell, MD.

Young J. Kim, MD/Ph.D.

# Table of Contents

<b>ABBREVIATIONS.....</b>	<b>VIII</b>
<b>CHAPTER I: BACKGROUND AND RESEARCH OBJECTIVES.....</b>	<b>1</b>
CLINICAL LANDSCAPE OF CANCER VACCINES .....	1
OVERVIEW OF THERAPEUTIC CANCER VACCINE COMPONENTS AND PROPOSED MECHANISM OF ACTION .....	3
CANCER VACCINE PLATFORMS.....	7
<i>Whole-cell cancer vaccines</i> .....	7
<i>Dendritic Cells</i> .....	9
<i>Proteins/Peptides</i> .....	15
<i>Nucleic Acids</i> .....	17
<i>Microbial (oncolytic and bacterial) vaccines</i> .....	20
<i>iPSC-based vaccines</i> .....	24
<i>Personalized Cancer Vaccine</i> .....	25
HURDLES FACING SUCCESS OF CANCER VACCINE THERAPY.....	29
<i>Development of tumor cell-intrinsic resistance mechanisms</i> .....	29
<i>T cell exclusion from solid tumors</i> .....	29
<i>Freeing immune cells from coinhibitory checkpoints and exhaustion</i> .....	30
<i>Immunosuppressive cells in the TME</i> .....	31
<i>Immunosuppressive metabolic barrier</i> .....	34
<i>The hypoxic environment of the tumor</i> .....	36
<i>Suboptimal Ag selection</i> .....	37
<i>Selection of patients, vaccine platform, time, dose, and route of delivery</i> .....	38
<i>Effect of microbiome</i> .....	41
RESEARCH OBJECTIVES.....	42
<i>Combine adjuvants to maximize immunogenicity</i> .....	42
<i>Modification of the tumor antigen source to boost antitumor immunity</i> .....	48

**CHAPTER II: MUSYC DOSING OF ADJUVANTED CANCER VACCINES OPTIMIZES ANTITUMOR RESPONSES..... 50**

INTRODUCTION ..... 50

RESULTS..... 54

*The MuSyC algorithm measures the synergy of STING and TLR agonists ..... 54*

*The MuSyC-dose can optimize activation for multiple APCs in vitro ..... 61*

*CDN-based vaccines induce optimal T-cell priming in vivo ..... 64*

*MuSyC-dose optimizes the antitumor response in vivo by modifying the tumor microenvironment. .... 67*

*The MuSyC-dose vaccine induces no additional weight loss and decreases the plasma concentration of IL-6 compared to the CDN vaccine ..... 73*

DISCUSSION: ..... 76

MATERIALS AND METHODS..... 80

*Mice ..... 80*

*Cell lines ..... 80*

*Adjuvants ..... 80*

*Antigens ..... 81*

*Vaccine formulations ..... 81*

*Antibodies and flow cytometry..... 81*

*Murine bone-marrow-derived dendritic Cell (mBDMC) and macrophage (mBMDM) generation ..... 83*

*In vitro mBMDC activation ..... 83*

*In vitro mBMDM and THP-1 activation ..... 84*

*In vivo APC activation ..... 84*

*In vivo cytotoxic T-Cell killing assay..... 85*

*In vivo T-cell proliferation ..... 85*

*In vivo tumor studies ..... 86*

*In vivo mouse weight analysis ..... 87*

*Plasma cytokine analysis ..... 88*

<i>The Multidimensional Synergy of Combinations (MuSyC) Analysis</i> .....	88
<i>Statistical Analysis</i> .....	89
<b>CHAPTER III: ABROGATION OF HLA-E/QA-1B EXPRESSION ON TUMOR CELLS SIGNIFICANTLY INCREASES</b>	
<b>ANTITUMOR IMMUNE RESPONSE ELICITED BY GVAX</b> .....	<b>90</b>
INTRODUCTION .....	90
RESULTS.....	92
<i>NKG2A blockade synergizes with GVAX to reduce tumor volume</i> .....	92
<i>Loss of Qa-1b does not alter expression of MHC I or PD-L1 on murine tumor cells</i> .....	93
<i>Knocking out HLA-E/Qa-1b on whole-cell vaccine significantly improves anti-tumor response</i> .....	95
.....	97
<i>QVAX does not increase tumor-specific T cells or cytotoxic function compared to GVAX</i> .....	97
<i>Human pancreatic cell lines used for clinical GVAX express HLA-E</i> .....	99
DISCUSSION .....	100
METHODS .....	102
<i>Mice</i> .....	102
<i>Cell lines</i> .....	102
<i>GVAX</i> .....	102
<i>Tumor studies</i> .....	103
<i>In vivo cytotoxic T-Cell killing assay</i> .....	103
<i>In vivo T-cell proliferation</i> .....	104
<b>CHAPTER IV: CONCLUSION AND FUTURE PERSPECTIVES</b> .....	<b>105</b>
CONCLUSION .....	105
FUTURE DIRECTIONS .....	106
<i>Combination of cancer vaccines with checkpoint inhibitors</i> .....	106
<i>Multi-layered analyses on the effect of cancer vaccines on hematopoiesis and immune infiltrate</i> .....	107

*Combination with epigenetic modulators, metabolic modulators, and cytokine/chemokine blockers to improve antitumor responses*..... 122

**REFERENCES** ..... 129

## List of Figures

FIGURE1- 1: A TIMELINE OF VACCINE DEVELOPMENT .....	1
FIGURE1- 2: THERAPEUTIC CANCER VACCINE FORMULATIONS .....	3
FIGURE1- 3: MECHANISM OF T CELL PRIMING AND CANCER CELL KILLING .....	6
FIGURE1- 4: NEW MODEL FOR DISCOVERING AND VALIDATING IMMUNOTHERAPIES .....	32
FIGURE1- 5: TLR SIGNALING PATHWAYS AND EFFECTS.....	43
FIGURE1- 6: STING SIGNALING AND EFFECTS.....	46
FIGURE1- 7: GVAX VACCINE WITH HLA-E (QA-1B IN MICE) DELETION PRECLINICAL HYPOTHESIS.....	49
FIGURE 2- 1: STING AGONIST IS THE MOST EFFICACIOUS ADJUVANT FOR STIMULATING MURINE DENDRITIC CELLS .....	55
FIGURE 2- 2: BOTH MPL-A AND R848 POTENTIATE THE STIMULATORY EFFECTS OF CDN ON DCs.....	56
FIGURE 2- 3: THE COMBINATION OF CDN AND MPL-A IS SYNERGISTICALLY POTENT .....	57
FIGURE 2- 4: THE COMBINATION OF CDN AND R848 IS SYNERGISTICALLY EFFICACIOUS AND POTENT .....	59
FIGURE 2- 5: MUSYC-DOSE CAN OPTIMIZE ACTIVATION FOR MULTIPLE APCs <i>IN VITRO</i> .....	62
FIGURE 2- 6: DOSE RESPONSES FOR MURINE BONE MARROW-DERIVED MACROPHAGES (MBMDM) AND HUMAN MONOCYTIC CELL LINE THP-1 .....	64
FIGURE 2- 7: CDN-BASED VACCINES INDUCE OPTIMAL T- CELL PRIMING. ....	66
FIGURE 2- 8: MUSYC DOSING OPTIMIZES THE ANTITUMOR RESPONSE <i>IN VIVO</i> THROUGH MODULATING THE TUMOR MICROENVIRONMENT.....	71
FIGURE 2- 9: GATING FOR TUMOR IMMUNOPHENOTYPING .....	73
FIGURE 2- 10: THE MUSYC-DOSE VACCINE INDUCES NO ADDITIONAL WEIGHT LOSS AND DECREASES THE PLASMA CONCENTRATION OF IL-6 COMPARED TO THE CDN VACCINE .....	75
FIGURE 3- 1: THERAPEUTIC TREATMENT OF MICE WITH NKG2A BLOCKADE AND GVAX SIGNIFICANTLY REDUCES TUMOR VOLUME.....	93
FIGURE 3- 2: MOC1 AND B16-MOVA QA-1B KO CELLS HAVE A NORMAL EXPRESSION OF MHCI, PD-L1, AND INCREASED SUSCEPTIBILITY TO NK CELL-MEDIATED KILLING. ....	94
FIGURE 3- 3: WHOLE-CELL VACCINE QVAX SIGNIFICANTLY REDUCES WT TUMOR VOLUME.....	96

FIGURE 3- 4: QVAX INDUCES SIMILAR LEVELS OF <i>IN VIVO</i> CD8 T CELL PROLIFERATION AS GVAX.....	98
FIGURE 3- 5: HLA-E IS UPREGULATED AFTER IFN $\gamma$ STIMULATION ON HUMAN PANC CELL LINES USED IN CLINICAL GVAX TREATMENT. ....	99
FIGURE 4- 1: QVAX-INDUCED ANTITUMOR RESPONSE IS MEDIATED BY CD8 <sup>+</sup> T CELLS.....	108
FIGURE 4- 2: THE HIERARCHY OF HEMATOPOIESIS .....	115
FIGURE 4- 3: MOUSE HEMATOPOIETIC STEM CELL (HSC) GATING .....	117
FIGURE 4- 4: STINGVAX SIGNIFICANTLY BOOSTS LSK HSCs IN THE BONE MARROW .....	119
FIGURE 4- 5: STINGVAX SIGNIFICANTLY ENHANCES LYMPHOPOIESIS .....	120
FIGURE 4- 6: STINGVAX SIGNIFICANTLY ENHANCES MYELOPOIESIS.....	122
FIGURE 4- 7: NEW MODEL FOR DISCOVERING AND VALIDATING IMMUNOTHERAPIES .....	127

## ABBREVIATIONS

HPV= Human Papilloma Virus

TAA= tumor associated antigens

CT= Cancer testis

Ags= antigens

HSIL= high-grade squamous

intraepithelial lesions

APC= antigen-presenting cell

MHC= major histocompatibility  
complexes

TIL= tumor-infiltrating lymphocyte

OS= overall survival

PFS= progression-free survival

ORR= overall response rate

Treg= regulatory T cells

PAMP= pathogen-associated molecular  
patterns

DAMP= damage-associated molecular  
patterns

PRR= pattern recognition receptor

TLR= Toll-like receptors

NLR= NOD-like receptors

RLR= retinoic acid-inducible gene 1 like  
receptors

AIM-2 like receptors

CLR= C-leptin receptor

STING= Stimulator of Interferon Genes

DAMP= danger-associated molecular  
patterns

HMGB1= high mobility group box 1

PTX3= pentraxin-3

HSP= heat shock proteins

moDC= monocyte-derived

SCF= Stem Cell Factor

DL1=Delta Like-1

PGE2= prostaglandin E2

IDO= indoleamine 2,3-dioxygenase

MPLA= monophosphoryl lipid A

5-FU= 5-fluorouracil

DFS= disease-free survival

IVT= in vitro

CEA= carcinoembryonic antigen

MAA= melanoma-associated antigen

ICI= immune checkpoint inhibitor

OV= Oncolytic viruses	RNS= reactive nitrogen species
APC= antigen presenting cells	NO= nitric oxide
PAMP= pathogen associated molecular patterns	ONOO-= peroxynitrite
DAMP= danger associated molecular patterns	IL= interleukin
iPSC= induced pluripotent stem cell	TNF- $\alpha$ = tumor necrosis factor-alpha
dLN= draining lymph nodes	TGF- $\beta$ = transforming growth factor beta
SNV= single nucleotide variation	FasL= fas ligand
PRO= patient-reported outcome	TRAIL= tumor-necrosis factor-related apoptosis-inducing ligand
ICAM-1= ntercellular adhesion molecule-1	MMP= matrix metalloproteinases
VCAM-1= vascular cell adhesion molecule-1	HIP1 $\alpha$ = Hypoxia Inducible Factor 1 $\alpha$
CAF=cancer-associated fibroblasts	EMT= epithelial to mesenchymal (EMT) phenotype
MDSC= myeloid-derived suppressor cell	GLU= glucose transporters
NK= natural killer cell	LDHA= lactate dehydrogenase A
tDC= tolerogenic dendritic cells	HK1= hexokinases 1
Breg= regulatory B cells	PTEN= phosphatase and tensin homolog)
VEGF= vascular endothelial growth factor	NSCLC= non-small-cell lung cancers
IDO= indoleamine 2,3-dioxygenase	RB= Retinoblastoma
ROS= reactive oxygen species	SCLC= small-cell lung cancer
	SCCHN= squamous cell carcinoma of the head and neck

MuSyC= Multidimensional Synergy of  
Combinations

mBMDC= murine bone-marrow-derived  
dendritic cells

GM-CSF= granulocyte-macrophage  
colony-stimulating factor

KLRG1= killer cell lectin-like receptor G1

Tcm= central memory T cell

Eem= effector memory T cells

# CHAPTER I: BACKGROUND AND RESEARCH OBJECTIVES

## CLINICAL LANDSCAPE OF CANCER VACCINES

The original attempt to generate therapeutic immunity against cancer was with James Coley’s heat-inactivated bacteria (Coley’s toxins) against inoperable sarcoma. Unfortunately, after this attempt, therapeutic cancer vaccine development has lagged drastically behind the success of prophylactic infectious disease vaccines (**Fig.1-1**). Prophylactic cancer vaccines target oncogenic microbes (i.e., human papilloma and hepatitis B viruses) before transforming into neoplastic cells. For example, in a seven-year Human papillomavirus (HPV) study in Scotland, from 8584 genotyped samples, the vaccine targeting HPV types 16 and 18 had an effective rate of 89.1% of preventing HPV for those vaccinated at age 12-13 (1). Another HPV vaccine study of over 500,000 women showed that women vaccinated sixteen and younger led to an incidence of less than 1.0% for either vulvar or vaginal high-grade squamous intraepithelial lesions (HSIL+) (2). These and many other prophylactic vaccine studies have successfully prevented viral-associated cancers.

Figure 1-1

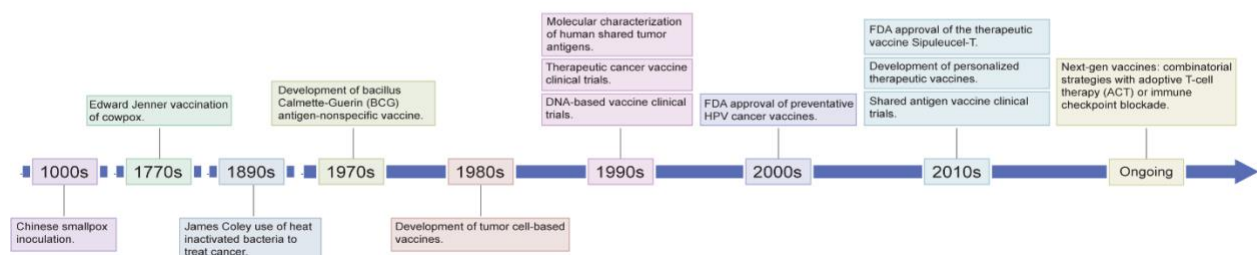


**Figure1- 1: A timeline of vaccine development**

Therapeutic cancer vaccines, in contrast, have yielded limited clinical benefits. For instance, a meta-analysis of 440 patients enrolled between 1995 and 2004 with metastatic disease and treated with different vaccines showed a low objective response rate of 2.6% (3). Early strategies on therapeutic cancer vaccines focused on tumor-associated antigens (TAA), which include overexpressed Ags (e.g., Her2/neu), cancer-testis (CT) Ags, developmentally regulated Ags (e.g., oncofetal proteins), or mutated neoantigens that are not found in normal cells (4, 5). Failure of these trials has been attributed to the generation of tolerance to TAA, low affinity/avidity of tumor-specific T cells and the homeostatic response to check hyper-responsive adaptive effectors cells (6). Other hurdles include suboptimal dose, mode of delivery, and improper or limited adjuvant selections. Moreover, this lack of success can partly be attributed to the immunosuppressive context of cancer vaccine utilization, i.e., high disease burden (metastasis), cancer-induced and cancer-therapy-induced immunosuppression, etc.). However, the FDA approval of immune checkpoint inhibitors (ICIs) has renewed enthusiasm for therapeutic cancer vaccines.

# OVERVIEW OF THERAPEUTIC CANCER VACCINE COMPONENTS AND PROPOSED MECHANISM OF ACTION

Therapeutic cancer vaccines manipulate and boost the immune system, the body's natural defense system, to target and kill cancer cells. The two significant components of cancer vaccines are an antigen source and an adjuvant, each having an essential role in eliciting cytolytic T-cell responses. The antigen source provides specific tumor antigen/s for the immune system to target and can have various formulations, i.e., genetic material or full-length proteins (**Figure 1-2**). Ideally, tumor antigens should be expressed specifically on cancer cells and not normal cells, ubiquitously expressed on cancer cells, essential for survival, and highly immunogenic (7).

Figure 1-2

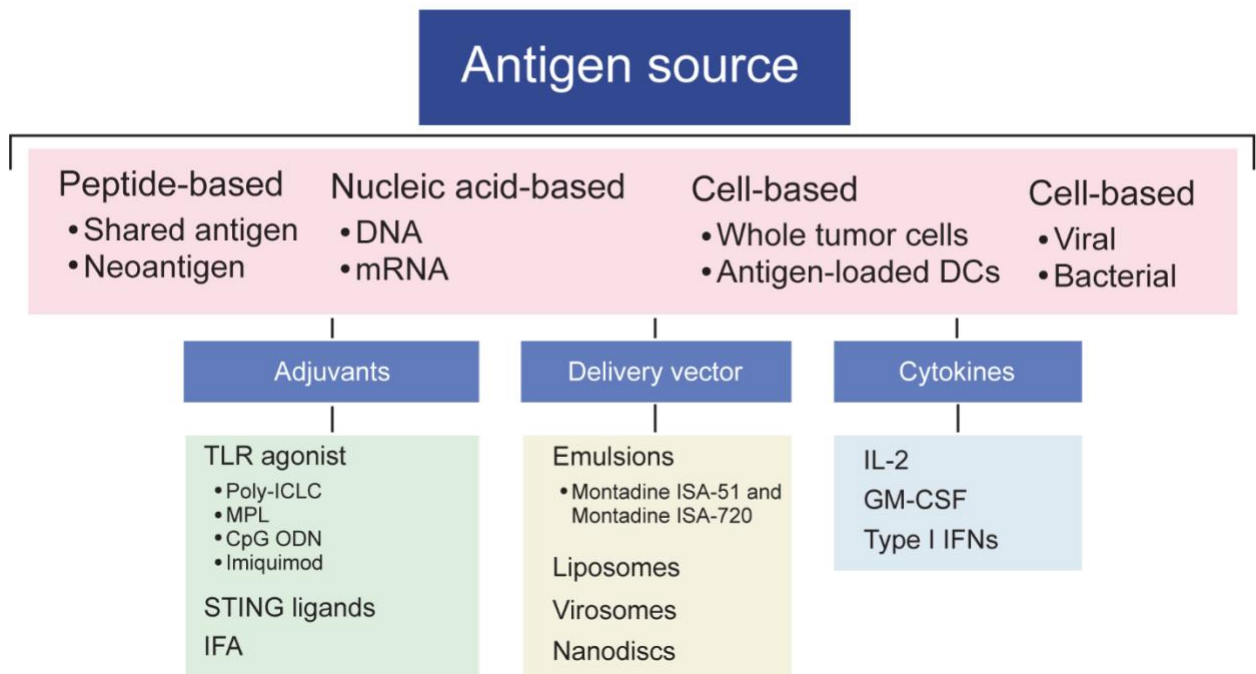


**Figure1- 2:** Therapeutic Cancer vaccine formulations

Figure 1-2: The essential components of an effective therapeutic cancer vaccine are illustrated here: i) source of tumor antigen- this can be either tumor-associated or neoantigens. Antigens can be derived from either whole cell lysate, peptides, overexpressed protein, tissue differentiation, cancer-testis (CT), oncofetal proteins and/or DNA or RNA. ii) Formulation- vaccines can be cell-based (whole cell or loaded into DC), protein or peptide-based, nucleic acid-based or microbial organism-based. iii) Adjuvants and/or cytokines used- different types of adjuvants and/or cytokines like TLR ligands, STING agonists, Type I IFNs, IL-12, and GM-CSF are used to improving vaccine efficacy and adaptive immunity activation. iv) Delivery vehicles- vaccines are bioengineered and formulated into emulsions, liposomes, virosomes or nanodiscs and other biological scaffolds to improve bioavailability

The currently accepted mechanism by which tumor antigens induce an immune response is as follows: (a) tumor antigen epitopes are presented on the surface of the antigen-presenting cells (APCs) by major histocompatibility complexes (MHCs); (b) naïve T-cells recognize those MHC/epitope complexes on APCs in the peripheral lymphoid organs leading to the clonal expansion of antigen-specific, tumor-reactive effector T-cells; (c) the effector cells infiltrate and eliminate the tumor cells expressing those MHC/epitope complexes (**Fig.1-3 A**) (8). The importance of CD8<sup>+</sup> TILs was identified in a meta-analysis of 33 immunotherapeutic studies where it showed a significant positive correlation between CD8<sup>+</sup> tumor-infiltrating lymphocytes (TILs) and clinical response (i.e., overall survival (OS), progression-free survival (PFS), and overall response rate (ORR) (9). Therefore, CD8<sup>+</sup> TILs are critical for immunotherapeutic responses. However, in the absence of a suitable adjuvant, tumor antigen sources alone fall short of inducing an effective CD8<sup>+</sup> antigen-specific immune response, leading

to T-cell anergy and exhaustion and increased production of regulatory T cells (Treg) that suppress cytotoxic effector cells (6).

Adjuvants represent a diverse range of pathogen-associated molecular patterns (PAMPs) or damage-associated molecular patterns (DAMPs) that, when bound to their respective pattern recognition receptors (PRRs), enhance the magnitude, breadth, quality, and longevity of antigen-specific immune responses (10). The proposed process of adjuvant-induced enhanced immune responses occurs in multiple steps. The first step involves the upregulation of MHCs [i.e., MHCI and MHCII] and costimulatory molecules [i.e., CD80, CD86, CD40] on APCs as both classes of molecules are necessary and sufficient for the priming of T-cells. Next, the upregulation of those molecules increases the MHC/peptide-T-cell receptor (TCR) [signal one] and costimulatory receptor-ligand [signal two] interactions, enhancing the clonal expansion of antigen-specific T-cells. Finally, this boosted T-cell expansion improves antitumor immunity (**Fig.1-3 B**) (11). As a result, adjuvants have been preclinically developed for immune-activating PRRs such as the Toll-like receptors (TLRs), NOD-like receptors (NLRs), retinoic acid-inducible gene 1 like receptors (RLRs), AIM-2 like receptors, C-leptin receptors (CLRs) and Stimulator of Interferon Genes (STING). With this 30,000 feet aerial view of the clinical landscape of cancer vaccines from its infancy to the latest generation of neoantigen-based platforms, we will survey some of the significant classes of vaccines, particularly those that have formidably crossed over the chiasmic divide into the clinical phase. Vaccine platforms are vast, and there are many excellent reviews that highlight their basic components with their advantages or limitations (27,

91, 92). In this introductory thesis section, we will highlight the recent developments, challenges and future prospect for some of the major classes of vaccines.

Figure 1-3

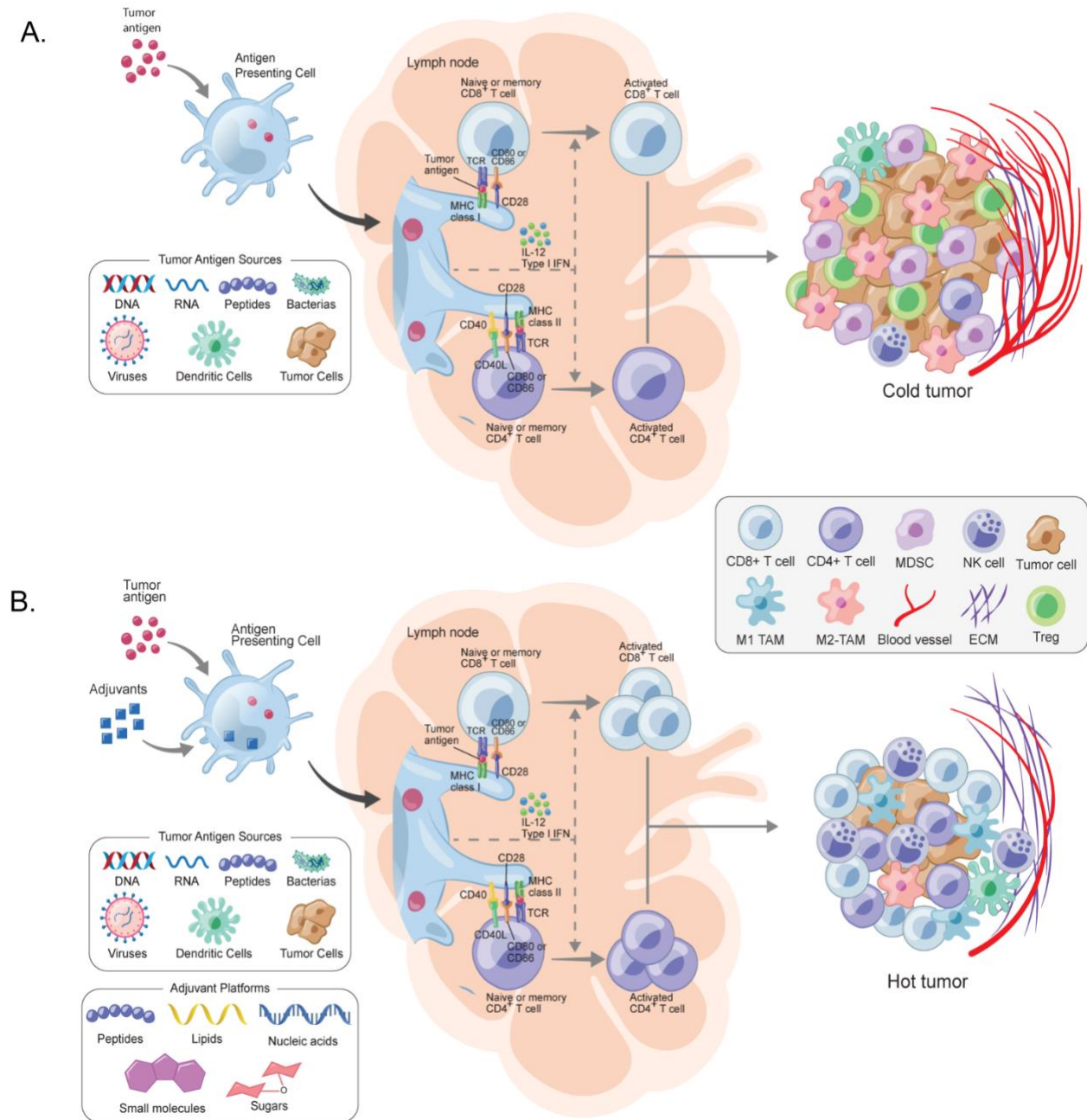


Figure1- 3: Mechanism of T cell priming and cancer cell killing.

Figure 1-3: **A)** Depending on the vaccine platform and antigen source used, the antigen presenting cells are primed and/or activated. This is followed by specific binding of a TCR on T cells in the tumor draining lymph nodes to its cognate peptide-major histocompatibility (MHC) complex displayed on an antigen-presenting cell (APC), like macrophages or dendritic cells. This, in combination with co-stimulatory signals and inflammatory cytokine release from activated APC can successfully transform resting naïve T cells (CD4<sup>+</sup>, CD8<sup>+</sup>) to activated effector cancer cell killing T cells and result in tumor regression. However, without proper co-stimulation tumor antigens alone generally lead to cold tumors. **B)** Co-stimulation may be improved by using adjuvants that activate the pattern recognition receptors on APC and upregulate the co-stimulatory ligands, leading to a more hot tumor.

## **CANCER VACCINE PLATFORMS**

### **Whole-cell cancer vaccines**

Whole tumor cell vaccines are prepared from whole tumor cells or tumor cell lysates generated by irradiation or repeated freeze-thaw cycles, derived from either autologous patient tumor tissues or heterologous tumor cell lines. These are often genetically modified to produce different cytokines/chemokines (GM-CSF) that can augment adjuvant function (recruit DCs and facilitate antigen uptake, cross-priming, and presentation to CD8<sup>+</sup> T cells). In addition, irradiated tumor cells can release danger-associated molecular patterns (DAMP) molecules such as high mobility group box 1 (HMGB1), pentraxin-3 (PTX3), heat shock proteins (HSP 70/90), and uric acid that can stimulate DC maturation and T cell responses against the tumor (12). One advantage

of using a whole cell vaccine is that the cells would be an unbiased source of a broad spectrum of tumor antigens, thereby eliminating the requirement of identifying an immunogenic antigen or potential concerns of antigen loss (12-14).

As mentioned earlier, tumor cell vaccines are often genetically modified to express different cytokines or chemokines or costimulatory molecules to stimulate a more robust immune response to the vaccine. Of different cytokines tested, a superior response was observed with irradiated melanoma cells transduced with GM-CSF. This vaccine (GVAX) showed promising results in early preclinical studies (15-22), which laid the groundwork for numerous clinical trials targeting a variety of cancers, including prostate, melanoma, NSCLC, and pancreatic cancer (23, 24). Unfortunately, most clinical trials failed to meet expectations (25-29). Despite these disappointing results, clinicians continue to test the efficacy of GVAX in combination with different treatment strategies, especially ICB molecules.

There are other whole-cell tumor vaccines: Oncovax (colon cancer; Vaccinogen) (30-32), and Reniale (renal cancer; Liponova) (33, 34), to name a few. Of these, Oncovax, prepared by irradiating patient tumor cells and administered with BCG bacteria as an adjuvant, significantly reduced the chances of recurrence post-surgery in several early phase trials in colon cancer patients (30-32). Based on these promising results, a randomized, multicenter Phase IIIb clinical trial (NCT02448173) is ongoing to test if Oncovax improves disease-free survival post-surgery. Unfortunately, the main disadvantage of an autologous whole cell vaccine approach is its inherent logistic hurdle

- it is time-consuming, expensive, and variable (15, 19, 35). Alternatively, allogeneic cells derived from different tumors could be used with the likelihood that the patient's tumor will share antigens with the vaccine.

## **Dendritic Cells**

Dendritic cells (DC) are the most potent antigen-presenting cells (APC), and depending on the context, DCs also provides either costimulatory or coinhibitory signals to T cells for activation or suppression (36-46). In the tumor microenvironment, immunosuppressive molecules and cytokines like TGF- $\beta$ , IL-10, VEGF, Arg-1, IDO interfere with DC maturation and arrest them in a dysfunctional state. Furthermore, additional factors like the expression of a high level of coinhibitory molecules like TIM3, PDL-1, and PD-1 on DCs, metabolic stress, antigen masking, and faulty antigen presentation facilitate the switch from inflammatory to tolerogenic phenotype. Hence, over the past decade, much effort was invested in understanding the complex interplay and biology of DCs with other immune cells in the tumor microenvironment and modulating them to activate T cells against the tumor.

Since DC can activate antigen-specific T cells, the DC vaccine aims to repair the immune suppression by administering "trained" DCs and starting the adaptive immune responses in the patient. Typically, monocytes are isolated from patients via leukapheresis and then differentiated using GM-CSF and IL-4 in vitro to yield immature DC. These are then loaded with either i) whole tumor preparation, ii) DC-tumor cell fusion, iii) virus, iv) defined, shared tumor-associated antigens (peptides, nucleic acid),

or v) unique neoantigens from the tumor cells. The antigen-loaded DCs are then further matured using a cytokine mixture that makes them competent for lymph node homing, antigen cross-presentation and activation of T cells, and production of pro-inflammatory cytokines (47-49). These *ex-vivo* matured DCs are then infused into the patient (39, 50).

DC vaccines have been applied to various malignancies (over 240 completed clinical trials), including melanoma, prostate, renal cell carcinoma, glioblastoma, and pancreatic cancer (36, 42, 48). In the earliest trials, the first-generation DC vaccines from blood monocytes that were only loaded with synthetic TAA peptides or tumor cell lysates were found to be safe and immunogenic. They were tested in various cancers (51-61), but only 3.3% of patients experienced tumor regression (42, 47, 48, 51-53). Many studies reported that regulatory T cell (Tregs) mediated immunosuppression hindered the efficacy of DC vaccines (52). Subsequently, the DCs were matured using a defined cocktail of cytokines, and these second-generation vaccines performed better with an overall objective response rate (ORR) in the range of 8%-15%. There is also an interesting strategy to use DC and tumor cell hybrid, improving immune responses in patients (NCT01096602) (54, 55).

Despite some modest clinical efficacy for DC vaccines, the early trials raised questions and challenges. One concern is that the specific details of DC vaccine manufacturing vary considerably and cover various aspects like the source and starting cell population, culture condition and maturation cocktail used, choice of antigen and antigen loading

technique, and time and route of administration. In addition, the DC subtypes are transcriptionally and functionally distinct in their developmental origin and localization (56, 57). A recent single-cell RNA sequencing study identified six different classes of circulating DC in peripheral blood (58). Some researchers argue in favor of using peripheral blood-derived DC to retain their physiological functionality after transfusion to patients. Indeed, studies report transcriptional and phenotypic differences in monocyte-derived (moDC) and conventional DCs (cDC) that translate to a poor migratory capacity of moDC to lymph nodes and T cell priming (59, 60).

Heterogeneity of the human DC population is further highlighted by studies showing potent antigen presentation by moDC (61, 62), whereas some studies indicated potent antigen presentation by BDCA1/CD1c+ moDCs and BDCA3/ CD141+ moDCs (42, 63). However, the use of cDC harvested from circulation is limited owing to their poor availability in the peripheral blood of cancer patients, the potential need for repeated dosing in a therapeutic setting, and their compromised capacity to present antigens and secrete pro-inflammatory cytokines (64). Still in its infancy, cDC vaccines are being tested as pilot trials in the European study, “Professional cross-priming for ovarian and prostate cancer” (PROCROP). A recent trial, however, used autologous naturally circulating DC and loaded with HLA-A2.1 restricted tumor antigen for stage IV melanoma patients (NCT01690377). Four of fourteen patients showed long-term progression-free survival, which correlated with developing cytolytic, multifunctional effector T cells (65). Scientists have also attempted to use plasmacytoid DC as vaccines (66).

Another important variable that dictates DC vaccine efficacy is the combination of cytokines that mature the DC. Scientists have differentiated DC from CD34<sup>+</sup> stem cells or cord blood by adding molecules like FLT3L, Stem Cell Factor (SCF), GM-CSF, Thrombopoietin, IL-7, Notch ligand Delta Like-1 (DL1), and IL-4, at the same time attempting to recapitulate physiological DC phenotype ex vivo by culturing the cells for different periods (one or three weeks) (60, 67-71). Unfortunately, there is no consensus for optimal DC maturation protocols and the maturation cocktail used. Earlier, the gold standard was to use a cocktail containing TNF- $\alpha$ , IL-1 $\beta$ , and IL-6 in combination with prostaglandin E2 (PGE2) (72). However, PGE2 has been shown to induce Tregs, increase the expression of indoleamine 2,3-dioxygenase (IDO) and reduce the secretion of IL-12 (73, 74). Therefore, scientists and clinicians have explored alternative maturation cocktails.

These include triggering of co-stimulatory pathways (e.g., CD40-CD40L), activation of Toll-Like Receptor (TLR) by using agonists like poly IC (TLR3), resiquimod (TLR7/8) pathway, and 3-O-deacylated monophosphoryl lipid A (MPLA) either as single agents or in combination (75-77). For instance, DC transfected on the TriMix platform with mRNA encoding constitutively active TLR4, CD40L and CD70 have been clinically tested in melanoma patients (78, 79). However, the combination of different agonists in varying doses and maturation times may alter the expression of inflammatory genes and chemokines that will translate to the efficacy of the DC vaccine in vivo (80). Recently, a novel method of transfecting DC with an mRNA cocktail encoding co-stimulatory

molecules (CD40L, CD70, and a constitutively active TLR4) has shown promising results in melanoma patients (NCT00074230, NCT01066390) (78, 81).

Another possible reason DC vaccines have shown limited efficacy is because many clinical trials were done with patients with late-stage diseases where dominant immunosuppressive mechanisms can dampen responses to DC vaccines and T cell activation. This is reflected in earlier studies that noted T cell activation in a higher fraction of patients receiving adjuvant DC vaccines than those with metastatic disease. This indicates that DC vaccines may perform better in adjuvant settings (54, 55, 82). Another potential for improvement is DC mobilization. Intradermal injection allows  $\leq 5\%$  of DCs to migrate to lymph nodes, whereas the intravenous route distributes DC to non-specific locations like the spleen, lungs, liver, and bone marrow. In addition, attempts have been made to manipulate DC by viral vectors to overexpress molecules to improve their trafficking to the tumor in vivo (83).

Other factors that significantly affect the DC vaccine efficacy are the choice and method of antigen loading. While a broad range of antigens have been explored, including defined peptides, whole tumor cell lysate, nucleic acids, irradiated tumor cells, neoantigen peptides, and viruses, how to generate the best immunogenic antigen and its loading technique to ensure maximum clinical response remains an open question. Oxidizing whole tumor lysate with hypochlorous acid or infecting the tumor cell with Newcastle Disease significantly improved DC vaccination outcomes in the preclinical setting (84-86). Combining chemotherapeutic drugs or oncolytic viruses that induce

immunogenic cell death of tumor cells is another way to improve DC vaccine outcomes. Lastly, the cost of production and the complexity associated with its manufacture has hindered its widespread clinical application.

Despite these challenges, several novel and state-of-the-art DC-based vaccines are currently being tested in different phases of clinical trials. For example, a placebo-controlled phase III trial is testing an autologous DC vaccine loaded with tumor lysate (DCVax-L) in glioblastoma patients in combination with radiation and chemotherapy (NCT00045968). The initial reports show DC vaccination improved overall survival to 23 months compared to 15-17 months in the case of patients who received standard-of-care therapy in earlier studies (87). Other phase III studies include investigating the efficacy of autologous RNA-loaded DC vaccine as an adjuvant to the standard of care in uveal melanoma (NCT01983748) and that of BDCA3<sup>+</sup> naturally circulating DC in stage 3 melanoma patients (NCT02993315). The patients will be assessed for 2-year recurrence-free survival.

Other trials are testing the efficacy of DC vaccines in combination with radiation, chemotherapy, targeted therapies, and depletion of myeloid cells and Tregs. In addition, the emergence of neoantigens has initiated the development and use of personalized neoantigen DC vaccines (88). For example, a recent meta-analysis reported that the objective response rate to DC vaccines in melanoma and glioblastoma was 8.5% and 15.6%, respectively (48). Hence, strategies to incorporate neoantigens into DC vaccines are ongoing (89) (NCT03300843). Lastly, in the light of current

understanding, like many other vaccine platforms, DC vaccines have been combined with ICB (90), including in combination with different PD-1 or CTLA-4 inhibitors in several cancers, including glioblastoma (and other brain tumors), colorectal cancer, and melanoma. In addition, DC vaccines can also be combined with other ICB-like antibodies targeting Tim-3, Lag-3, and NKG2A, currently in different stages of clinical development.

### **Proteins/Peptides**

Peptide-based vaccines that initially targeted tumor-enriched antigens (91, 92), can be classified into two distinct categories: tumor-associated antigens (TAA) and neoantigens (tumor-specific antigens, TSA). TAAs are enriched on cancerous cells but also expressed on some normal cells and are further subcategorized to a) aberrantly overexpressed antigens (e.g., Her2/neu (93) and survivin (94), b) lineage-restricted antigens (e.g., gp100 (95), prostate-specific antigen (96), and tyrosinase (97) c) cancer-testis (CT) antigens (e.g., MAGE family (98) and NY-ESO-1 (99)), and d) oncofetal antigens (e.g., Carcinoembryonic antigen (100-102)), and e) oncogenic viral antigens (HPV E6/E7). On the other hand, neoantigens are developed from somatic mutations (e.g., insertions, deletions, translocations) (103) in the tumor triggered by DNA-damage events, resulting in specific expression in the tumor.

Early clinical trials utilized TAA-based vaccines, such as the MAGEA3 vaccine (104), to treat established cancers and generally resulted in good safety profiles but lacked objective clinical responses (105). Various forms of adjuvants (Montanide, TLR

agonists, incomplete Freund's adjuvant, etc.) are an essential component of these vaccines (106-108), and some early studies showed modest signs of clinical benefits for recurrence and disease-free survival compared to non-vaccinated patients (109). However, even with the added anti-cancer benefits from immunostimulants or delivery vehicles, no peptide-based vaccine has been FDA approved to treat cancer. One biological reason may be the low immunogenicity of the TAAs, which is why it may be more beneficial to target neoantigens for peptide vaccines. An illustrative example is the Kras-based neoantigen vaccine that showed no clinical benefit (110-112).

To address immunosuppression from advanced tumor burden, combination strategies have been adopted to increase immunogenic cancer cell death, for example, by using approved chemotherapeutic agents like gemcitabine, cyclophosphamide, fluorouracil (5-FU), or folfirinox, among others. These treatments were also reported to suppress the tumor-promoting functions of Tregs and MDSCs (113-122). For instance, gemcitabine was shown to specifically reduce the number of Gr1<sup>+</sup> MDSC in spleens of tumor-bearing mice. This decrease in splenic MDSCs was accompanied by the increased antitumor activity of CD8<sup>+</sup> T cells and NK cells (113). Similarly, 5-FU significantly contracted the number of MDSC in the spleen and tumor bed, concomitantly increased IFN- $\gamma$  production by CD8<sup>+</sup> T cells, and promoted T cell-dependent antitumor activity (117).

The effect of chemotherapy on Tregs is also appreciated. Chemotherapy can selectively reduce the number of Tregs in the tumor bed, tumor-draining lymph nodes, and peripheral blood (115, 123, 124). Cyclophosphamide may also reduce the number

of Tregs by inducing apoptosis and inhibiting proliferation (115). Based on these encouraging results, multiple trials have employed this combinatorial strategy but have failed to show any significant clinical effect. For example, a phase II clinical study for patients with resected pancreatic cancer determined that gemcitabine plus OCV-C02, a three peptide cocktail, had no significant effect on disease-free survival (DFS) compared to gemcitabine alone (125). Another strategy explored is the combination of peptide vaccines and ICB because of ICB's ability to intensify immunogenic responses. This combination strategy is still in its infancy, and these clinical trials are still ongoing.

### **Nucleic Acids**

Nucleic acids have been well recognized as potent adjuvants (126, 127) and come in multiple flavors (128, 129). Both RNA and DNA have been used as adjuvants, but these also offer the ability to code for TAA. For RNA vaccine, RNA is transcribed in vitro (IVT) by a DNA template encoding the antigen and bacteriophage RNA polymerase (130). Pertinent biological factors for these platforms have been discussed elsewhere (128, 131). While there are examples of naked RNA vaccines that code for carcinoembryonic antigen (CEA) exhibiting strong immune responses when challenged with CEA overexpressing cancer cells (132), the stability of RNA has been an issue. Some of this work has been adopted by bioengineers as a delivery problem, and various forms of alternative vaccine delivery methods ("gene gun", protamine condensation, encapsulation) have been used (133-136).

An example is CV9103 comprising mRNA encoding four prostate cancer-associated antigens condensed with protamine for castration-resistant prostate cancer. The vaccine was well tolerated and showed antigen-specific T cell responses in 36 patients with metastatic prostate cancer. The vaccine showed a median overall survival of 30 months compared to the predicted 16.5 months (EudraCT number: 2011-006314-14) (92, 137). A similar approach for lung cancer patients is ongoing (138-140). To improve RNA half-life and delivery in vivo, naked RNA IVT is often encapsulated in nanoparticles and cationic lipid complexes for patient delivery (141)(NCT03313778). Details about similar studies can be found on the ClinicalTrials.gov website (NCT03289962) (NCT03815058).

The RNA and DC platform can be combined, whereby DCs can be pulsed with either total tumor RNA, TAA RNA, or neoantigen RNA. There are currently over 24 ongoing clinical trials investigating RNA-loaded DC vaccines. The advantage (or the disadvantage) of using whole tumor RNA for DC priming is it presents the entire constellation of antigens without the requirement of identification of immunogenic epitopes. Most of these early studies have shown little toxicity and potential to elicit an antitumor immune response (142-146). In a recent Phase II trial with Rocabudencel-T or AGS-003, moDC was co-electroporated with whole tumor RNA plus RNA encoding a costimulatory gene CD40L and administered to treatment naïve patients with clear cell renal cell carcinoma and evaluated in combination with sunitinib. The mixture was well tolerated and yielded supportive immunologic responses and a significant increase in OS (147). Alternatively, DCs can also be loaded with single or multiple TAA encoding

IVT mRNAs and infused back into the patients. With this method, the antigen must be immunogenic enough to activate the T cells, and these TAA pulsed DCs have been tested in multiple clinical trials (148-152). DCs have also been stimulated with mRNA encoding melanoma antigens (MAGEA3, melanoma-associated antigen C2 (MAGEC2), tyrosinase and melanocyte lineage-specific antigen GP100, and other mRNAs encoding immune co-stimulatory genes like CD40 ligand (CD40L), a constitutively active mutant form of TLR4 and CD70 (NCT01066390) (78, 79, 153, 154). Trimix vaccine is currently being tested in a placebo-controlled clinical trial in breast cancer patients (NCT03788083).

A DNA-based vaccine is the other flavor of nucleic acid vaccines, and much like RNA, their clinical development is focused on delivery and combination with ICB. The biological basis of DNA-based vaccines are reviewed elsewhere (127, 155). The commonly used techniques to deliver the vaccine are electroporation, sonoporation, gene gun, or DNA tattooing. For gene gun mediated intradermal injection, Langerhans cells, the antigen-presenting cells (APCs) residing in the skin, directly engulf the plasmids and express the antigen, which MHC I then presents to prime naïve T cells in the lymphoid tissues. For the intramuscular route, myocytes take up the plasmids. However, they are not potent inducers of immune activation. Instead, they recruit DCs, which phagocytose the infected cells and then mount T cell response and memory. These techniques have been comprehensively reviewed elsewhere (156). Unfortunately, DNA vaccines as monotherapy have often shown limited clinical success

(155). Several clinical trials are testing the potential of DNA vaccines in combination with ICB in various tumors (Clinicaltrials.gov).

### **Microbial (oncolytic and bacterial) vaccines**

Oncolytic viruses (OV) have recently emerged as one of the most promising treatment options in cancer therapy. In brief, oncolytic viruses infect and replicate within tumor cells, causing cell death and releasing antigens and viral debris (156, 157). Phenotypic “hallmarks of cancer,” including the high metabolic activity within tumor cells and driver mutations, have been shown to increase the replication of viruses inside the cancer cells. The significant advantage of oncolytic viruses is that they can specifically target and lyse neoplastic tissue while sparing healthy cells, thus theoretically limiting systemic toxicity. Also, in contrast to drug pharmacokinetics that decreases with time, the viral dose in tumor increases due to *in situ* replication. Furthermore, viral receptors can be overexpressed by tumor cells, and recombinant viruses can be modified to target tumor-specific receptors and to overexpress cancer-specific genes (for example, apoptosis-inducing or immune stimulating) to amplify the antitumor effects. OV can be either DNA or RNA virus and either single-stranded or double-stranded. They establish the lytic cycle in cancer cells by either replicating preferentially in cancer cells by using activated oncogenic pathways or have been genetically modified to replicate selectively in malignant cells. Oncolytic virus details have been extensively reviewed elsewhere (157-162).

In brief, immune stimulatory properties of OV stem from their ability to induce immunogenic cell death like programmed necrosis or necroptosis (163-167) to activate immune cells against the infected malignant cells as well as prime *de novo* T cell response against tumor-associated as well as neoantigens that were not exposed earlier. OV-induced lysis of cancer cells releases endogenous nuclear and cellular contents, including pathogen associated molecular patterns (PAMPs), danger associated molecular patterns (DAMPs), viral proteins and nucleic acids, tumor-associated antigens, immunogenic neoepitopes (159, 168, 169) and activate antitumor immune response cascades. PAMPs, DAMPs, and tumor antigens thus released can be phagocytosed by macrophages or dendritic cells and fuel the release of inflammatory and immune-activating cytokines. These then can activate immune cells against the infected malignant cells and prime *de novo* T cell response against tumor-associated and neoantigens that were not exposed earlier. Type I Interferons and DAMPs can also directly activate NK cells which will now effectively kill cancer cells that have downregulated their expression of MHC I, a common occurrence in most cancers. OV can also be genetically modified to express anti-angiogenic molecules to target tumor angiogenesis (170). OVs have also been reported to produce the abscopal effect - the regression or delayed progression of metastatic sites distant from the site of injection (170).

Currently, numerous OVs are being tested in clinical trials to treat different types of cancers (171). The FDA has approved the HSV-1-based oncolytic virus, talimogene laherparepvec, or T-VEC (Imlygic™), for treating surgically metastatic melanoma

nonresectable. TVEC is comprised of genetically modified HSV-1 made to overexpress GM-CSF (90, 172-174). Twenty-eight trials are active and testing TVEC in various cancers, including pancreatic cancer, sarcoma, breast cancer, and melanoma, among others, either alone or in combination with radiation, chemotherapy, or immune therapy. Another example of oncolytic virus therapy showing promising results in early phase trials is a genetically modified poliovirus: rhinovirus chimera, PVSRIPO. The virus elicited effective antitumor immune responses in patients with recurrent glioblastoma (175, 176). A phase II trial is currently underway testing the efficacy of PVSRIPO with or without the chemotherapy drug lomustine (Gleostine®) in glioblastoma patients. Based on the promising results, the FDA granted PVSRIPO's 'breakthrough' status. Other examples of OV are the human Orthoreovirus which can cross the blood-brain barrier to activate cytotoxic T cell response against brain tumors (177), and the Maraba virus isolated from a variety of sandflies in Brazil to treat triple-negative breast cancer (TNBC) (178).

With the expansion of OV in clinical trials, there is now an urgent need for biomarker discovery, optimal dosing, and combinatorial pathways (179, 180) to identify patients that may benefit more from the virus therapy either as a stand-alone drug or in combination with other immunomodulating agents. In addition, with the wealth of well-characterized microbial agents, several other viral vectors are currently being investigated in preclinical phases for translations.

The other microbial vector is the bacterium, and other reviews are available that discuss this platform in detail (181-186). Commonly used strains include *Clostridium*, *Salmonella*, and *Listeria*. A modified *Salmonella* vaccine was tested for dose, safety, tolerability, and immune response in patients with refractory solid tumors (NCT00006254, NCT00004216). *Salmonella* modified to express IL-2 has been orally administered to patients with refractory hepatic metastases from solid tumors in a phase I study (NCT01099631). One ongoing phase I trial will test the safety and dosage of orally administered live *Salmonella* vaccine modified to produce survivin in patients with multiple myeloma and induce survivin antigen-specific T cell response (NCT03762291). In phase I clinical trial with one patient presenting retroperitoneal leiomyosarcoma, the *Clostridium* vaccine showed extensive tumor necrosis and improved quality of life (NCT01924689)(184). The *Clostridium* vaccine is currently being tested in combination with pembrolizumab in solid tumors (NCT03435952).

Lastly, in early phase trials, *Listeria* strains modified to express the tumor antigen mesothelin (CRS207), have also been tested in mesothelioma, lung, pancreatic, or ovarian cancers. Both vaccines were well tolerated in patients and induced tumor-specific immune T and NK cell responses (187). CRS207 was next investigated in a phase II trial in combination with GVAX and cyclophosphamide (NCT02004262) in previously treated pancreatic metastatic patients. A phase I clinical trial is ongoing to test the safety, dose, and immune response of a live *Listeria* vaccine (ADU623) expressing EGFRvIII and NY-ESO-1 to treat patients with astrocytic tumors (NCT01967758). Ongoing trials focus on combining *Listeria* vaccines with conventional

treatment options or immunotherapies (Clinicaltrials.gov). For example, the *Listeria* vaccine is currently being tested in combination with anti-PD-1 (NCT03847519) or as an adjuvant after chemotherapy (NCT01675765) in non-small cell lung carcinoma and malignant mesothelioma, respectively. Another study by Aduro Biotech Inc aimed to test the efficacy of a personalized live attenuated *Listeria* vaccine in metastatic colorectal cancer patients (NCT03189030).

### **iPSC-based vaccines**

The concept of embryonic tissue being used for vaccination dated back to 1906, when Georg Schöne reported that mice immunized with fetal tissue rejected transplanted tumors (188, 189). Published reports indicate that embryonic and tumor cells share transcriptome profiles and antigen repertoire (190, 191). Induced pluripotent cell-based vaccines circumvent the ethical roadblock and are the newest addition to the cancer vaccine family. Reports show that induced pluripotent stem cells (iPSCs) share nearly identical gene expression profiles with embryonic stem cells and cancer cells and have immunogenic properties (192-198). The concept has recently been tested by Kooreman et al. In their elegant study, the authors have developed an autologous vaccine from irradiated mouse pluripotent stem cells (to arrest their proliferation in vivo and prevent the formation of teratoma). The vaccine was used prophylactically to prevent tumor formation in syngeneic models of breast cancer, mesothelioma, and melanoma and showed clear indications of humoral and cellular immune responses. The vaccine culminated in mature antigen-presenting cells in the draining lymph nodes (dLN) and increased local and systemic helper and cytotoxic T cells. In an adjuvant

setting, it reduced metastatic tumor burden and potentially altered immune responses characterized by fewer Th<sub>17</sub> cells and increased infiltration of Gr1<sup>+</sup>CD11b<sup>+</sup> myeloid cells into the tumors. Interestingly, when the authors adoptively transferred T cells from vaccinated tumor-bearing mice, it elicited an antigen-specific antitumor response in unvaccinated recipients (199).

One significant advantage of the autologous iPSC vaccine is that it circumvents the challenge of patient-specific tumor antigen selection. Also, it will be readily available from the patient skin or blood. However, there are a few safety concerns that need to be noted. iPSCs are immature progenitor cells that do not have growth restraint and may give rise to teratomas once injected. Genetic modifications with suicide gene *ex vivo* are potentially feasible soon. Another issue is the labor-intensive process of reprogramming iPSCs *ex vivo*, which introduces concerns regarding the cost and time required to prepare the vaccine. Although iPSC-based vaccines showed encouraging results in preclinical settings, their translation in patients is pending.

### **Personalized Cancer Vaccine**

As mentioned earlier, tumor-associated antigens are often expressed at low levels in normal tissue and hinder immune responses to vaccine therapy through central and peripheral tolerance or autoimmunity. Thus, the lack of enough “foreignness” may have been the past failure of many vaccine studies. As cancer evolves, it accumulates mutations that alter the amino acid sequences in proteins. The most common types of mutations are single nucleotide variation (SNV), insertion, deletion, and fusion or

duplications. These mutations can either result in a single amino acid mutation or change the open reading frame yielding mutated peptides/proteins called neoepitopes. These can vary within different regions of the same tumor and are tumor-specific antigens. There are reports of shared neoantigens, but most are not shared across tumor types and are specific to the patient (200). Personalized vaccines targeting the unique set of neoantigens in an individual's tumor have been developed; this platform's challenges are primarily immunogenicity and heterogeneity.

Early examples in murine Lewis Lung carcinoma models in 1994 of mutated connexin 37 showed the biological basis of these neoantigen-based platforms. Still, their translational potential was spurred by advancements in next-generation sequencing and bioinformatics (201-206). The typical workflow for developing a personalized neoantigen vaccine involves whole exome and RNA sequencing of tumor and matched normal tissue, followed by bioinformatics platforms to analyze the clonal ancestry for determining the neoantigen clonality in the tumor and intratumor heterogeneity. Potential vaccine neoepitopes are next predicted based on their binding affinity to the HLA subtype defined in the patient. NetMHC and IEDB consensus are two such platforms. Finally, the validated epitopes are selected for vaccine formulation and administered to the patients. In some settings, immunogenicity can be determined with ELISPOT using synthetic peptides. In one such study, three melanoma patients were treated with autologous DCs loaded with seven HLA-A2 restricted synthetic 7-mer peptides representing the individual antigenic mutations in the patients (89). In addition to the neoepitope vaccine, they also received melanoma gp100-derived peptides G209-

2M and G280-9V (positive vaccine controls). The treatment was well tolerated in the patients who developed neoantigen-specific T cell responses.

Multiple combinatorial approaches have been exploited to deliver different neoantigen-based vaccines (205, 207-215). Examples range from direct injection of unformulated antigens to DC pulsed with immunogenic neoantigens (89) or bioengineered neoantigen delivery formulations (216-218). It is noteworthy that based on the recent developments, multiple personalized vaccines are now ongoing or in the pipeline, awaiting their evaluation in clinical settings. RNA-based personalized vaccine RO7198457 (Genentech) is currently in a Phase Ia/Ib dose-escalation study either as a single agent or in combination with Atezolizumab (MPDL3280A, an engineered anti-PD-L1 antibody). Neovax (formulated with poly-ICLC) will be combined with Ipilimumab in a cohort of 18-20 patients diagnosed with stage III/IV clear cell renal cell carcinoma (ccRCC)(NCT02950766). NEO-PV-01, a personalized cancer vaccine containing up to 20 neoantigens individually selected for each patient diagnosed with advanced melanoma, bladder cancer, or non-small cell lung cancer (NSCLC), is also ongoing (NCT01970358). A second Phase II study is continuing to evaluate the efficacy, safety, pharmacokinetics, and patient-reported outcomes (PROs) of RO7198457 plus Pembrolizumab (PD-1 blocking agent) compared with Pembrolizumab alone in patients with previously untreated advanced melanoma.

The design and development of neoantigen-based personalized cancer vaccines involve the rapid and accurate identification of a patient's mutanome and thus heavily

rely on the robustness of in silico modeling and derivation of neoantigens- working with the patient sample to sequencing and bioinformatics analysis. This is especially imperative for tumors with lower mutation load. There are still significant gaps in HLA presentation prediction based solely on Kd vs. actual immunogenicity that is not accounted for in the sequencing-based methods to generate these personalized vaccines. However, current bioinformatics algorithms face significant challenges in accurately assessing MHC binding affinity and specificity partly due to limited knowledge about several HLA alleles. Recent studies showed CD8<sup>+</sup> T cell response against predicted high-affinity binders as low as 29%, warranting improvements to the current algorithms (219). In addition, researchers are exploiting other methods, including mass spectrometry, to identify actual neoantigens presented on HLA molecules. For example, mass spectrometric analysis of peptide-HLA complexes revealed the HLA ligandome derived from human tumors (220-224). Collectively, this entire process of identification of patient tumor neoantigen, validating their presentation on HLA molecules, and demonstrating their immunogenicity may take up to several weeks or months, which may not be a feasible option if the patient is diagnosed with large tumor burden or an advanced stage of cancer. Lastly, the platform also introduces the concern for affordability by most patients.

## **HURDLES FACING SUCCESS OF CANCER VACCINE THERAPY**

### **Development of tumor cell-intrinsic resistance mechanisms**

The heterogeneity of cancer cells in tumors results in developing resistance mechanisms, and clinical persistence or disease recurrence to immunotherapy manifests this critical mechanism. For example, epigenetic modifications often trigger alternate signaling pathways in cancer cells (225). Also, genetic mutations in genes following therapeutic intervention (“immuno-editing”) can render immune therapy ineffective. One study investigated the genetic mutations in patients responsible for acquired resistance to Pembrolizumab. Surprisingly, two patients were found to have mutations in JAK1 or JAK2 genes that interfered with IFN- $\gamma$  signaling. A third patient had a mutation in  $\beta$ 2M gene that was important for the recognition and elimination of cancer cells (226). These tumor intrinsic resistance mechanisms have been extensively discussed elsewhere (227).

### **T cell exclusion from solid tumors**

A common mechanism of immune evasion by tumors is excluding T cells from the TME (concept of immunologic ignorance). Leaky tumor vasculature and hypoxic regions resulting in spatial differences in metabolites are essential factors that influence T cell extravasation, survival, and function in the TME (227). Also, tumor blood vessels' endothelium often downregulates the expression of leucocyte adhesion molecules like intercellular adhesion molecule-1 (ICAM-1) and vascular cell adhesion molecule-1 (VCAM-1) or increases the level of Endothelin B receptor in the tumor microvasculature

that dampen T cell entry. TAMs and MDSC also secrete chemokines that support Tregs trafficking but prevent cytotoxic T cells. Tumor cells and TAMs also express Fas ligand (FasL) to induce apoptosis in infiltrating T cells (227). Such molecular mechanisms may explain the solid desmoplastic reaction in pancreatic cancer, which can trap T cells in the stroma and prevent migration to the tumor cell-rich areas.

### **Freeing immune cells from coinhibitory checkpoints and exhaustion**

Immune checkpoint molecules are essential for maintaining immune homeostasis and autoimmunity. They regulate the breadth and magnitude of T cell response by balancing co-stimulatory and coinhibitory signals for T cell activation. However, cancer cells often hijack these molecules to suppress T cell activation as a mechanism to escape immune killing. Further, due to chronic antigen stimulation, tumor-infiltrating T cells become exhausted and attain a hyporesponsive state characterized by progressive loss of effector functions (228, 229). In this context, combinatorial ICB involving CTLA-4, PD-1, and its ligands PDL-1/PDL-2 and LAG3 have become attractive targets in cancer immune therapy. Immune checkpoint mechanisms have been extensively reviewed elsewhere and are beyond the scope of this introductory thesis section (230-233). In brief, CTLA-4 competes with CD28 for binding with CD80 and CD86 and provides a coinhibitory signal to prevent T cell activation by antigen-presenting cells (APC).

PD-1 on T cells can bind to PDL-1 or PDL-2 expressed by cancer cells or TAMs, which can arrest T cells in a non-activated state. For example, in a clinical trial using the

TG4010 Muc-1 vaccine in lung cancer, patients with lower PDL-1 expression showed higher progression-free survival (234). Antibodies targeting immune checkpoints are now widely used in clinical trials as a single agent or combination therapy for boosting the immune response (235). The best clinical responses have been demonstrated in melanoma, where PD-1 and CTLA4 blocking antibodies (response rates of 45-60%) are now standard care. Combining cancer vaccines with checkpoint blockade may yield superior immune responses in patients. This was observed in a phase II clinical trial with the DC vaccine and Ipilimumab. Patients who received combination therapy responded better than those who received monotherapy (78). In addition to checkpoint blockade, several co-stimulatory agonists like OX40 and 4-1BB have shown synergistic effects in preclinical studies (236, 237) and are now being tested in clinics (235).

### **Immunosuppressive cells in the TME**

The solid tumor microenvironment is a highly complex structure. It is often heavily infiltrated by endothelial cells, cancer-associated fibroblasts (CAF), TAMs, tolerogenic DC, MDSCs, suppressive regulatory B cells,  $\gamma\delta$  T cells, and Tregs. They engage in a complex cross-talk to collectively establish an environment of immune suppression (227, 238-244) and aid in cancer cell survival, growth, and metastases. For instance, TAMs and MDSC secrete suppressive cytokines like IL-10, TGF- $\beta$ , and IL-4 to dampen T cell function, induce T cell apoptosis, and favor Tregs formation. Similar suppressive activity has been reported for regulatory B and  $\gamma\delta$  T cells (245-250). Additionally, TAMs upregulate the expression of coinhibitory molecules like PDL-1 to drive T cells to

suppression. They are also crucial for pre-metastatic niche formation. Each of these TME members are well-known contributors to therapy failure (**Fig.1-4**).

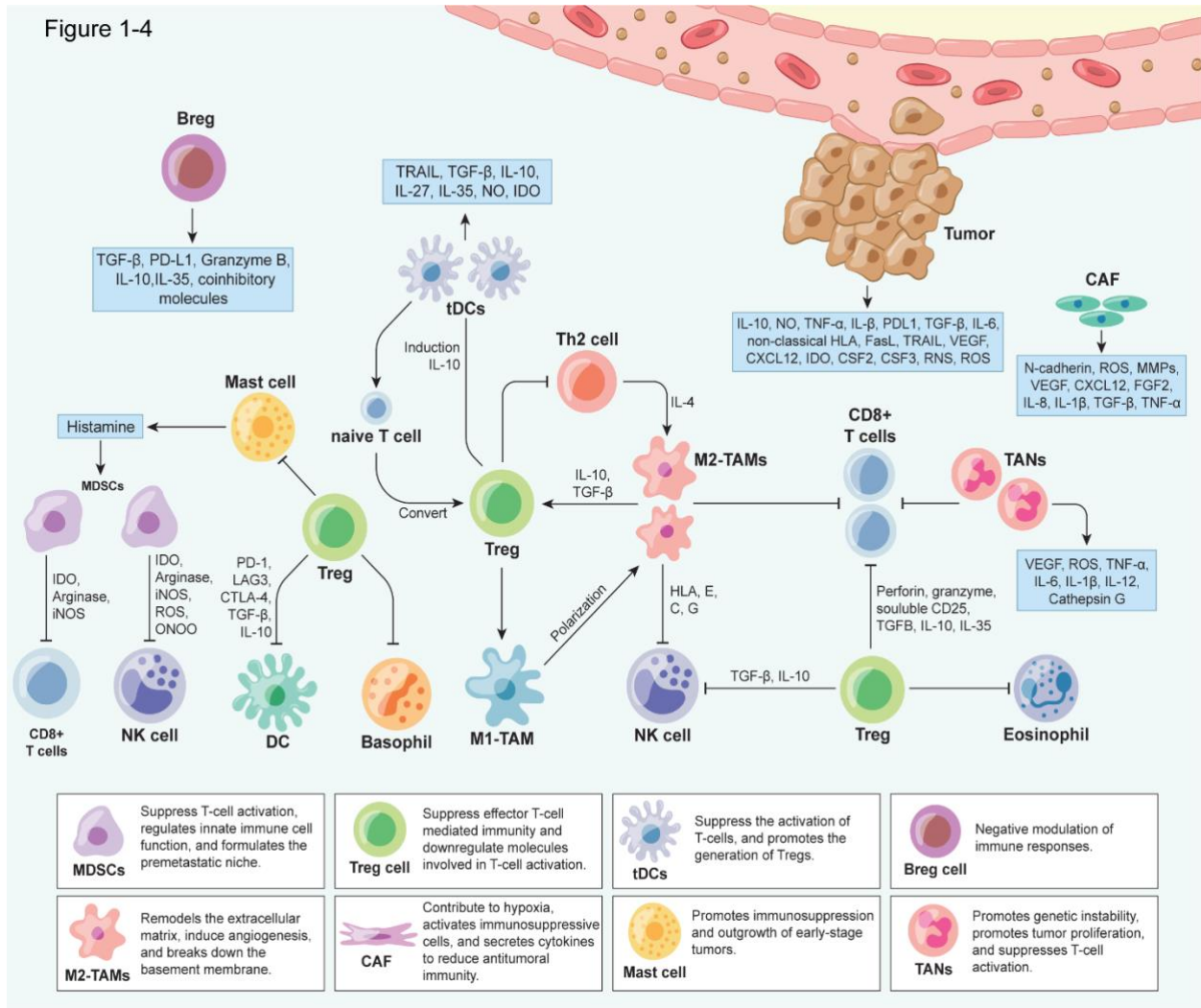


**Figure1- 4:** New model for discovering and validating immunotherapies

Figure 1-4: Tumor cells significantly hinder antitumor immunity by lowering the pH and glucose but enhancing the secretion of growth factor VEGF, metabolites IDO, ROS, RNS, NO, or ONOO-, and anti-inflammatory cytokines such as IL-10 and TGF- $\beta$ . In addition, the tumor can express non-classical HLAs and death ligands FasL and TRAIL. These resistance mechanisms allow tumors to evade effector immune cells, recruit stromal cells, and facilitate tumorigenesis. Cancer-associated stromal cells, such as CAFs, have the protumoral function by suppressing the immune responses and inducing other immunosuppressive cells. CAFs also promote blood vessel formation, invasion, and tumor progression. Bregs also contribute to the immunosuppressive microenvironment by releasing anti-inflammatory cytokines and expressing coinhibitory molecules. Tregs can block the function of effector T cells, eosinophils, basophils, and mast cells. Moreover, Tregs also stimulate tDC to secrete IL-10 polarizing M1 TAMs to M2 TAMs. When this polarization occurs, M2 TAMs eradicate effector cells by secreting immunosuppressive cytokines, depriving the microenvironment of nutrients, and expressing coinhibitory molecules. Also, M2 TAMs stimulate angiogenesis and promote metastasis. MDSC is similar to M2 TAMs as it hinders effector function and releases anti-inflammatory cytokines to generate a protumoral microenvironment. TANs also play a role in eliminating cytolytic T cells. (Note- Tregs: regulatory T cells; TAMs: tumor-associated macrophages; TANs: tumor-associated neutrophils; CAF: cancer-associated fibroblast; MDSCs: myeloid-derived suppressor cells; NK: natural killer cell; tDC: tolerogenic dendritic cells; Breg: regulatory B cells; VEGF: vascular endothelial growth factor; IDO: indoleamine 2,3-dioxygenase; ROS: reactive oxygen species; RNS: reactive nitrogen species; NO: nitric oxide; ONOO-: peroxynitrite; IL: interleukin; TNF- $\alpha$ : tumor necrosis factor-alpha; TGF- $\beta$ : transforming growth factor beta; FasL: fas ligand; TRAIL: tumor-necrosis factor-related apoptosis-inducing ligand; MMP:

Another emerging mechanism in the human TME is the immunosuppressive process of efferocytosis. It has recently been reported that phagocytosis of apoptotic debris in the TME drives macrophages towards an immunosuppressive phenotype (163, 251, 252). This is one factor contributing to the relapse of the disease in a more aggressive form. In addition, circulating MDSCs often increase in therapy patients (253). Various strategies are being tested to target TAMs or MDSCs in clinics and are discussed elsewhere (235). For example, STING agonists can reprogram suppressive MDSCs to an activated inflammatory type (254). In a clinical trial with the NY-ESO1-ISCOMATRIX vaccine in melanoma, poor response to the vaccine correlated with more Tregs in metastatic patients compared to early-stage patients (255). Antibody-mediated Tregs depletion or adding low-dose CpG-ODN to the ISCOM formulation restored the vaccine's efficacy in preclinical models (256). However, selective depletion of Tregs in patients is challenging. Using cyclophosphamide has shown some success, achieved by metronomic scheduling (257). As said in one review, “there is no particular hierarchy in immunosuppression in solid tumors, and the dynamic nature and the potential redundancy of suppressive mechanisms” (227) continue to remain one of the biggest hurdles for vaccine therapy.

### **Immunosuppressive metabolic barrier**

Another important consideration is the metabolic demands of the tumor immune cells and the limited metabolic milieu of the TME that can affect their metabolic requirements and, therefore, functional polarization (258-264). For effective vaccines, naïve T cells need to mature into multifunctional effector cells for which they heavily rely on aerobic

glycolysis. However, inside the tumor microenvironment, factors like hypoxia, areas of necrosis as well as the rapid proliferation of tumor cells create nutrient constriction. The metabolic landscape is generally hostile and does not support effector T cell activation. The glycolytic cancer cells outcompete the T cells for glucose consumption (265-267). This directly reduces TCR signaling, proliferation, and production of tumor cell-killing cytokines (268-273). Furthermore, lactate produced by glycolysis is detrimental to T cell proliferation and IFN- $\gamma$  release (274). Glucose restriction, on the other hand, does not affect Tregs, which depend on oxidative phosphorylation for their function (275). In addition to glucose, glutamine addiction is common for many cancer types. For example, ovarian cancer cells metabolize glutamine to glutamate. This is taken up by CAFs, which convert it back to glutamine and thus foster a vicious feed-forward loop with cancer cells. Unfortunately, glutamine is also essential for T cell proliferation. Hence glutamine deprivation faced by T cells in TME affects their antitumor activity (227).

An amino acid-dependent mechanism of immunosuppression in the TME is indoleamine-2,3-dioxygenase (IDO). This enzyme converts tryptophan to kynurenines and is highly expressed on tumor cells, DC, and suppressive myeloid populations. Tryptophan is essential for T cell activation, and its depletion restricts the tumoricidal effector function of T cells. Additionally, IDO can directly recruit myeloid cells and Tregs and blunt NK cell function (227). A high level of Arginase-1 by myeloid cells contributes to T cell dysfunction in TME. Although Arginase-1 inhibitors are in clinical

development, we are unaware of any clinical trial using Arginase-1 inhibitors in combination with vaccines.

### **The hypoxic environment of the tumor**

As a tumor grows, large areas within can become hypoxic. The tumor compensates by producing more angiogenic factors like Vascular Endothelial Growth Factor (VEGF), but most often, the neoangiogenic and lymphangiogenic blood vessels fail to induce normoxia. Also, in highly desmoplastic tumors like pancreatic adenocarcinoma, blood vessels collapse and further contribute to the hypoxic tumor microenvironment. The lack of oxygen within cancer profoundly affects several aspects of tumor growth, metastases, metabolism, and associated immune response. Hypoxia induces the expression of Hypoxia Inducible Factor 1  $\alpha$  (HIF1 $\alpha$ ), a key mediator of hypoxia signaling, which drives angiogenesis, procurement of epithelial to mesenchymal (EMT) phenotype, glycolysis in cancer cells, and immune suppression. Hypoxia also induces the expression of targetable CD47 in tumor cells, relaying the “do not eat me” signal to macrophages or DCs. It can also influence the expression of HLA-G. This important negative immune modulator dampens the functionality of macrophages, NK cells, T cells, and B cells by binding to cognate receptors expressed by these cells.

Hypoxia also affects immune cells within the tumor. For example, hypoxia increases the expression of PDL-1 in macrophages, MDSCs, and dendritic cells to promote immune suppression of T cells. In addition, one of the hallmarks of cancer is aerobic glycolysis, where glucose is converted to lactate instead of being shuttled to oxidative

phosphorylation. This way, the intermediates from glycolysis can be used for the biosynthesis of other macromolecules. HIF1 $\alpha$  upregulates the expression of several glucose transporters and glycolytic genes like such as glucose transporters 1 and 3 (GLUT1 and GLUT3), pyruvate dehydrogenase, lactate dehydrogenase A (LDHA), phosphoglycerate kinase 1, and hexokinases 1 (HK1). This restricts glucose availability to effector T cells which rely on glycolysis to mature into multifunctional T cells. Also, the lactate produced from glycolysis dampens the activity of T cells and NK cells. All these collectively pose a significant hurdle to rewiring vaccine-mediated antitumor immunity. Various metabolic modulators are currently being studied or in the clinical developmental stage. Combining them with existing cancer vaccines may improve patient responses (227).

### **Suboptimal Ag selection**

Since the discovery of the first tumor antigen, MAGE-1, in 1911, extensive efforts have been undertaken to design and develop efficient vaccines to eradicate the tumor. The selection of appropriate immunogenic antigens is essential for the reliable activation of immune responses. TAAs like EGFR or gp100 overexpressed on cancer cells and often shared across multiple cancer types have been targeted for vaccine development. However, they are also expressed in low levels in non-cancerous tissues resulting in a weaker immune response due to central and peripheral tolerance (276). Thus, more recent approaches have focused on antigens that are mutated in individual tumors. These neoantigens or tumor-specific antigens are identified through next-generation sequencing and are unique to cancer and patient. As discussed above, their expression

levels can vary within different tumor clones in the same individual. Also, among the identified neoepitopes, not all will be immunogenic enough to stimulate T cell responses. Therefore, the current personalized vaccines are designed to target multiple neoepitopes, usually up to 20 (276-278).

### **Selection of patients, vaccine platform, time, dose, and route of delivery**

It is now appreciated that distinct genetic and phenotypic populations co-exist within the same tumor or between tumors in the same patient. Even for cancer of the same histological type, patient-specific factors such as germline genetic and somatic mutation profile (point mutations, single nucleotide variation, insertion, deletion, copy number variation, allelic loss, karyotype aberrations) either present before/at the time of treatment or acquired at progression (temporal heterogeneity), epigenetic changes and environmental factors contribute to the development of intra-tumor and inter-patient heterogeneity. For example, germline genetic polymorphism analysis across multiple cancer types has been shown to influence lymphoid and myeloid cell infiltration into the tumor, affecting clinical response since inflamed tumors are more likely to respond to checkpoint therapies like anti-PD-1 or anti-PDL-1 (279). Another example comes from the loss of heterozygosity at the human leukocyte antigen (HLA-C\*08:02) locus in the resistant clones during treatment with T cell clones engineered to recognize KRAS<sup>G12D</sup>. Since this allele was necessary to present the KRAS<sup>G12D</sup> neoantigen epitope, its loss enabled immune escape (280).

In a recent study, the rapid autopsy performed on breast cancer patients harboring activating PIK3CA mutations (phosphatidylinositol-4,5-bisphosphate 3-kinase, catalytic subunit alpha, PI(3)K $\alpha$ ) with metastases revealed intertumoral variations where some patients lost the original PIK3CA mutation, whereas some developed bi-allelic loss of PTEN (phosphatase and tensin homolog) with disease progression and treatment (281). Similarly, analysis of non-small-cell lung cancers (NSCLCs) patients showed a complete loss of the Retinoblastoma (RB) gene in the course of treatment in cases where the disease transformed to small-cell lung cancer (SCLC) in a subset of patients, also acquiring elevated expression of neuroendocrine markers (282). In addition, an extensive genomic characterization in glioblastoma patients identified differences in mutations in responders versus non-responders to immune checkpoint inhibitors (283). These tumor heterogeneity issues have been extensively discussed elsewhere (284-292) and highlighted in several recent research articles (279, 293-296) and are beyond the scope of this review. Unless carefully detected and characterized, these factors can have detrimental effects by misdirecting treatment decisions. Collectively, these form the basis for precision medicine targeting specific genetic alterations in a particular tumor instead of a “one size fits all” treatment strategy.

The selection of patients who are likely to respond remains a crucial challenge. For example, one study assessing GVAX + ipilimumab in pancreatic cancer suggested that higher TCR clonality correlated with more long-term survival (297). Cancers like melanoma, NSCLC, bladder cancer, gastric cancer, and squamous cell carcinoma of the head and neck (SCCHN) carry a heavier mutational load and more inflamed tumor

microenvironment compared to “cold” cancers like pancreatic adenocarcinoma or prostate cancer, may also be better targeted for vaccine development (298, 299). Another recent study showed that patients with maximal heterozygosity of HLA class I locus (HLA-A, B, and C) showed more remarkable survival following treatment with either anti-PD-1 or anti-CTLA-4 (296). Other factors include the type of vaccine administered to a kind of cancer, the combination therapy employed, the dose, and the timing of treatment. For many cancers, the standard of care is either radiation or chemotherapy. However, chemotherapeutic agents have a profound effect on non-malignant cells as well. Therefore, it is possible when the patient receives a vaccine or any immune therapy after radiation or chemotherapy; the immune cells are already in a compromised state and too weak to mount a robust response.

Similarly, the timing could play a vital role when using vaccines and checkpoint blockade as combinatorial therapy. For example, CTLA-4 and PD-1 blockade were more effective in preclinical models after GVAX or TG4010 (Muc-1-targeted MVA vaccine) treatment (300, 301). In contrast, a PSA-targeted DNA vaccine worked better when used concurrently with PD-1 blockade (302). Another concern is the selection of the route of delivery of the drug. Following parenteral administration, vaccines quickly spread in circulation and minimal amounts home to lymph nodes for T cell activation. Hence, researchers are now focusing on developing other effective vaccine delivery methods, like nanoparticles, bioscaffolds, etc.

## **Effect of microbiome**

Recently, there has been a renewed interest in the >100 trillion microbes in each person. Emerging evidence suggests host microbiome can increase one's susceptibility to developing a particular type of cancer and affect response to therapy by regulating the immune system. Gut microbes have been shown to affect therapeutic efficacy in preclinical models and patient cohorts (303). For example, patients who respond to anti-PD-1-based therapy have a higher diversity of gut bacteria and differences in composition that correlate with prolonged progression-free survival (304, 305). The mechanism for these correlative findings is still early, and their use as a clinical biomarker has yet to be validated.

## RESEARCH OBJECTIVES

### **Combine adjuvants to maximize immunogenicity**

Immune checkpoint inhibitors (ICI) are FDA approved to treat various cancer types, but their efficacy is low. Since ICI mediates its action through T-cells, therapeutic cancer vaccines have been developed, which by themselves are not clinically effective (306). Hence, combinatorial immunotherapy that combines ICI and cancer vaccines has been advanced. While cancer vaccines are developed to target tumor antigens, these vaccines require adjuvants that activate the antigen-presenting cells (APCs) to prime effector T-cells against those antigens. Approved adjuvants are toll-like receptor (TLR) agonists that stimulate the myeloid differentiation factor 88 (MyD88) and TIR Domain Containing Adaptor Inducing Interferon-Beta (TRIF) intracellular signaling pathways (307) **(Fig.1-5)**. Since MyD88-TRIF stimulating adjuvanted vaccines failed multiple phase III trials (306), combining FDA-approved TLR adjuvants with clinically safe MyD88-TRIF independent adjuvants may synergistically enhance immune-stimulatory capacity. This combinational approach is a viable strategy for the translational development of cancer vaccines.

Figure 1-5

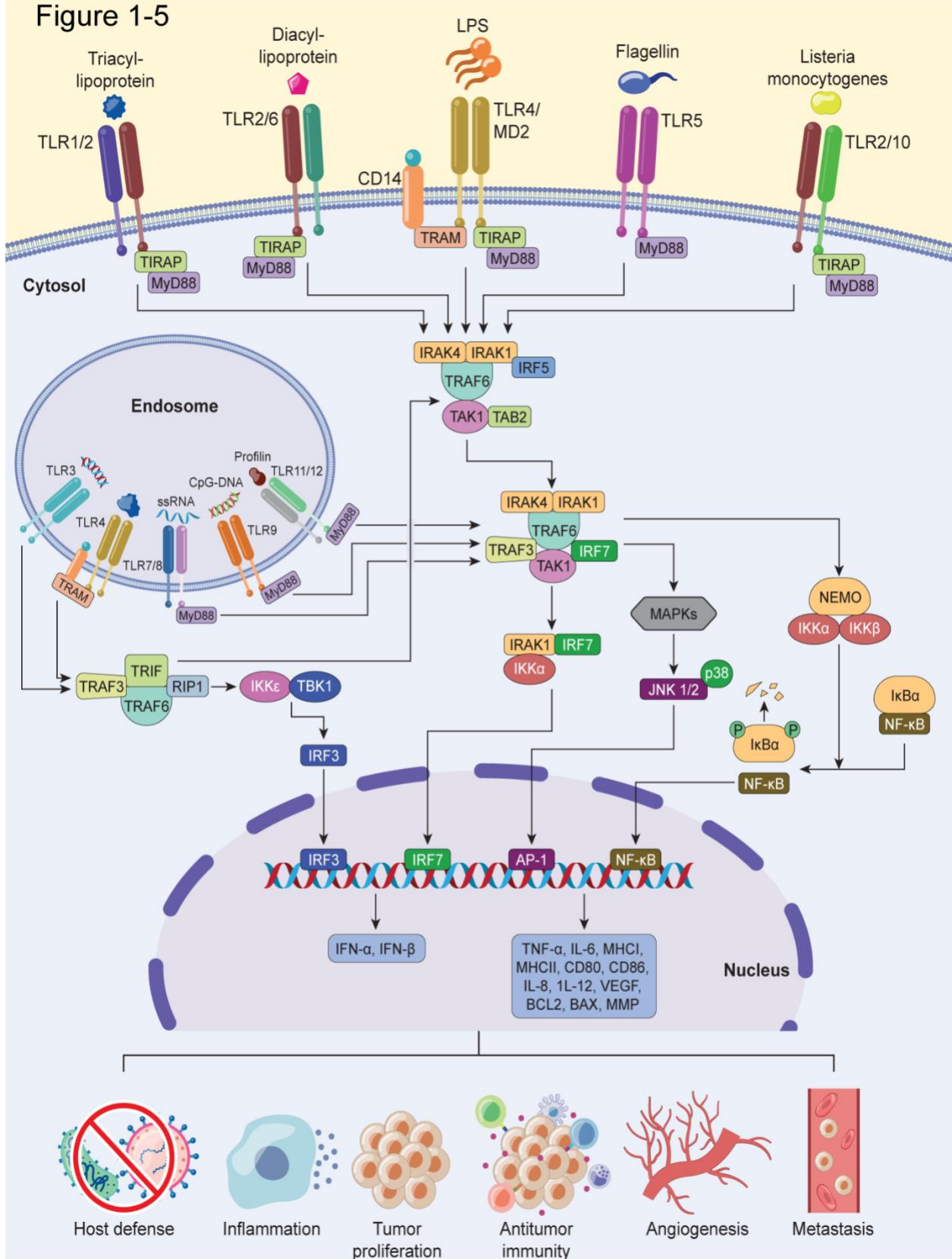
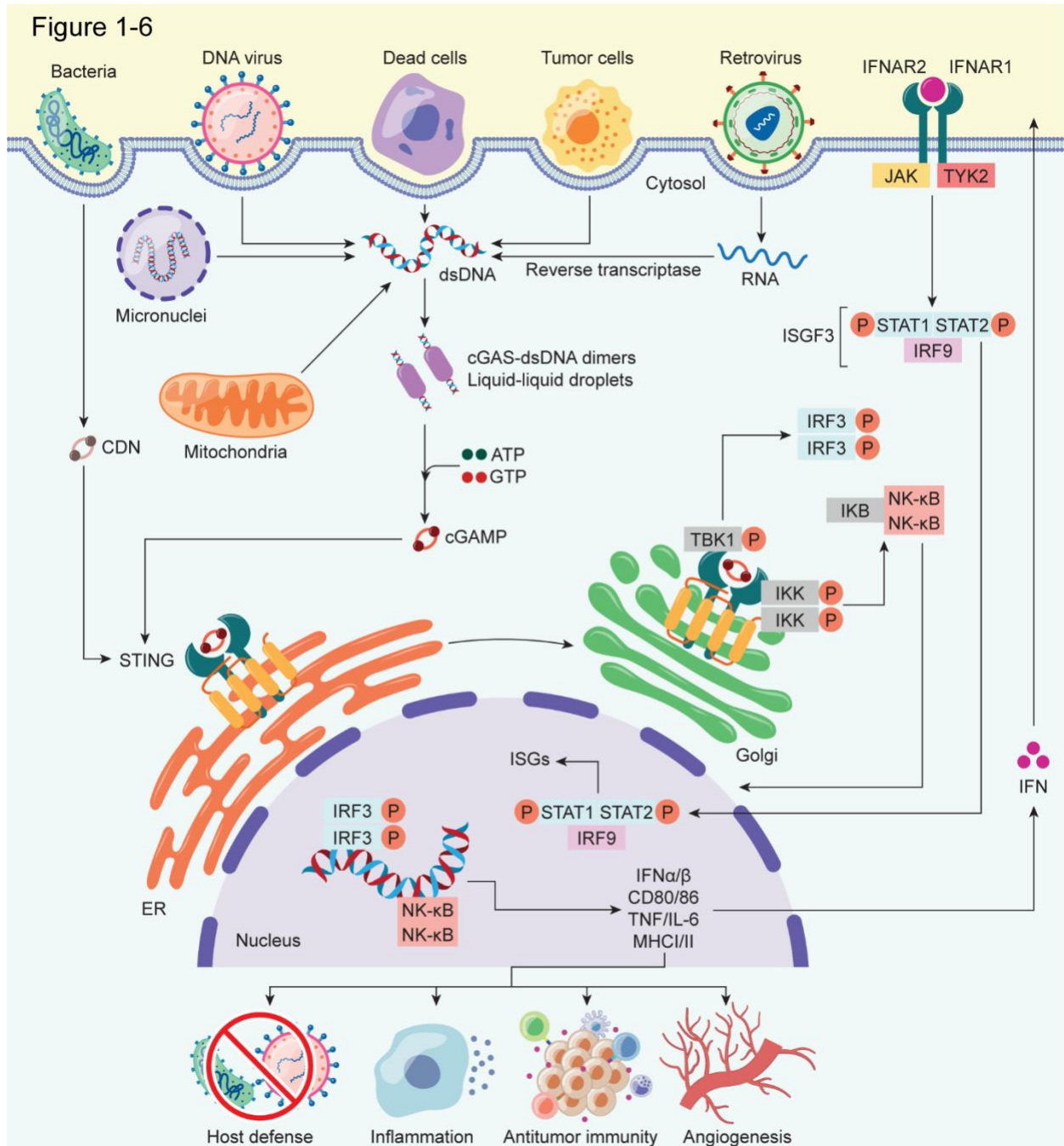


Figure1- 5: TLR signaling pathways and effects

Figure 1-5: Toll-like receptors (TLRs) are located on the cell surface and the intracellular endosomal compartment of innate immune cells (i.e., DCs and macrophages) and nonimmune cells (i.e., fibroblast and epithelial cells). After binding its respective PAMPs and DAMPs, most TLRs signal through MyD88-dependent axes. The only TLR to signal through a MyD88-independent pathway is TLR3. TLR4 can signal through both paths. In the MyD88-dependent signaling cascade, MyD88 binds with IRAK4 and IRAK1. Next, IRAK4 phosphorylates IRAK1 and promotes the recruitment of TRAF6, which serves as a protein complex platform to associate and activate the kinase TAK1. The activation of TAK1 stimulates the IKK complex, comprised of IKK $\alpha$ , IKK $\beta$ , and NEMO (IKK $\gamma$ ), which catalyzes the phosphorylation and subsequent degradation of I $\kappa$ B. After I $\kappa$ B degradation, it liberates transcription factor NF- $\kappa$ B (i.e., p50/p65), allowing NF- $\kappa$ B to translocate from the cytoplasm to the nucleus, which binds to DNA and regulates the transcription of multiple genes. IRF7, another transcription factor, is activated downstream of TLR7, 8, and 9 stimulation. Direct phosphorylation of IRF7 by IRAK1 leads to translocation to the nucleus. The binding of IRF7 to the nucleus induces the transcription of Type I IFN. In the MyD88-independent (TRIF) signaling pathway, TRIF associates with TRAF3 to activate TBK1 and IKKi, resulting in the dimerization and activation of transcription factor IRF3. IRF3 translocates to the nucleus and induces Type I IFN. These transcription factors target various genes involved in processes such as inflammation and angiogenesis that directly or indirectly affect tumor progression. (Note- IFN: interferon; IL: interleukin; TRAF: tumor necrosis factor receptor (TNF-R)-associated factor; IRF: interferon regulatory factor; JNK: c-Jun N-terminal kinase; MAPK: mitogen-activated protein kinase; MyD88, myeloid differentiation primary response 88; NF- $\kappa$ B, nuclear factor  $\kappa$ B; TRIF: TIR-domain-containing adapter-inducing interferon- $\beta$ ; IRAK: Interleukin-1 receptor-associated kinases; TBK1: TANK-binding kinase 1; TIRAP:

The Stimulator of Interferon Genes (STING) receptor signals through a MyD88-TRIF independent pathway and correlates with increased priming of tumor antigen-specific CD8+ cytotoxic T cells (**Fig.1-6**) (308). Our lab has advanced synthetic STING adjuvants - 2'3'-c-di-AM(PS)<sub>2</sub> (Rp, Rp) (ML RR-S2 CDA) – since a) these phosphodiesterase resistant molecules had higher efficacy in preclinical settings (309), b) were shown to activate all known human STING alleles (309), and c) is found to be safe in early phase 1 clinical trials. In this proposal, we aim to assess the TLR and STING adjuvant combinations to test the hypothesis that combinatorial STING and TLR adjuvanted vaccines synergize to increase antitumor response through T cell priming.



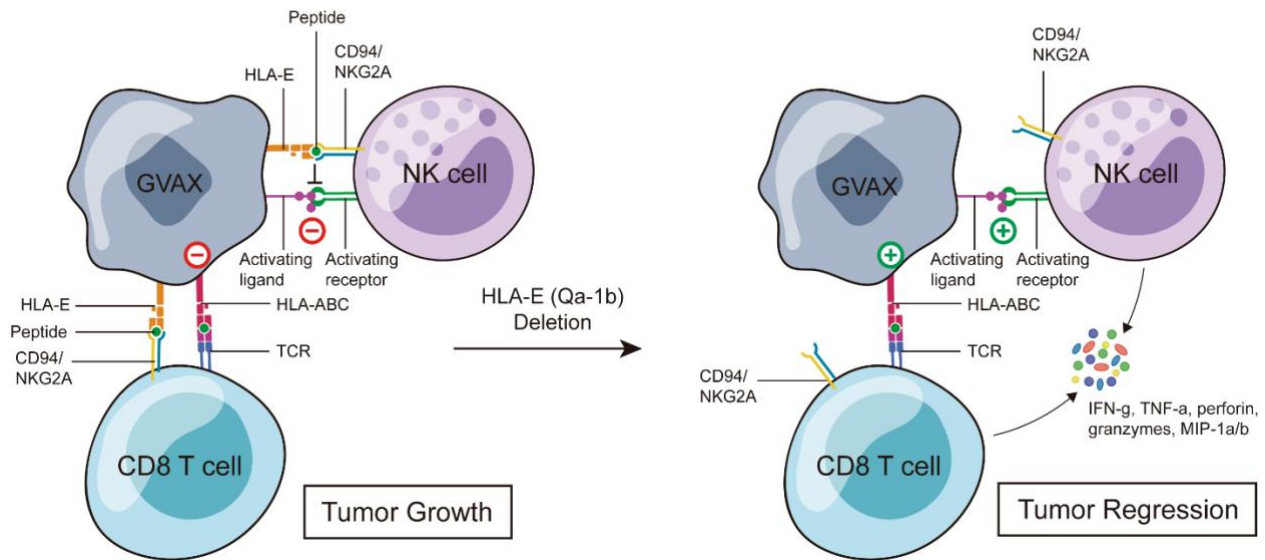
**Figure1- 6: STING signaling and effects**

Figure 1-6: The enzyme cyclic GMP-AMP synthase (cGAS) is an innate immune sensor that identifies various cytoplasmic double-stranded DNA (dsDNA) sources, including viral, bacterial, mitochondrial, and micronuclei. Upon binding dsDNA in a minimal 2:2 complex, cGAS catalyze the production of 2',3'-cyclic GMP-AMP (cGAMP) in the presence of substrates GTP and ATP. Next, the second messenger, cGAMP, binds and activates STING at the endoplasmic reticulum (ER), inducing a higher-order oligomerization to form tetramers and translocation to the Golgi complex. Palmitoylation of cys88 and cys91 on STING at the Golgi leads to recruitment of TANK binding kinase 1 (TBK1). TBK1 transphosphorylates the C-terminal of STING, which leads to the recruitment and activation of the transcription factor IRF3. STING also activates IKK, which catalyzes the phosphorylation and subsequent degradation of I $\kappa$ B. After I $\kappa$ B degradation, it liberates transcription factor NF- $\kappa$ B (i.e., p50/p65). IRF3 and NF- $\kappa$ B translocate to the nucleus, bind to DNA, and regulate the expression of Type I IFN (IFN- $\alpha$  or IFN- $\beta$ ) and NF $\kappa$ B-driven inflammatory genes (i.e., CD80, CD86, IL-12), respectively. Type I IFN can have autocrine and paracrine effects by binding the IFNAR1/2 complex, triggering the phosphorylation of Janus kinase 1 (JAK1) and tyrosine kinase 2 (TYK2). This event leads to recruitment and phosphorylation of transcription 1 and 2 (STAT1 and 2) to form a heterodimer. The STAT1/2 heterodimer associates with IFN-regulatory factor 9 (IRF9) to form the IFN-stimulated gene factor 3 (ISGF3) complex. ISGF3 translocates to the nucleus to induce genes regulated by IFN-stimulated response elements (ISRE), resulting in the expression of several immunoregulatory cytokines, cell death factors, and proteins related to antiviral response. Also, Type I IFNs block the generation of angiogenic factors released by cancer cells and suppress blood vessel proliferation and secretion, which are responsible for chemotaxis and

### **Modification of the tumor antigen source to boost antitumor immunity**

Multiple tumor antigen sources (i.e., peptide, DNA, and RNA) have been utilized in clinical trials but generally failed as a monotherapy. We chose to adopt and modify the whole-cell GVAX vaccine platform, which is irradiated cancer cells genetically modified to secrete granulocyte-macrophage colony-stimulating factor (GM-CSF). Clinically, GVAX is safe and tolerable in multiple types of cancer patients and some cases, led to curable states (310). Hence the translational potential for the GVAX platform is high. Secondly, GVAX presents an unbiased repertoire of tumor antigens that can generate its cognate antitumor T-cell repertoire (311). Multiple studies have shown an increase in antitumor response by blocking or deleting the checkpoint/ligand interactions on the tumor, allowing more cytolytic effector cells to eliminate the tumor. In this proposal, we block or delete checkpoint protein or its ligand on the GVAX vaccine to test the hypothesis that modifying GVAX will enhance immunogenicity and improve the antitumor response. Specifically, we block the recent checkpoint/ligand interaction of HLA-E (Qa1b in mouse) and NKG2a (**Fig.1-7**).

Figure 1-7



**Figure1- 7:** GVAX vaccine with HLA-E (Qa-1b in mice) deletion preclinical hypothesis

Figure 1-7: Without HLA-E (Qa-1b) deleted on whole-cell tumor cell vaccine GVAX, it acts as a coinhibitory ligand to NKG2a expressed on NK and CD8 T cells potentially blocking their activation at the site of vaccination. GVAX alone will lead to minimal to modest tumor response, eventually leading to tumor growth. Deletion of HLA-E will negate the NKG2a interaction, allowing the NK and CD8 T cells to activate and elicit its effector functions, thereby enhancing and prolonging the antitumor response.

## **CHAPTER II: MUSYC DOSING OF ADJUVANTED CANCER VACCINES OPTIMIZES ANTITUMOR RESPONSES**

### **INTRODUCTION**

FDA approval of T cell-dependent immune checkpoint inhibitors (ICI) in multiple tumors has re-engaged translational strategies to increase tumor-specific T cells' frequency, diversity, and/or function (312-314). Consensus evidence supports this rationale since high T cell infiltration in the tumor microenvironment often correlates with clinical response to approved  $\alpha$ PD1 and  $\alpha$ PDL1 blocking antibodies (315, 316). Hence, one promising approach to promote ICI's clinical efficacy is developing therapeutic cancer vaccines that can generate an increased tumor-specific T cell response (309, 317, 318). However, previous clinical trials of cancer vaccines as monotherapies have suggested these early generations of cancer vaccines cause only a modest tumor infiltration of tumor-specific T cells (319-321). While the limited efficacy of cancer vaccines in cancer patients has been attributed to several mechanisms, one limitation of vaccine trials may stem from suboptimal antigen-presenting cell (APC) stimulation and potentially toxic inflammatory side effects of the adjuvants.

Several signaling pathways sense adjuvants for APC stimulation, namely NOD-like receptors (NLRs), RIG-I-like receptors (RLRs), Toll-like receptors (TLRs), and the Stimulator of Interferon Genes (STING) receptor. Adjuvant agonism of these targets leads to the upregulation of costimulatory molecules (i.e., CD80, CD86, and CD40) and major histocompatibility complexes (i.e., MHC I and MHC II) to promote T cell priming

and activation (322-325). In general, single adjuvanted cancer vaccines have failed to produce a sufficient tumor-specific response against cancer, prompting the exploration of adjuvant combinations as a strategy to strengthen antitumor T cell responses (326-329). In addition, preclinical studies from different classes of TLR agonists have shown that their combination could increase the antitumor response compared to the single agents (330-333). However, combining a MyD88-dependent adjuvant with another MyD88-dependent adjuvant (334, 335), or utilizing more than two adjuvants, has led to modest antineoplastic responses (331), making the combinatorial choice imperative for optimizing responses. Altogether, the primary shortcoming of these studies is that they are efficacy-focused without consideration of potency (Table 2-1) and toxicity. Clinically, combining adjuvants without optimization, for instance, using a high dose of both adjuvants, leads to an increase in toxicities (336, 337). In short, these empirical approaches have not adopted a rigorous quantitative definition of the synergy of adjuvants.

Optimal dosing of adjuvants importantly addresses the critical concept of "off-target" and adverse effects in patients. For example, MyD88 and NF- $\kappa$ B signaling in the tumor through TLR stimulation has been shown to have oncogenic potential (338-342). Additionally, adjuvants have been demonstrated to induce the systemic release of TNF, IL-6, IL-1, and MIP1- $\alpha$ , which can mediate cytokine storm and limit clinical combination strategies (334, 343). Therefore, the development of adjuvanted cancer vaccines must minimize some of these "off-target" consequences through appropriate dosing while maximizing T cell tumor infiltration. Towards this goal, we extended our recently

described synergy framework, the Multidimensional Synergy of Combinations (MuSyC), for the adjuvant combination (344-346). MuSyC distinguishes between two types of synergy: synergy of efficacy, which quantifies the maximal effect, and synergy of potency, which measures potency change due to the combination (344-346). Furthermore, the MuSyC framework removes the inherent biases and ambiguities of the two most common drug synergy principles, Loewe's Dose Equivalence Principle (DEP) and the Multiplicative Survival Principle introduced by Bliss (346). The MuSyC algorithm unifies these two principles to make a consensus framework for quantifying drug combination synergy. Therefore, we hypothesized that utilizing the MuSyC algorithm to guide how we combine adjuvants will maximize therapeutic efficacy and minimize the total dose/off-target effects in developing cancer vaccines.

Table 2-1. Key Definitions	
Potency	The amount of drug required to produce an effect. Generally, it is quantified by measuring the $EC_{50}$ , the concentration or dose of drug that causes 50% of maximum effect. The lower the $EC_{50}$ , the more potent the drug.
Efficacy	The maximum effect that a drug can produce regardless of dose. Classically, efficacy is quantified by the maximal effect ( $e_{max}$ ).
Synergistic Potency	Increase in the potency (decrease in $EC_{50}$ ), owing to the presence of another drug.
Synergistic Efficacy	Increase in $e_{max}$ with the combination compared to the most efficacious single agent.

## RESULTS

### The MuSyC algorithm measures the synergy of STING and TLR agonists

To determine the optimal adjuvant combination for activating antigen-presenting cells (APCs), we screened the following major PRR class adjuvants known to activate murine bone-marrow-derived dendritic cells (mBMDC): STING agonist cyclic dinucleotides (CDN), TLR4 agonist monophosphoryl lipid A (MPL-A), TLR7/8 agonist resiquimod (R848), TLR9 agonist CpG oligonucleotide (CpG), NLR agonist tri-DAP (NLL), and RLR agonist 5'ppp-dsRNA (RLL) (323, 325, 347, 348). After identifying saturating doses for CD86 for each adjuvant, we identified CDN as the most efficacious single agent for inducing MHCI, CD86, and TNF (signal 1, signal 2, and signal 3, respectively) on murine bone-marrow-derived dendritic cells (mBMDCs) (**Fig.2-1**). With the saturating dose of CDN, we combined it with the saturating amount of the other adjuvants, which we termed “Max-dose”. At Max-dose for the combinations, CDN significantly enhances all three signals compared to the single agents alone (**Fig.2-2**). However, NLL, RLL, and CpG Max-dose combinations significantly antagonized MHCI, CD40, and TNF than CDN alone (**Fig.2-2**). Only Max-dose combinations of R848 or MPL-A significantly improved at least one of the signals compared to CDN alone (**Fig.2-2**). Therefore, we chose MPL-A or R848 as potential choices to combine with CDN.

Figure 2-1

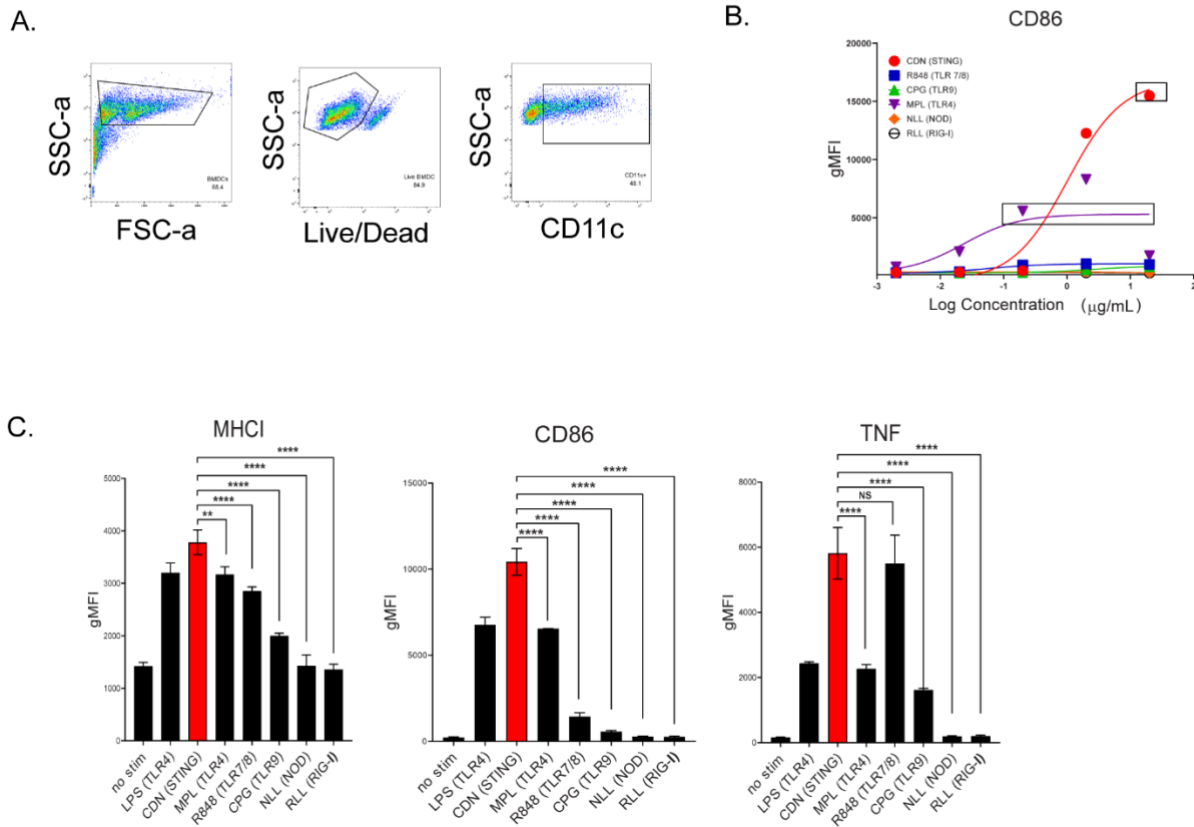


**Figure 2- 1:** STING agonist is the most efficacious adjuvant for stimulating murine dendritic cells

Figure 2-1: **A)** Gating strategy for murine bone-marrow-derived dendritic cells (BMDCs) **B)** Dose-response to identify saturating dose for CD86 signal (geometric mean fluorescence intensity, gMFI) for STING (CDN), TLRs (CpG, MPL-A, and R848), NOD (NLL), and RIG-I (RLL). Saturating doses: CDN (20 $\mu\text{g/mL}$ ), R848 (2 $\mu\text{g/mL}$ ), CpG (20 $\mu\text{g/mL}$ ), MPL-A (2 $\mu\text{g/mL}$ ), NLL (0.02 $\mu\text{g/mL}$ ), and RLL (0.02 $\mu\text{g/mL}$ ). 1 $\mu\text{g/mL}$  is the dose used for LPS. **C)** Expression levels of MHCII, CD86, and TNF at the saturating dose for each adjuvant. All data are given in mean  $\pm$  S.D. of 3 technical replicates. \*P < 0.05, \*\*P < 0.01, \*\*\*P < 0.001, \*\*\*\*P < 0.0001, one-way analysis of variance (ANOVA) for multiple comparisons.

Figure 2-2

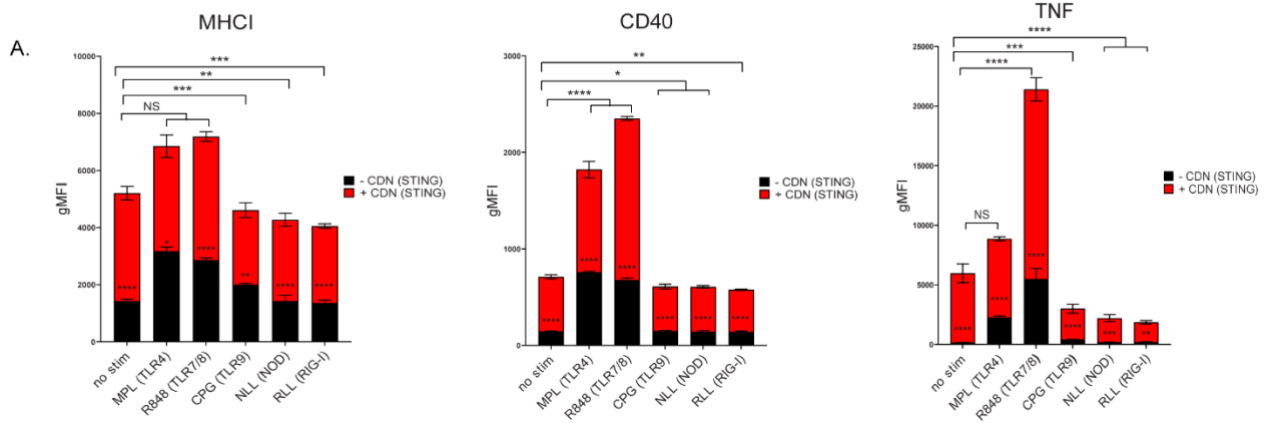


**Figure 2- 2: Both MPL-A and R848 potentiate the stimulatory effects of CDN on DCs**

Figure 2-2: TNF, CD40, and MHC I expression on mouse bone-marrow-derived dendritic cells (mBMDCs) after stimulation with saturating CD86 dose (**Fig.2-1**) of CDN (STING) plus saturating dose of TLRs (CpG, MPL, and R848), NOD (NLL), and RIG-I (RLL) termed the Max-dose. All data are given in mean  $\pm$  S.D. of 3 technical replicates. \*P < 0.05, \*\*P < 0.01, \*\*\*P < 0.001, \*\*\*\*P < 0.0001, one-way analysis of variance (ANOVA) for multiple comparisons (bracket) of STING alone versus the combinations and two-way ANOVA analysis of variance for comparison (non-bracket) of no CDN vs. the addition of CDN.

The STING-TLR titrations using geometric mean fluorescence intensity (gMFI) of CD86, MHCII, CD80 and CD40 signals were analyzed by the Multidimensional Synergy of Combinations (MuSyC) algorithm generates three-dimensional drug synergy diagrams to assess synergistic potency and efficacy (**Table 2-1 and Fig.2-4 A**). The results show no change in the MPL-A and CDN combination for the maximal activation ( $e_{max}$ ) of MHCII, CD40, CD86, and CD80 markers compared to CDN alone, the most efficacious single agent (**Fig.2-3 B-C**). However, CDN increased its potency (left shift in the  $EC_{50}$ )

in the presence of MPL-A for CD40 and CD80, and MPL-A increased its potency in the presence of CDN for MHCII (Fig.2-3 B-C). Therefore, the combination of CDN and MPL-A is considered synergistically potent.

Figure 2-3

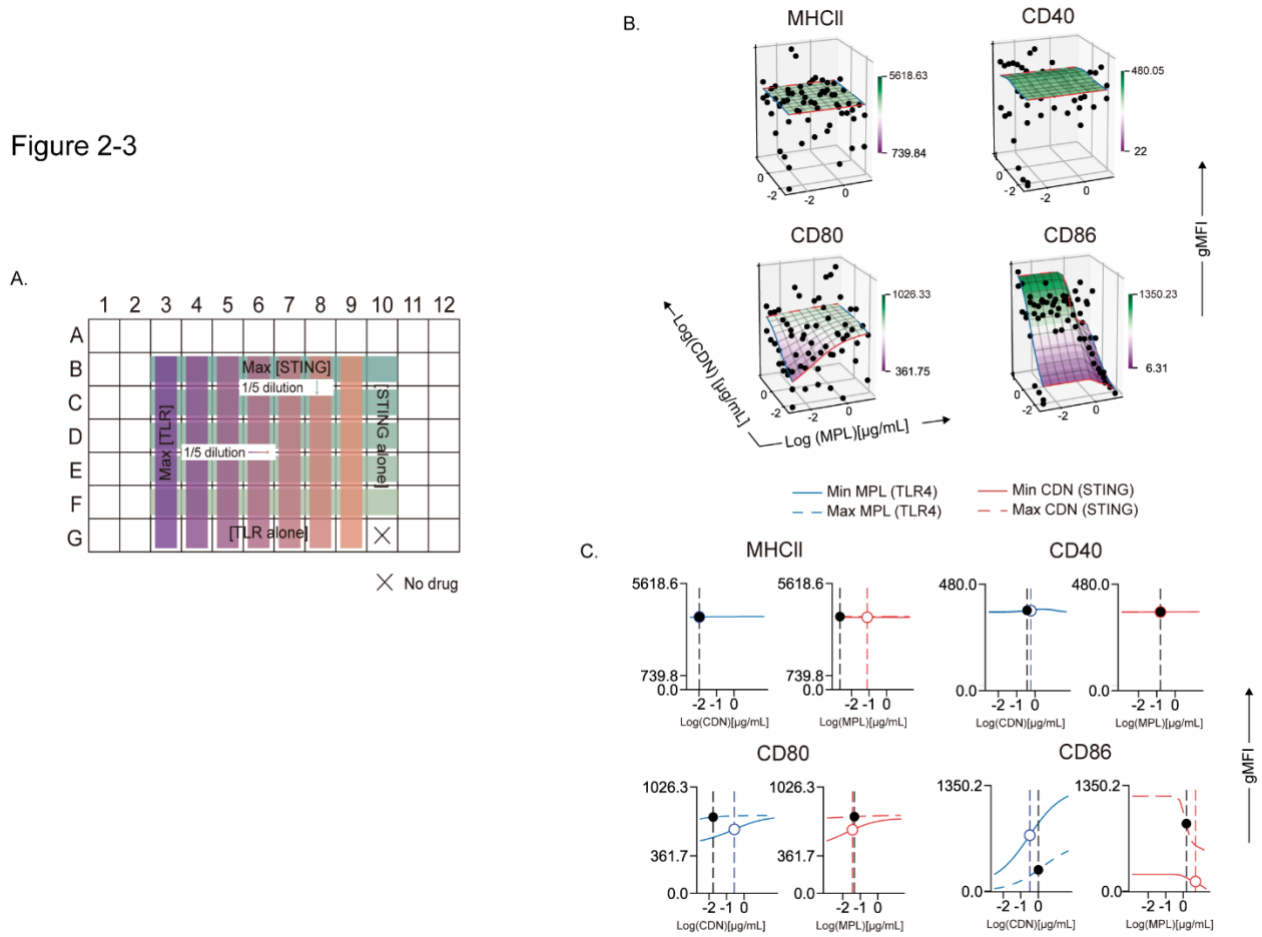


Figure 2- 3: The combination of CDN and MPL-A is synergistically potent

Figure 2-3: **A)** Comprehensive checkerboard plate map for combining STING and TLR agonists. **B)** MuSyC algorithm-generated drug synergy diagrams for STING and TLR4 agonists to activate mBMDCs. The y-axis is the log concentration of CDN (STING), the x-axis is the log concentration of MPL (TLR4), and the z-axis is the geometric mean fluorescence intensity (gMFI) of multiple activation markers. Points are experimentally measured conditions. The surface is the fit to the MuSyC equation, which quantifies the synergistic potency and efficacy. The solid red line is the MPL single-agent dose-response. The solid blue line is CDN single-agent dose-response. The hashed blue line is the max dose of MPL plus increasing amounts of CDN. The hashed red line represents the max dose of CDN plus increasing doses of MPL. **C)** One-dimensional graphs displaying an open circle for the  $EC_{50}$  for the single agents and a solid black circle for the new  $EC_{50}$  in the presence of the combinatorial agent. The vertical hashed lines represent the  $EC_{50}$  of the

In contrast, the R848 and CDN combination increased the  $e_{max}$  compared to CDN alone for MHCII, CD40, and CD80 (**Fig.2-4 B**). Also, R848 increases its potency in the presence of CDN for the same markers (**Fig.2-4 B**). Hence, this combination is synergistically potent and efficacious for mBMDC activation (**Fig.2-4 B**). However, R848 plus CDN, as with the MPL-A combination, antagonized the costimulatory molecule CD86, revealing an antagonistic effect with the combination that may affect the priming of T-cells (**Fig.2-3 B and Fig.2-4 B**). To offset this “antagonistic” effect, we derived a MuSyC synergy dosing strategy (MuSyC-dose) for the CDN and R848 combination, where we use the saturating dose from CDN and one-tenth of the saturating amount of R848 (**Fig.2-4 C**). The MuSyC-dose strategy could potentially

rescue the antagonistic effect on CD86 activation while maintaining a similar  $e_{max}$  for the other markers. Therefore, the MuSyC algorithm can enable the combination dosing strategy that simultaneously maximizes multiple costimulatory molecules' expression while minimizing the amount of adjuvant necessary.

Figure 2-4

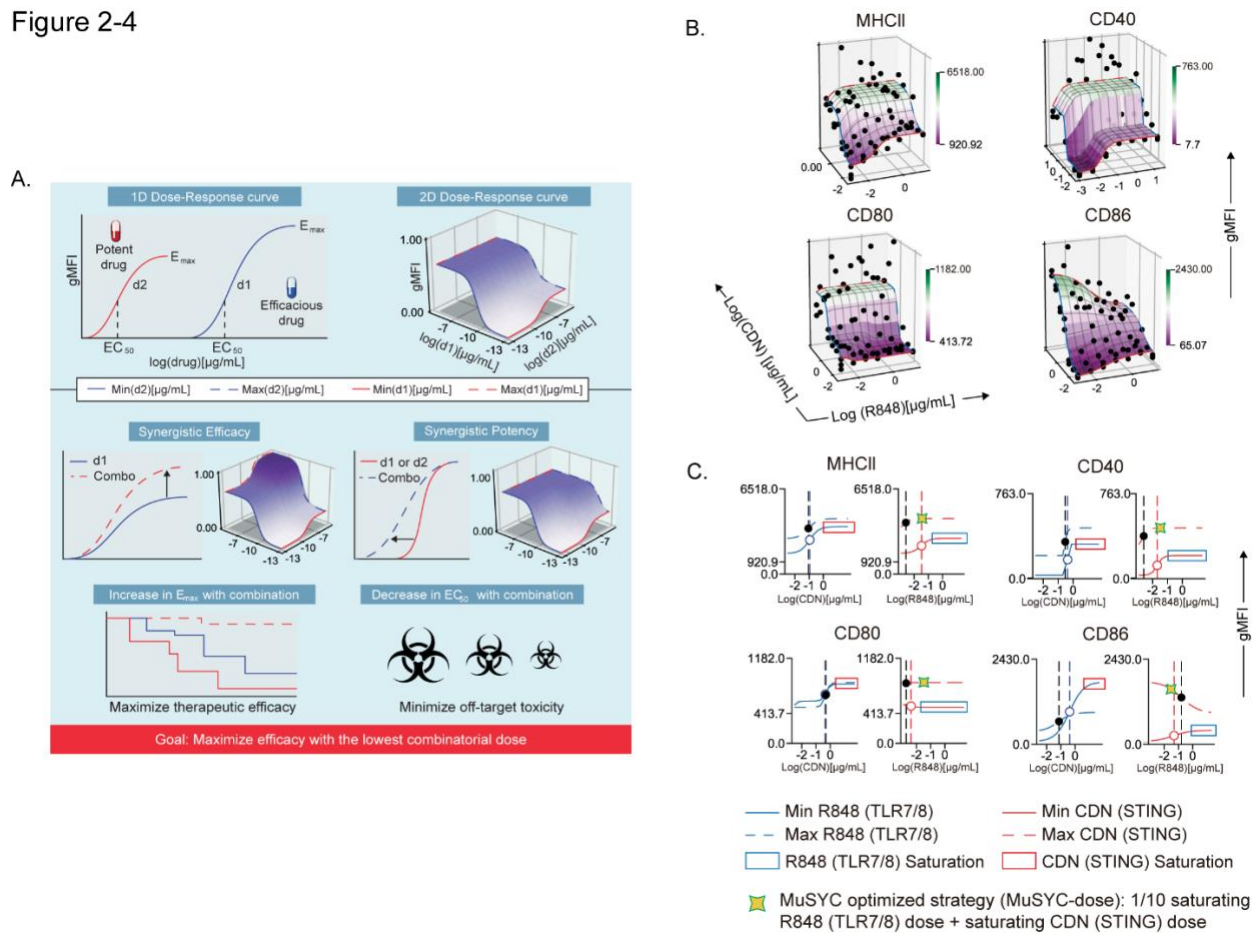


Figure 2- 4: The combination of CDN and R848 is synergistically efficacious and potent

Figure 2-4: **A)** MuSyC algorithm classification scheme. **B)** MuSyC algorithm-generated drug synergy diagrams for STING and TLR7/8 agonists activation of bone marrow-derived dendritic cells (mBMDCs). The y-axis is the log concentration of CDN (STING), the x-axis is the log concentration of R848 (TLR7/8), and the z-axis is the geometric mean fluorescence intensity (gMFI) of multiple activation markers. Points are experimentally measured conditions. The surface is the fit to the MuSyC equation, which quantifies the synergistic potency and efficacy. The solid red line R848 single-agent dose-response. The solid blue line represents CDN single-agent dose-response. The hashed blue line is the max dose of R848 plus increasing amounts of CDN. The hashed red line represents the max dose of CDN plus increasing doses of R848 **C)** One-dimensional graphs displaying an open circle for the  $EC_{50}$  for the single agents and a solid black circle for the new  $EC_{50}$  in the presence of the combinatorial agent. The vertical hashed lines represent the  $EC_{50}$  of the respective curve. Optimization and derivation of the MuSyC-dose for the combination [1/10 saturating

### **The MuSyC-dose can optimize activation for multiple APCs in vitro**

To test and validate that the MuSyC-dose strategy [saturating CDN plus one-tenth saturating R848] maximizes  $e_{\max}$  and counteracts potential antagonistic effects, we utilized the same mBMDC activation model. We first performed dose-response to determine the saturating quantity for CDN and R848 (**Fig.2-5 A**). We found that the Max-dose group had synergistic efficacy, as demonstrated by enhanced average expression of MHCI, MHCII, and CD40 on mBMDCs compared to CDN (STING) alone (**Fig.2-5 B**). The MuSyC-dose maintained or significantly increased that synergistic efficacy at a lower total combinatorial dose, confirming the synergistically efficacious and potent effects of the MuSyC-dose strategy for mBMDCs (**Fig.2-5 B**). We also saw a slight decrease in average expression for Max-dose compared to CDN for CD86 and a rescue effect with MuSyC-dose, which we predicted the MuSyC-dose would counteract (**Fig.2-5 B**). Hence, we can validate the MuSyC-dose without performing the checkerboard method with MuSyC analysis (50 samples) and instead utilize single-agent dose responses with the MuSyC-dose strategy (10 samples).

Next, we wanted to determine if the MuSyC-dose would translate to other types of APCs. Therefore, we established a dose-response for R848 and CDN on murine bone-marrow-derived macrophages (mBMDM) (**Fig.2-6 A**) and human monocytic cell line (THP-1) (**Fig.2-6 B**) and identified the saturating dose for each agent per model. We then compared the Max-dose and MuSyC-dose (CDN-max R848 1/10<sup>th</sup> max) for mBMDM (**Fig.2-5 C**) and human THP-1 cells (**Fig.2-5 D**). We showed that MuSyC dosing potentially enhanced stimulatory effects compared to CDN alone, and similar or

better activation effects relative to the Max-dose combination in THP-1 cells and mBMDMs. This data suggests that the MuSyC-dose strategy developed using mBMDC applies to both mBMDM and human THP-1 cells.

Figure 2-5

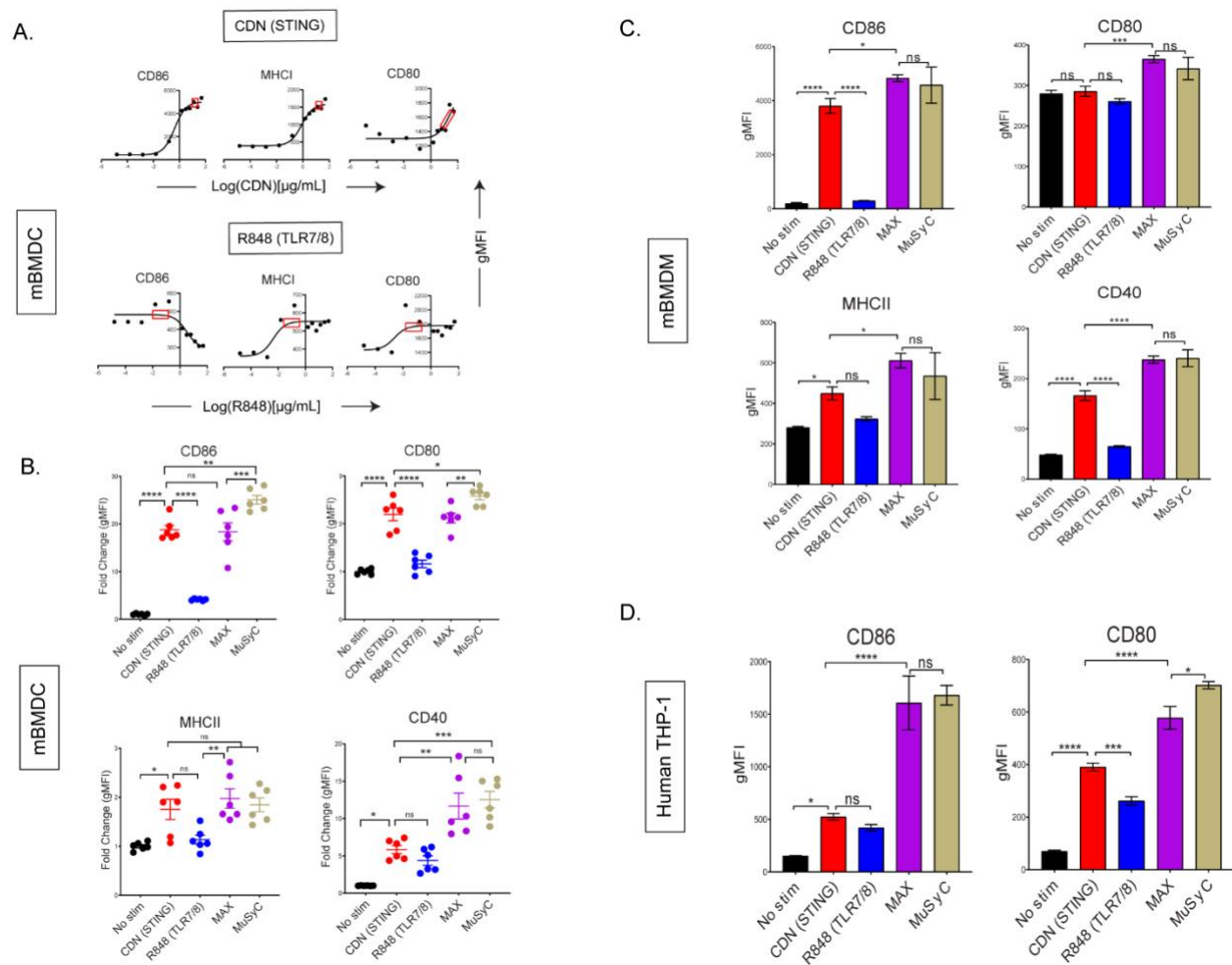
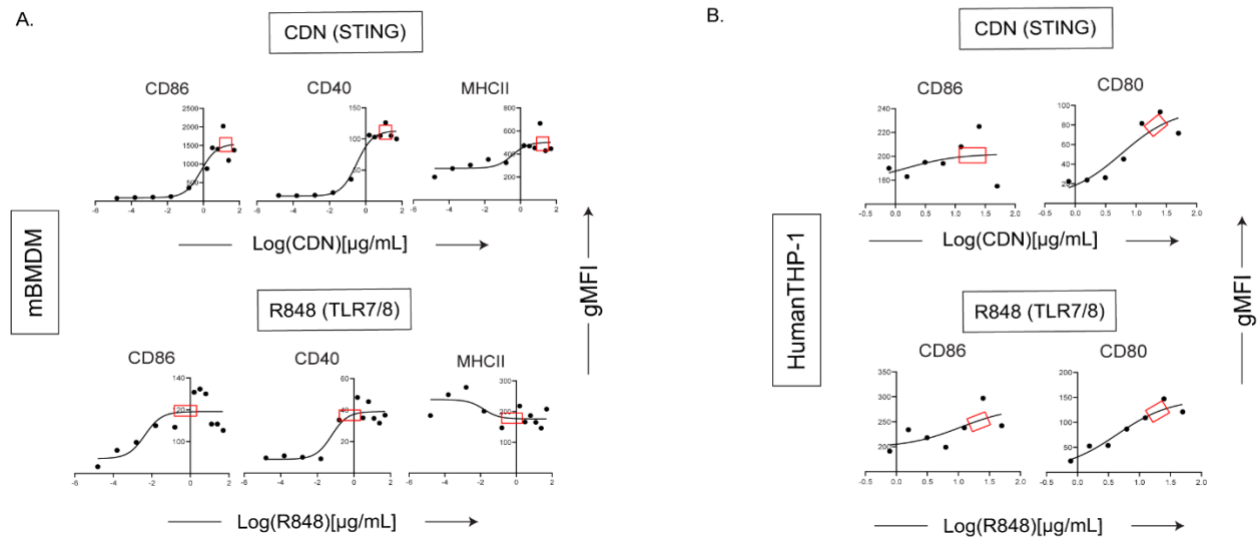


Figure 2- 5: MuSyC-dose can optimize activation for multiple APCs *in vitro*.

Figure 2-5: **A)** Corresponding dose-response curves for CDN (STING) and R848 (TLR7/8) for the activation of mBMDCs with the saturation range for each adjuvant in the red box. 20µg/mL was chosen for CDN and 0.1µg/mL was chosen for R848. **B)** mBMDCs activated with R848, CDN, Max-dose (20µg/mL CDN + 0.1µg/mL R848), and MuSyC-dose (20µg/mL + 0.01µg/mL R848). The gMFI of the activation markers are shown **C)** Murine bone marrow-derived macrophages (mBMDM) activation with the doses selected through the corresponding dose-response (**Fig.2-6 A**). **D)** Human monocytic cell line (TH-P1) activation with appropriate doses (**Fig.2-6 B**). All data are given in mean ± S.D. of 3 technical replicates. \*P < 0.05, \*\*P < 0.01, \*\*\*P < 0.001, \*\*\*\*P < 0.0001, one-way analysis of variance (ANOVA) for multiple comparisons.

Figure 2-6



**Figure 2- 6:** Dose responses for murine bone marrow-derived macrophages (mBMDM) and human monocytic cell line THP-1

Figure 2-6: **A)** Corresponding dose-response curves for CDN (STING) and R848 (TLR7/8) for the activation of mBMDM with saturation range in the red box.  $10\mu\text{g/mL}$  was chosen for CDN, and  $1\mu\text{g/mL}$  was chosen for R848. **B)**  $25\mu\text{g/mL}$  was chosen for CDN, and  $25\mu\text{g/mL}$  was chosen for R848 for the activation of human monocytic cell line THP-1.

### CDN-based vaccines induce optimal T- cell priming *in vivo*

After demonstrating that MuSyC generated combination dose (MuSyC-dose) of CDN and R848 is equivalent/comparable to the Max-dose across multiple APC models *in vitro*, we tested whether the MuSyC-dose also leads to synergistic T cell activation *in vivo* (**Fig.2-7 A**). First, we established the saturating doses of the adjuvants R848 and CDN *in vivo* using the maturation of  $\text{CD11c}^+$   $\text{MHCII}^+$  dendritic cells in the draining

lymph node with CDN and R848 adjuvanted ovalbumin-based peptide vaccines (OVA) (**Fig.2-7 B**). Then, we identified 2µg/mouse for R848 and 20µg/mouse for CDN (**Fig.2-7 B**) as the saturating dose based on the expression of MHCII, CD86, MHCI, and CD80 on draining lymph node DCs.

Comparing MuSyC-dose to Max-dose and CDN resulted in similar DC activation for surrogate markers MHCII, CD86, PDL1, and CD40 (**Fig.2-7 C**). R848 alone, in general, had only a modest impact on the activation of the combinations (**Fig.2-7 C**). Thus, the activation status for the combinations is primarily CDN-driven. Finally, we analyzed the MuSyC dosing strategy to optimize T-cell priming *in vivo*. Adoptive transfer of CFSE-labeled OVA-specific T cells followed by vaccination and five-day incubation determined that CDN and both combinations led to at least 95% of CD45.1 OT-1 T-cells proliferating (not shown), essentially saturating that effect. Furthermore, there was no significant difference between CDN and the combinations in the CD45.1+ CD8+ percentage of the live splenocytes (**Fig.2-7 D**). On the other hand, the R848 adjuvanted peptide vaccine did not increase the CD45.1+CD8+ rate compared to OVA alone. Again, the response of the combinations seems to be CDN-based. Next, we tested the effect of the proliferative response on the antigen-specific killing by vaccinating the mice and intravenously injecting CFSE-high labeled ova-specific splenocytes and CFSE-low nonspecific splenocytes. Sixteen hours post-vaccination, the splenocytes were extracted, and antigen-specific killing was calculated. Yet again, as with the T-cell proliferation and APC activation, there was no significant difference between the CDN adjuvanted peptide vaccine and the combinations in cytolytic activity (**Fig.2-7 E**).

Additionally, the R848-based vaccine did not significantly induce killing compared to the vaccine alone. Collectively, the CDN saturates the T-cell priming effect.

Figure 2-7

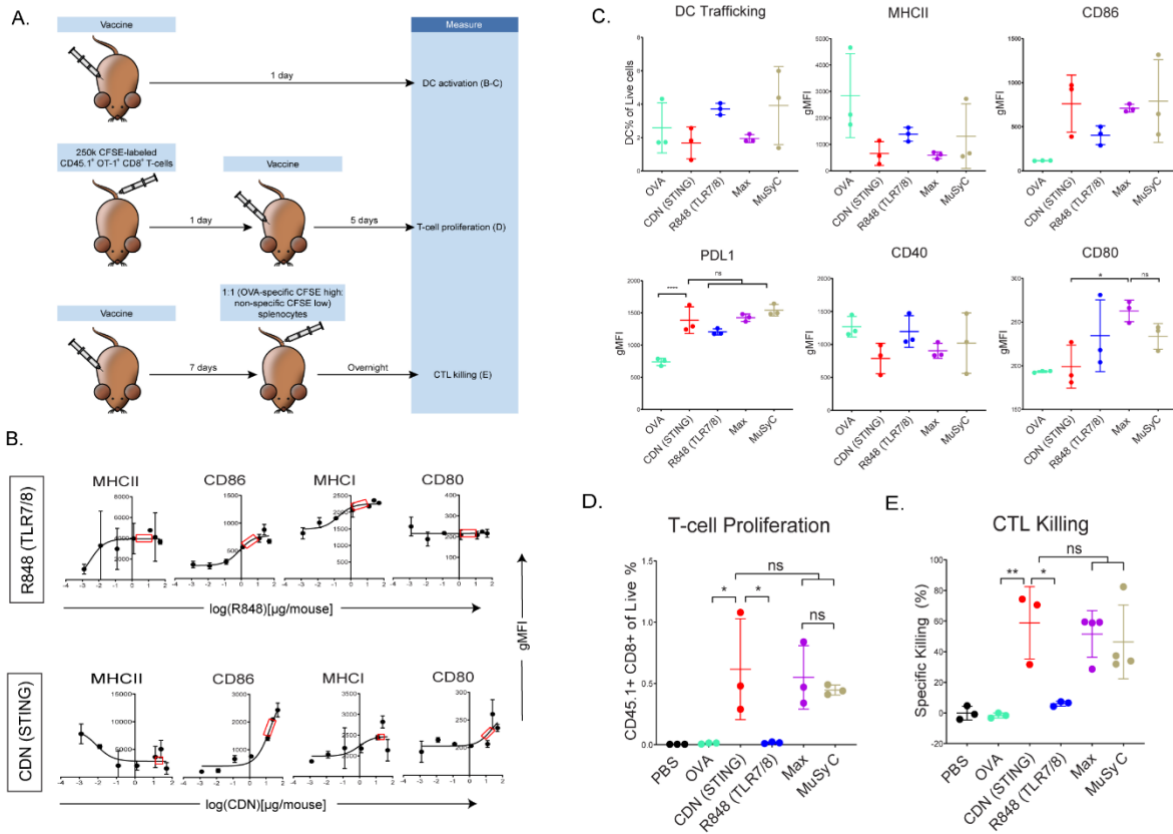


Figure 2-7: CDN-based vaccines induce optimal T-cell priming.

Figure 2-7: **A)** *In vivo* T-cell priming schematic **B)** Female C57BL/6 mice (n = 2) were subcutaneously injected with 20µg of full-length ovalbumin protein vaccine with increasing doses of R848 (TLR7/8) and CDN (STING). CD11c + MHCII+ DCs activation status is shown. Saturating doses of 2ug was chosen for R848 and 20ug for CDN for all remaining *in vivo* experiments. **C)** Female C57BL/6 mice (n = 3) were injected with OVA alone or OVA plus R848, CDN, Max-dose (2ug/mouse R848 + 20ug/mouse CDN), and MuSyC-dose (0.2ug/mouse R848 + 20ug/mouse CDN). The gMFI for activation/inhibitory receptors (CD80, CD86, PDL1, MHCII, and CD40) and the percentage of murine DCs of total live cells in the lymph node were measured. **D)** 250k CFSE-labeled CD45.1+ OT-1 CD8 T-cells were intravenously injected into female C57BL/6 mice (n = 3). Mice were injected with the corresponding vaccine. The percentage of CD45.1+ of the live cells is shown **E)** C57BL/6 mice (n = 3-4) were subcutaneously injected with PBS or the appropriate vaccine. 1:1 CFSE high ova peptide-pulsed: CFSE low splenocytes were intravenously injected. The specific killing percentage was measured with the equation shown [Ratio= Low Peak (nonspecific) High peak (ova-specific). Specific killing = 1- (PBS ratio average) / (Exp. ratio) \* 100]. All data are given in mean ± S.D. \*P< 0.05, \*\*P< 0.01, \*\*\*P < 0.001 , \*\*\*\*P < 0.0001, one-way analysis of variance (ANOVA) for multiple comparisons.

**MuSyC-dose optimizes the antitumor response *in vivo* by modifying the tumor microenvironment.**

Next, we tested the antitumor response of Max-dose and MuSyC-dose *in vivo*. We first compared Max and MuSyC adjuvant doses using a therapeutic vaccine model with B16

melanoma tumor cells expressing the model tumor antigen ovalbumin (B16-mOVA). Mice were injected with B16-mOVA tumors on the flank, and five days later, vaccinated on the opposite flank (**Fig.2-8 A**). The peptide vaccine consisted of endotoxin-free ovalbumin as the antigen source with or without the adjuvants. As expected, vaccination with OVA alone did not reduce tumor volume, indicating adjuvants' critical role in the antitumor immune response to vaccination. The addition of R848 to the OVA vaccine enhanced the antitumor response, but the effect seems to start to diminish twelve days post-treatment. In contrast, the CDN-based vaccine significantly decreases the tumor volume and is more durable than the R848 vaccine (**Fig.2-8 B**). The Max-dose vaccine does not add any additional benefit to the CDN vaccine. However, utilizing one-tenth of R848, the MuSyC-dose, significantly reduced the tumor volume than the other groups, including Max-dose and CDN alone vaccines (**Fig.2-8 B**). This tumor reduction trended with the tumor weights, but the MuSyC-dose tumor weight was not significant compared to Max-dose and CDN (**Fig.2-8 B**).

We also adopted the cell-based GVAX vaccine platform, irradiated cancer cells genetically modified to secrete granulocyte-macrophage colony-stimulating factor (GM-CSF) (15). We determined the antitumor effects of MuSyC-dose versus Max-dose adjuvanted GVAX using two murine tumor models, B16-mOVA melanoma and the head and neck tumor MOC1. In both cases, MuSyC-dose or Max-dose significantly lowers the tumor volume compared to PBS or GVAX alone (**Fig.2-8 C**). However, there was no significant difference in the Max-dose and the MuSyC-dose responses (**Fig.2-8 C**). Therefore, similar to our *in vitro* findings, utilizing a lower total dose of combinatorial

R848 plus CDN (MuSyC-dose) either has better or similar reactions to Max-dose, validating the MuSyC algorithm.

Next, we wanted to identify immune cell types involved in the antitumor response. Therefore, we utilized the ovalbumin-based peptide vaccine with the B16 m-OVA tumor cell melanoma model. Twenty-one days post tumor inoculation, tumors were extracted and immunophenotyped through flow cytometric analysis. We first examined the makeup of the CD45+ immune cell infiltrate, including CD8+ T-cells, CD4+ T-cells, natural killer (NK) cells, myeloid-derived suppressors cells (MDSCs), DCs, and macrophages (MACs) (**Fig.2-9 A**). Results indicate various measured immune cell populations induced by vaccine alone, including approximately 30% of total MDSCs (**Fig.2-8 D**). In addition, the R848 vaccine reduced the MDSC percentage of CD45+ by roughly half and doubled the CD8+ T-cells compared to the vaccine alone (**Fig.2-8 D**). CDN vaccine further decreased the rate of MDSCs and increased the CD8+ T-cell, NK cell, and CD4+ T-cell percentages compared to the R848 vaccine alone (**Fig.2-8 D**). Interestingly, the MuSyC-dose and Max-dose groups had over fifty-five percent macrophages, potentially meaning that the efficacious antitumor response was myeloid-derived (**Fig.2-8 D**). However, there are no significant differences in the percent of CD45+ immune populations between CDN, Max-dose, and MuSyC-dose vaccines (**Fig.2-8 D**).

Finally, we measured the percent of total live for the immune infiltrate. The vaccine alone treatment group led to an average of 2% of CD45+ immune cells in the tumor

**(Fig.2-8 E).** R848 adjuvanted vaccine had no impact on the infiltration of total CD45+ infiltrate **(Fig.2-8 E)**. However, the R848-based vaccine decreased the average total MDSC penetration compared to the vaccine alone, which is a potential mechanism by which this treatment induced an antitumor response. Both CDN and Max-dose vaccines increased the average rate of CD45+ in the tumor by more than 2.5 times compared to R848 or vaccine alone **(Fig.2-8 E)**. Moreover, although not significantly, both groups enhanced the percentage of NK cells, CD8 T-cells, CD4 T-cells, and CD68+ MACs and decreased total MDSCs. The CD8+ T-cells, specifically, have significantly higher CD69 and PD-1 making them more activated in CDN and Max-dose groups than the R848 and vaccine-only groups.

Interestingly, the MuSyC-dose treatment group had the highest average percentage of CD45+ immune cells in the tumor at approximately 12%, significantly higher than R848 and vaccine alone and roughly two times higher than CDN and Max-dose treatment groups **(Fig.2-8 E)**. These higher CD45+ immune infiltrates induced by the MuSyC-dose treatment led to an enhanced percentage of CD8+ T-cells, CD4+ T-cells, NK cells, and CD68+ MACs in the tumor compared to the other groups **(Fig.2-8 E)**. Of those CD68+ MACs, the ratio of M1:M2 MACs was approximately 4:1 with the MuSyC-dose vaccine, which is significantly higher than the vaccine alone **(Fig.2-8 F)**. Also, MuSyC-dose, as with the CDN and Max-dose, had significantly higher activated CD8 T-cells and lower total MDSC infiltrate to R848 and vaccine-only treatment groups **(Fig.2-8 E)**. Altogether, using MuSyC to guide combination dosing rationally, we achieved a tumor

burden reduction that either outperforms or is similar to naively combining both drugs at the saturating dose.

Figure 2-8

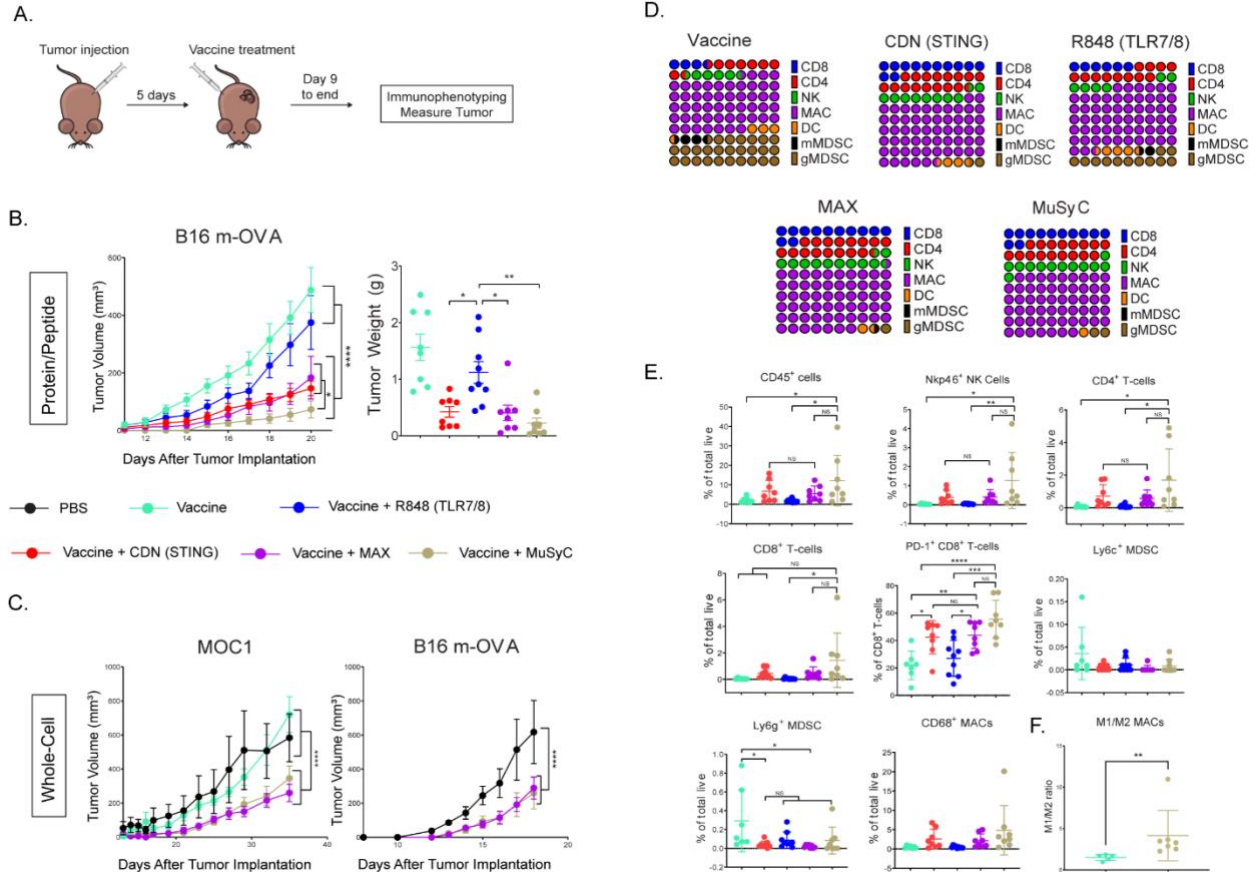


**Figure 2- 8: MuSyC dosing optimizes the antitumor response *in vivo* through modulating the tumor microenvironment.**

Figure 2-8: **A)** General vaccination strategy for tumor models **B)**  $10^5$  B16 m-OVA tumor cells were subcutaneously injected on one flank of C57BL/6 mice (n=10-11). Mice were then subcutaneously injected with 20 $\mu$ g of full-length ovalbumin protein vaccine alone, 20 $\mu$ g vaccine administered with 2 $\mu$ g/ mouse R848 (TLR7/8), 20 $\mu$ g/mouse CDN (STING), Max-dose (2 $\mu$ g/mouse R848 + 20 $\mu$ g/mouse CDN), or MuSyC-dose (0.2 $\mu$ g/mouse R848 + 20 $\mu$ g/mouse CDN) in the opposite flank. B16 m-OVA tumor curve and final day tumor weights are shown. **C)**  $10^5$  B16 m-OVA and  $2 \times 10^6$  MOC1 were subcutaneously injected in one flank C57BL/6 mice (n=8-12). Mice were subcutaneously injected with PBS,  $10^6$  whole-cell vaccine GVAX (B16 m-OVA or MOC1-derived GVAX), and GVAX administered with Max-dose and MuSyC-dose. B16 and MOC1 tumor curves are shown. **D)** Percentage of CD45 for the following cell types are shown for B16-mOVA peptide vaccination model: NK cells (CD11b-Nkp46+), CD8+ T-cells (CD11b-Nkp46-CD4-CD8+), CD4+T-cells (CD11b-Nkp46-CD8-CD4+), gMDSC (CD11b+MHCII-CD68-CD11c-Ly6G+), mMDSC(CD11b+MHCII-CD68-CD11c-Ly6C+), DC (CD68-CD11c+MHCII+), and MACs (CD11c-CD68+). **E)** Percentage of total live of different cell types that include CD45+ immune cells, NK cells, CD4+ T-cells, CD8+ T-cells, PD-1+ CD8+ T-cells, CD69+ CD8+ T-cells, mMDSC, gMDSC, DCs, and MACs. **F)** M1(CD206-)/M2(CD206+) ratio of CD68+ MACs. MOC1 whole-cell and B16 m-OVA peptide models are given in mean  $\pm$  SEM with two independent experiments. All other data are given in mean  $\pm$  S.D. of biological replicates. \*P < 0.05, \*\*P < 0.01, \*\*\*P < 0.001, \*\*\*\*P < 0.0001, one-way or two-way analysis of variance (ANOVA) for multiple comparisons.

Figure 2-9

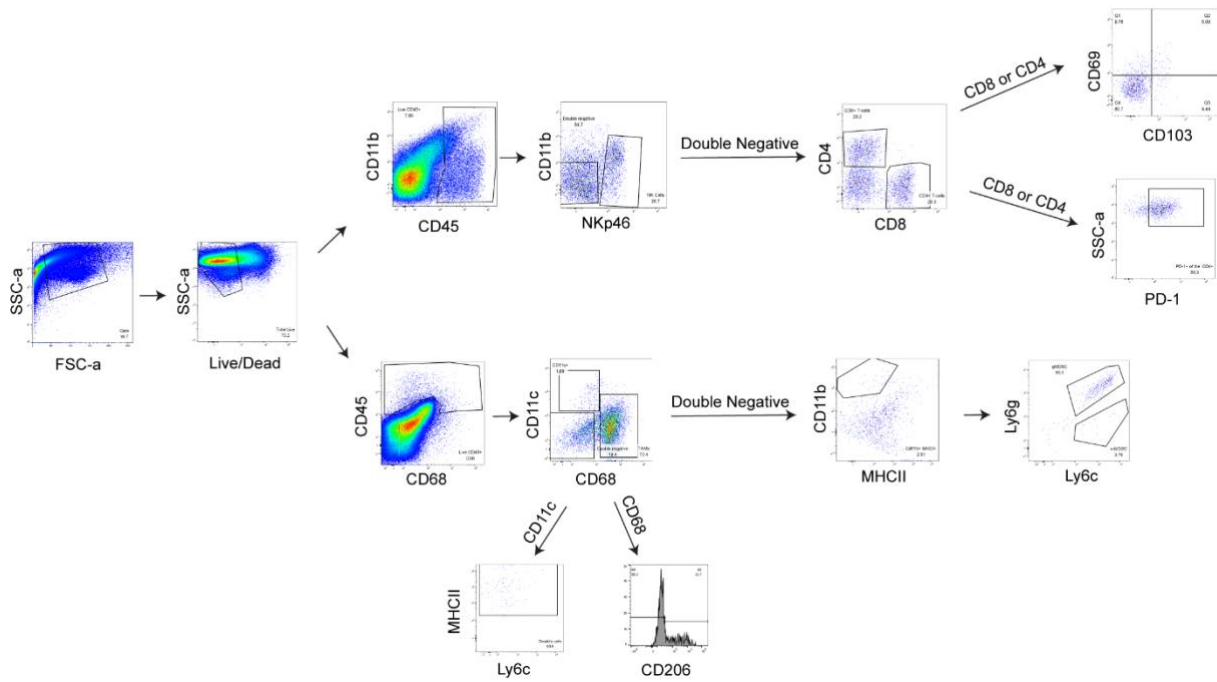


Figure 2- 9: Gating for tumor immunophenotyping

**The MuSyC-dose vaccine induces no additional weight loss and decreases the plasma concentration of IL-6 compared to the CDN vaccine**

A vital component of the MuSyC algorithm is to reduce “off-target” effects through synergistically potent combinations. Therefore, we measured mouse weight and plasma cytokine levels to test potential adjuvanted vaccine-induced toxicities (**Fig.2-10 A**). To measure vaccine-induced weight changes, mice were weighed for their initial weight (100%) and subsequently injected with PBS or the appropriate vaccine. Twenty-four hours post-injection, all adjuvanted vaccine mouse groups significantly lost weight compared to the vaccine alone (**Fig.2-10 B**). Also, the weight loss was the least

significant in the MuSyC-dose group compared to the vaccine alone (**Fig.2-10 B**). The MuSyC-dose vaccinated mice recovered more significantly than CDN and Max-dose groups than the R848 vaccine forty-eight hours post-injection. However, MuSyC-dose does not significantly affect weight loss compared to CDN or Max-dose vaccines for the twenty-four and forty-eight hour timepoints. Interestingly, R848 single-agent vaccines induced persistent weight loss (**Fig.2-10 B**). Moreover, CDN ablates the combinations' R848-induced ongoing weight loss effects, showing beneficial CDN-driven results. Overall, the combinations have no significant weight changes compared to CDN alone, showing no additional potential toxic effects.

Next, we evaluated plasma cytokine levels generated by adjuvanted vaccine treatment six hours post-vaccination. The results show that R848 adjuvanted vaccine does not significantly change plasma cytokine levels compared to PBS or vaccine alone (**Fig.2-10 C**). Compared to PBS, vaccine alone and the R848 vaccine, the CDN vaccine significantly increased IL-6, IL-27, and MCP-1 (CCL2). IL-6 is considerably lower in the MuSyC-dose treatment group than in the CDN group (**Fig.2-10 C**). Strikingly, Max-dose or MuSyC-dose vaccines do not significantly affect the remaining cytokines to the CDN treatment. Therefore, the Max-dose or MuSyC-dose does not potentiate weight loss or plasma cytokines compared to CDN alone, unlike the common clinical trend where Max-dose combinations increase toxicities.

Figure 2-10

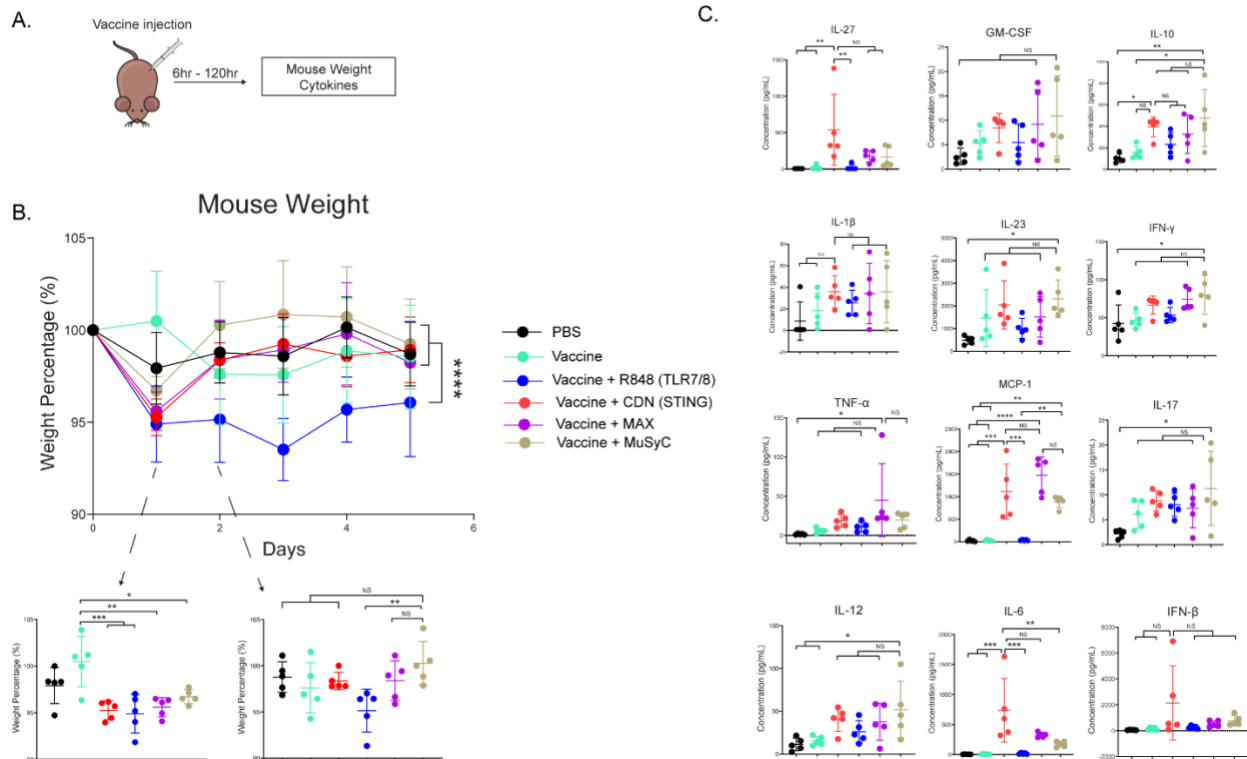


**Figure 2-10:** The MuSyC-dose vaccine induces no additional weight loss and decreases the plasma concentration of IL-6 compared to the CDN vaccine

Figure 2-10: **A)** Vaccination schematic for mouse weight and cytokines **B)** C57BL/6 mice (n = 5) were weighed initially and then were subcutaneously injected with PBS, 20 $\mu$ g of full-length ovalbumin protein vaccine alone, 20 $\mu$ g vaccine administered with 2 $\mu$ g/ mouse R848 (TLR7/8), 20 $\mu$ g/mouse CDN (STING), Max-dose (2 $\mu$ g/mouse R848 + 20 $\mu$ g/mouse CDN), or MuSyC-dose (0.2 $\mu$ g/mouse R848 + 20 $\mu$ g/mouse CDN) in one flank. Mouse weight was measured daily. **C)** C57BL/6 mice (n = 5) were subcutaneously injected with the appropriate treatment. Six hours post-injection, mouse plasma was collected and measured for cytokines. \*P < 0.05, \*\*P < 0.01, \*\*\*P < 0.001, \*\*\*\*P < 0.0001, one-way or two-way analysis of variance (ANOVA) for multiple comparisons.

## DISCUSSION:

Here we extended the MuSyC algorithm, previously used to classify targeted chemotherapeutic drug combinations, to guide dose selection when combining immune-activating agents. Our approach optimizes the adjuvant combinations to maximize efficacy and minimize total dose for *in vitro* and *in vivo* applications. The MuSyC algorithm classified the combination of CDN and R848 as synergistically efficacious and potent for APC activation. We then rationally calculated an optimal dose, termed the MuSyC-dose, by multiparametric optimization of immune activation across a matrix of dose combinations. Future work includes defining a Pareto front enabling the optimization of dosing selection algorithmically rather than heuristically; for example, by combining our approach with system biology models of the immune dynamics. This would allow optimizing combinatorial doses for CDN and TLR mixtures. Regardless, our derivation of the MuSyC-dose for the CDN and R848 induced similar or better APC activation effects compared to Max-dose *in vitro* for multiple models.

To the best of our knowledge, we are the first to utilize an algorithm *in vitro* to derive a synergy dosing strategy for immune-activating agents for *in vivo* experimentation. However, in the present study, our *in vitro* APC activation data did not recapitulate the APC activation effects *in vivo* for Max-dose or MuSyC-dose because of CDN stimulation's overpowering impact leading to the saturating effects on the clonal expansion of cytotoxic T-cells. Strikingly, consistent with previous studies, the “free” R848-adjuvanted peptide vaccine did not lead to or provide any additional benefit to T-cell priming for the combinations (322, 349, 350). Multiple approaches to improve the

T-cell responses of R848, CDN, or other TLR-based vaccines have been reported, which include the following: utilizing higher doses to allow the agent to remain in the body longer (351-353), formulating with emulsion agents to generate a slow-release “depot effect” (354, 355), and encapsulating with nanoparticles to improve delivery (349, 350, 356). Nevertheless, our present work and other studies have shown that R848 and CDN induce myeloid-based mechanisms, i.e., reduction of MDSCs (357, 358), to reduce tumor burden. Hence, APC activation and T-cell priming should not be the final determining factor on which adjuvant combinations will be successful at therapeutically curing tumors as CDN, MuSyC-dose, and MAX-dose had similar T-cell priming effects. Still, the MuSyC-dose vaccine increased the antitumor responses compared to CDN alone.

This disconnect emphasizes the challenges in translating between *in vitro* and *in vivo* dosing strategies. As stated earlier, we predicted the synergistic MuSyC-dose for *in vitro* APC activation would be similar for APC activation *in vivo* and would lead to synergistic T-cell priming and antitumor response. However, the MuSyC-dose only led to synergistic effects on the antineoplastic response, similar to when TLR agonist and GVAX are combined (359). Thus, tumor models are the most accurate way to gauge how a combination will work. For that reason, one could argue we should bypass the *in vitro* work, *in vivo* APC activation, and T-cell priming assays and perform tumor models with MuSyC analysis. The two apparent flaws to this approach are time (tumor processing and immunophenotyping) and cost (approximately seventy-five mice per tumor model and combination). Moreover, the MuSyC analysis and optimization

strategy would be more complex due to the numerous parameters that would need to be included, such as final day tumor volume, T-cell infiltration, and MDSC percentage. Therefore, we currently believe utilizing *in vitro* APC activation with MuSyC analysis/optimization and translating that to *in vivo* is a sufficient and cost-effective approach for combining adjuvants, as demonstrated with the *in vitro* derived MuSyC-dose leading to a synergistic decrease in tumor volume and modulation of the tumor microenvironment.

Clinically, the importance of therapeutic cancer vaccines manipulating the host-tumor interaction has increasingly become evident for inducing clinical responses, considering that many tumors have immunosuppressive microenvironments (360-362). Both R848 and CDN have been used in clinical trials either as a single agent intratumoral/topical treatment (363, 364) or as an adjuvant for vaccine formulations (365), but the combination has yet to be studied. Generally, CDN and R848 treatments are well tolerated clinically, and we show that the combination possibly will not potentiate the side effects. Clinical trials have utilized combinatorial adjuvants for cancer treatments and are identifying methods to optimize the combinations. Here we utilized the MuSyC algorithm to generate a ratio for the CDN + R848 as a strategy to optimize APC activation for T cell priming. Although we have data showing this ratio works for human monocytes, dosing strategies will have to be identified in non-human primates for clinical trials. Here, we provide a proof-of-concept by which one can identify logical combinations and optimization methods for those future trials.

The present study treated tumor-bearing mice with R848 and CDN-based vaccine treatments and performed immunophenotyping on the tumors sixteen days post-treatment. Specifically, the MuSyC-dose adjuvanted vaccines optimized the antitumor response and induced novel changes to the tumor microenvironment. Moreover, the MuSyC-dose vaccine significantly increased cytotoxic T-cells in the tumor, and correlations have shown that increased CD8+ infiltrate is associated with a better response to anti-PD-1 therapy (316). The boost in CD8 T-cells and enhanced PD-1 expression make MuSyC-dose adjuvanted cancer vaccines a good candidate for combination with checkpoint blockade.

In addition to the increase in tumor-infiltrating lymphocytes, the MuSyC-dose vaccine CD45+ population contained a high percentage of macrophages, suggesting a myeloid-based mechanism for the antitumor response. Furthermore, CDN and R848 without antigen have been shown to cause an antineoplastic reaction, meaning responses in these studies were not due to the priming of antigen-specific T-cells (40-43). Overall, we believe MuSyC-dose-based vaccines modulate the tumor microenvironment to optimize tumor response. In conclusion, our work questions the long-standing assumption regarding the superiority of using the maximum permissible concentrations when combining immunoadjuvants. Instead, by measuring multiple markers of immune activation, our work detailed a more nuanced view of adjuvant synergy, paving the way for a more rigorous approach to deriving dosing strategies for vaccine adjuvants.

## **MATERIALS AND METHODS**

### **Mice**

Female C57BL/6 [strain #: 000664], female and male C57BL/6-Tg(TcraTcrb)1100Mjb/J (OT-1) [strain #: 003831], and female and male B6.SJL-Ptprca Pepcb/BoyJ (CD45.1) [strain #: 002014] mice were purchased from The Jackson Laboratory. OT-1 x CD45.1 and all other mice were housed according to the Vanderbilt University Medical Center Animal Care and Use Committee rules. All animal experiments were reviewed and approved by the Institutional Animal Care and Use Committee at Vanderbilt University Medical Center (M1900004-00). According to NIH guidelines, the Animal Welfare Act, and US Federal law, all experiments were performed.

### **Cell lines**

B16 m-OVA melanoma, Mouse Oral Squamous Cell Carcinoma (MOC1), B78H1-GM-CSF and human monocytic THP-1 were grown in complete RPMI (cRPMI), which consisted of RPMI supplemented with 10% heat-inactivated Fetal Bovine Serum (FBS), 5% Penicillin-Streptomycin, 5% HEPES, 5% GlutaMAX, and 0.5%  $\beta$ -Mercaptoethanol.

### **Adjuvants**

All adjuvants were purchased from Invivogen. These adjuvants include the following: TLR4 agonist Lipopolysaccharide from *Escherichia coli* 055:B5 (LPS) [catalog #: tlrl-pb5lps], STING agonist Bisphosphorothioate analog of 2'3'-c-di-AMP (CDN) [catalog #: tlrl-nacda2r], Vaccigrade STING agonist 2'3'-c-diAM(PS)2(Rp,Rp) endotoxin-free (CDN) [catalog #: vac-nacda2r], TLR7/8 agonist Resiquimod R848 [catalog #: tlrl-r848-5],

Vaccigrade TLR7/8 agonist Resiquimod (R848) [catalog #: vac-r848], TLR4 agonist Monophosphoryl Lipid A from Salmonella minnesota R595 (MPL-A) [catalog #: tlrl-mpla], TLR9 agonist Stimulatory CpG ODN, Class C, Human / mouse (CpG) [catalog #: tlrl-m362-1], Rig-like agonist 5' triphosphate double stranded RNA (RLL) [catalog #: tlrl-3prna-100], and NOD1 agonist L-Ala-gamma-D-Glu-mDAP (NLL) [catalog #: tlrl-tdap].

### **Antigens**

Endofit Ovalbumin (OVA) [catalog #: vac-pova] was purchased from Invivogen. GVAX is a lethally irradiated (100Gy) tumor cell (MOC1 or B16 m-OVA), and B7H8, a GM-CSF secreting B16 melanoma cell line.

### **Vaccine formulations**

GVAX was formulated from irradiated  $10^6$  B16 m-OVA or MOC1 tumor lines with  $10^5$  B7H8. Each peptide vaccine contained 20 $\mu$ g of endotoxin-free ovalbumin (OVA). Stimulator of interferon genes (STING) ligand, cyclic dinucleotides (CDN), formulations consisted of 0.0012-50 $\mu$ g of ML-RR-S2-CDA. Resiquimod (R848), a TLR7/8 adjuvant, based formulations are composed of 0.0012 to 50 $\mu$ g of R848.

### **Antibodies and flow cytometry**

The anti-mouse antibodies specific for FITC CD11c (clone HL3) [catalog #: 553801] , BV650 CD80 (clone 16-10A1) [catalog #: 564158], APC CD86 (clone GL1) [catalog #: 558703], BV786 CD8a (clone 53-6.7) [catalog #: 563332], BV421 MHC I (clone AF6-88.5), BV650 TNF (clone MP6-XT22) [catalog #: 563943], BV786 MHC II (clone

M5/114.15.2 [catalog #: 557000], PE-594 F4/80 (clone T45-2342) [catalog #: 565613], PE CD40 (clone 3/23) [catalog #: 553791], PE-594 CD80 (clone 16-10A1) [catalog #: 562504], BV786 CD11c (clone HL3) [catalog #: 563735], BV786 CD45 (clone 30-F11) [catalog #: 564225], PE CD11c (clone HL3) [catalog #: 553802], BV786 CD4 (clone GK1.5) [catalog #: 563331], BB515 CD45 (clone 30-F11) [catalog #: 564590], and PE CD8 (clone 53-6.7) [catalog #: 553032] were purchased from BD Bioscience. Anti-human antibodies specific for BV786 CD80 (clone L307.4) [catalog #: 564159] and APC CD86 (clone 2331 (FUN-1) [catalog #: 555660] were purchased from BD Biosciences. The anti-mouse antibodies specific for PE-594 CD40 (clone 3/23) [catalog #: 124630], FITC MHC I (clone 28-8-6) [catalog #: 114606], BV605 PD-L1 (clone 10F.9G2) [catalog #: 124321], BV421 MHC II (clone M5/114.15.2) [catalog #: 107632], Alexa Fluor 700 CD11b (clone M1/70) [catalog #: 101222], Zombie aqua live/dead BV510 [catalog #: 423102], BV421 Ly6c (clone HK1.4) [catalog #: 128032], BV605 Ly6g (clone 1A8) [catalog #: 127639], Alexa Fluor 488 CD45 (clone FA-11) [catalog #: 137012], APC MCH II (clone M5/114.15.2) [catalog #: 107614], BV421 CD69 (clone H1.2F3) [catalog #: 562920], BV605 CD103 (clone 2E7) [catalog #: 121433], APC Nkp46 (clone 29A1.4) [catalog #: 137608], APC CD45.1 (clone A20) [catalog #: 110714], and PE-594 PD-1 (clone 29F.1A12) [catalog #: 135228] were purchased from Biolegend. Flow cytometry was performed using BD FACS Celesta Flow Cytometer. Analysis was done using FlowJo software (FlowJo LLC).

## **Murine bone-marrow-derived dendritic Cell (mBDMC) and macrophage (mBMDM) generation**

Briefly, bone marrow from the leg of C57BL/6 mice was plated on day zero into 250mL or 500mL tissue culture flasks (Corning, Corning, NY) at  $10^5$  cells/mL. These extracted bone marrow cells were plated in DC medium, which consisted of cRPMI supplemented with 20ng/mL of GM-CSF (Biolegend) [catalog #: 576308]. On day three, the same volume of DC medium was added to the flask. On day six, half of the nonadherent cells were spun down and added back to the flask with an equal amount of DC media. The nonadherent cells were harvested on day eight or nine for mBMDM. For mBDMC, the adherent cells were harvested.

### ***In vitro* mBMDM activation**

On day eight, harvested mBMDMs were stimulated and cultured with monesin (for cytokines only) [catalog #: 554724], LPS (1 $\mu$ g/ml), CDN (.002 $\mu$ g/mL to 50 $\mu$ g/ml), R848 (.00128 $\mu$ g/mL to 20 $\mu$ g/ml), MPL-A (.00128 $\mu$ g/mL to 20 $\mu$ g/ml), CPG-ODN (.002 $\mu$ g/mL to 20 $\mu$ g/ml), RLL (.002 $\mu$ g/mL to 20 $\mu$ g/ml), or NLL (.002 $\mu$ g/mL to 20 $\mu$ g/ml) for twenty-four hours for surface markers and four hours for intracellular cytokines in a ninety-six well plate. DCs were stained for anti-mouse CD11c, CD86, CD80, CD40, MHCII, MHCI, and TNF. Gated DC population (CD11c+) was probed for surface markers (MHCI, MHCII, CD86, CD80, and CD40) and intracellular cytokine analysis (TNFa) after permeabilization by geometric mean fluorescence intensity (gMFI). No data points were excluded.

### ***In vitro* mBMDM and THP-1 activation**

For twenty-four hours, harvested BMDMs were stimulated and cultured on day eight with CDN (.0000156µg/mL to 50µg/ml) and R848 (.0000156µg/mL to 50µg/ml) for the dose-response in a ninety-six well plate. 10µg/mL was the saturating CDN dose, and 1µg/mL was the saturating R848 dose. The Max-dose combines the saturating amounts of CDN (10µg/mL) plus R848 (1µg/mL), and the MuSyC-dose is saturating dose of CDN (10µg/mL) plus one-tenth saturating dose of R848 (0.1µg/mL). The mBMDMs were stained for anti-mouse F4/80, CD86, CD80, CD40, and MHCII. Gated mBMDM population (F4/80+) was measured for surface markers (MHCII, CD86, CD80, and CD40) by gMFI. The THP-1 cells were stimulated with CDN (0.78125µg/mL to 50µg/mL) and R848 (0.78125µg/mL to 50µg/mL) for the single-agent dose responses. 25µg/mL was the saturating CDN dose, and 25µg/mL was the saturating R848 dose. The Max-dose was 25ug/mL CDN plus 25ug/mL R848, and the MuSyC-dose was 25µg/mL CDN plus 2.5µg/mL R848. The THP-1 cells were stained for anti-mouse CD86 and CD80 and measured by gMFI. No data points were excluded.

### ***In vivo* APC activation**

Six- to twelve-week-old female C57BL/6 were subcutaneously injected with 20µg of Endofit ovalbumin (OVA) administered with increasing doses (0.0012µg to 50µg) of vaccigrade CDN (STING) or R848 (TLR7/8). Twenty-four hours later, the draining lymph nodes were extracted and stained for activation markers (MHCI, MHCII, CD40, CD86, and CD80). The *in vivo* doses of 20µg and 2µg were selected for CDN and R848, respectively, based on single-agent dose responses. These doses were used for

the remaining *in vivo* studies. Next, the same experiment was performed, comparing the Max-dose (20µg CDN and 2µg R848) to MuSyC-dose (20µg CDN and 0.2µg R848). No data points were excluded.

### ***In vivo* cytotoxic T-Cell killing assay**

Six- to twelve-week-old female C57BL/6 mice were vaccinated with PBS alone (n = 3), 20µg of Endofit ovalbumin (OVA) alone (n = 3), or OVA administered with 20µg of CDN (n = 3), 2µg of R848 (n = 3), Max-dose (2µg R848 and 20µg CDN) (n =4), and MuSyC-dose (0.2µg and 20µg CDN) (n = 4) [n = 20 total]. Seven days post-vaccination, splenocytes were extracted from non-vaccinated mice. Half of the splenocytes were given a high dose of 5µM CFSE with 1µg/mL SINFEKL peptide (specific splenocytes), and the other half was given a low dose of 0.5µM CFSE with no SINFEKL peptide (nonspecific splenocytes). The splenocytes were mixed 1:1, and then  $5 \times 10^6$  cells were injected intravenously into the vaccinated mice. Sixteen hours later, mice were euthanized, and spleens were extracted. Splenocytes were analyzed by flow cytometry and specific killing was calculated with the following equation: Ratio= Low Peak (non-specific) / High peak (ova-specific); Specific killing =  $(1 - (\text{PBS ratio average}) / (\text{Exp. ratio})) * 100$ . No data points were excluded. No animals were excluded.

### ***In vivo* T-cell proliferation**

CD8+ T-cells were isolated from six- to twelve-week-old female CD45.1 OT-1+ mouse spleens. The CD45.1+ OT-1+ CD8+ T-cells were 5µM CFSE stained.  $2.5 \times 10^5$  CFSE stained CD8 T-cells were intravenously injected into naïve WT CD45.2 C57BL/6 mice (n

= 3 per treatment) [n = 18 total]. Twenty-four hours later, the CD45.2 C57BL/6 mice were vaccinated with PBS alone, 20µg of Endofit ovalbumin (OVA) alone, or OVA administered with 20µg of vaccigrade CDN (STING), 2µg of vaccigrade R848 (TLR7/8), Max-dose (2µg R848 and 20µg CDN), and MuSyC-dose (0.2µg and 20µg CDN). Five days post-vaccination, mice were euthanized, and spleens were extracted. Spleens were stained for CD45.1 and CD8 for flow cytometry. Percent proliferation and percentage of CD45.1+ CD8+ of total live splenocytes were calculated. No data points were excluded. No animals were excluded.

### ***In vivo* tumor studies**

Based on priori power multiple analysis of variance (MANOVA) analysis at a 95% confidence interval, power of 80%, with an intermediate (0.50) [B16 m-OVA peptide vaccine] or large effect size (.75) [GVAX models], the total number of mice needed to reach significance is the following for each tumor model: 25 for the B16 m-OVA GVAX model, 26 for the MOC1 GVAX model, and 34 for the B16 m-OVA peptide model. For all vaccination models, six- to twelve-week-old female C57BL/6 mice were subcutaneously injected with the following amount of cells for different tumor models in the right flank:  $10^5$  B16 m-OVA tumor cells and  $2 \times 10^6$  MOC1 tumor cells. Five days after tumor inoculation, mice were randomized and then injected with 100µL of GVAX B16 m-OVA [n = 28 total mice] or GVAX MOC1 [n = 43 total mice] in PBS plus or minus vaccigrade 20µg CDN, 2µg R848, Max-dose (20µg CDN + 2µg R848) or MuSyC-dose (20µg CDN + 0.2µg R848) on the opposite flank. In addition, 100uL of PBS alone was used as a negative control. For the peptide vaccine, 20µg of Endofit ovalbumin (OVA)

(n = 11) plus or minus vaccigrade 20 $\mu$ g CDN (n = 11), 2 $\mu$ g R848 (n = 10), Max-dose (20 $\mu$ g CDN + 2 $\mu$ g R848) (n = 11) or MuSyC-dose (20 $\mu$ g CDN + 0.2 $\mu$ g R848) (n = 11) [n = 54 mice total] on the opposite flank. Tumor measurements were initiated once palpable utilizing calipers. The following formula calculated tumor volume: Length (longer dimension) x Width (shorter dimension)<sup>2</sup>/2. OVA-based vaccine-treated tumors were extracted and weighed sixteen days post-treatment. These tumors were processed and stained for immunophenotyping via flow cytometry. The percent of CD45+ and the percent of total live were evaluated utilizing the following gating: NK cells (CD11b-Nkp46+), CD8+ T-cells (CD11b-Nkp46-CD4-CD8+), CD4+T-cells (CD11b-Nkp46-CD8-CD4+), gMDSC (CD11b+MHCII-CD68-CD11c-Ly6G+), mMDSC (CD11b+MHCII-CD68-CD11c-Ly6C+), DC (CD68-CD11c+MHCII+), MACs (CD11c-CD68+), M1 MACs (CD206- MACs), and M2 MACs (CD206+ MACs). No data points were excluded. Animals were excluded if the negative control had zero tumor growth throughout the entire study for a specific model, thereby excluding other zero growth from the treatment groups in the same model. One mouse from the PBS, MuSyC-dose, and Max-dose groups from the MOC1 GVAX model fits this exclusion criterion.

### ***In vivo* mouse weight analysis**

Six- to twelve-week-old female C57BL/6 mice (n = 5 per group) [n = 30 total] were weighed to get their initial weight, considered 100%. Next, the mice were vaccinated with PBS alone, 20 $\mu$ g of Endofit ovalbumin (OVA) alone, or OVA administered with 20 $\mu$ g of CDN (STING), 2 $\mu$ g of R848 (TLR7/8), Max-dose (2 $\mu$ g R848 and 20 $\mu$ g CDN), and MuSyC-dose (0.2 $\mu$ g and 20 $\mu$ g CDN). Mice were weighed every twenty-four hours

for one hundred and twenty hours. The percent weight change was calculated daily. No data points were excluded. No animals were excluded.

### **Plasma cytokine analysis**

Six- to twelve-week-old mice female C57BL/6 (n = 5 per group) [n = 30 total] were vaccinated with PBS alone, 20 $\mu$ g of Endofit ovalbumin (OVA) alone, or OVA administered with 20 $\mu$ g of CDN (STING), 2 $\mu$ g of R848 (TLR7/8), Max-dose (2 $\mu$ g R848 and 20 $\mu$ g CDN), and MuSyC-dose (0.2 $\mu$ g and 20 $\mu$ g CDN). Six hours post-vaccination, mice were euthanized, and whole blood was drawn via heart puncture. Plasma was separated from the blood. The following plasma cytokines were analyzed by flow cytometry utilizing the Legendplex kit (catalog #: 740150) [lot #: B326302]: IL-1 $\alpha$ , IL1 $\beta$ , IL-6, IL-10, IL-12p70, IL-17A, IL-23, IL-27, CCL2(MCP-1), IFN- $\beta$ , IFN- $\gamma$ , TNF- $\alpha$ , and GM-CSF. The Biolegend Legendplex QOGNIT software quantified the concentration for each cytokine. No data points were excluded. No animals were excluded.

### **The Multidimensional Synergy of Combinations (MuSyC) Analysis**

Synergy was calculated using the MuSyC algorithm as previously described using a monte carlo non-linear least squares regression [35, 36]. MuSyC distinguishes two types of drug synergy, synergistic efficacy ( $\beta$ ) and synergistic potency ( $\alpha$ ), both relating to geometric transformations of the dose response surface. These transformations are analogous to the transformations in the 1D Hill equation for potency (horizontal shift in the EC<sub>50</sub>) and efficacy (vertical shift in e<sub>max</sub>). Synergy was calculated by fitting a dose-response surface relating the observed effect (i.e. change in surface marker expression)

to the concentrations of CDN and the tested adjuvant (Figures 1, S3). As the maximal effect of the drugs ( $e_{\max}$ ) is larger than the basal effect ( $E_0$ ) when quantifying mBMDC activation, synergistic efficacy ( $\beta$ ) is defined as  $(e_{\max} - \max(E_1, E_2)) / (\max(E_1, E_2) - E_0)$  where  $E_3$  is the effect observed at the maximum of both drugs,  $E_1$  is the maximum effect for drug 1 alone, and  $E_2$  is the maximum effect for drug 2 alone. No bounds were required for the non-linear regression to converge.

### **Statistical Analysis**

Multiple comparison tests of datasets were achieved with a one-way or two-way analysis of variance (ANOVA). Error bars reflect the standard error of the mean (SEM) or the standard deviation (S.D.). Tests of significance are reported as P values, a two-tailed distribution, and calculated at 95% confidence. All data analyses were performed using Graphpad prism. A priori analyses were performed utilizing the G-power 3.1.9.7 calculator.

# **CHAPTER III: ABROGATION OF HLA-E/QA-1b EXPRESSION ON TUMOR CELLS SIGNIFICANTLY INCREASES ANTITUMOR IMMUNE RESPONSE ELICITED BY GVAX**

## **INTRODUCTION**

Whole-cell vaccines are an attractive platform for cancer immunotherapy as they provide an unbiased set of tumor antigens to stimulate the immune system. In this report, we tested the whole cell vaccine platform GVAX in which irradiated tumor cells are mixed with granulocyte monocyte colony-stimulating factor (GM-CSF) producing cells. GVAX has been shown to induce a potent immune response in preclinical models and humans (15, 366). The idea behind GVAX is that GM-CSF produced by the bystander cells recruits and activates antigen-presenting cells, which take up tumor antigens from the irradiated tumor cells and induce tumor-specific T cells. However, clinically GVAX has had only modest success as a single agent, with multiple clinical trials ongoing combining GVAX with various immunotherapy and chemotherapy agents (366-369). One potential problem with GVAX is that the critical component, tumor cells, express a wide variety of immune suppressive molecules. We hypothesize that suppressive molecules expressed on the tumor cells used in GVAX potentially limit the anti-tumor immune response elicited.

One novel immunosuppressive molecule found on cancer cells is the non-classical HLA molecule HLA-E. HLA-E is expressed by all nucleated cells at deficient levels but can

be upregulated by interferon-gamma (IFN $\gamma$ ). A wide range of cancer types often overexpresses HLA-E compared to normal tissue (370, 371). HLA-E is the ligand for the natural killer group 2 A (NKG2A)/CD94 complex, which upon stimulation, induces immune suppression through two ITIM domains (372). NKG2A is constitutively expressed by most NK cells and on subsets of CD8 T cells. The role of the NKG2A/HLA-E axis in the immune system is to survey cells for the presence of MHC I, which is required for HLA-E to be stably expressed on the surface of cells. We and others have found that NKG2A is significantly upregulated on tumor-infiltrating CD8 T cells (373, 374), making NKG2A a good candidate for immunotherapy. Consequently, NKG2A blockade is currently being tested in HNSCC patients with promising early results (373). In addition, we found that blockade of NKG2A is effective when combined with peptide vaccine in pre-clinal tumor models (374).

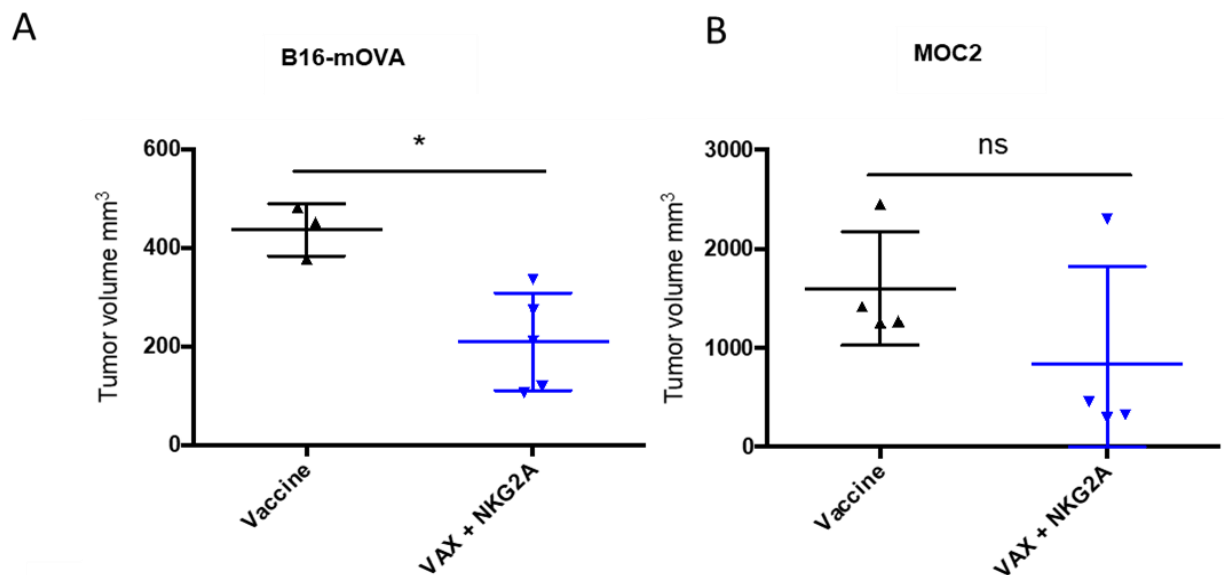
Since we have demonstrated the role of NKG2A/HLA-E blockade in improving peptide-based vaccines, we wanted to extend these findings to GVAX. We hypothesized that HLA-E ligands expressed on the tumor cells comprising GVAX would inhibit the immune response elicited. Therefore, the anti-tumor immune response to GVAX could be improved by disrupting the NKG2A/HLA-E axis. However, since HLA-E is expressed by both the primary tumor and the cells comprising GVAX, it would be difficult to ascertain the contributions of NKG2A blockade at the site of vaccination from the primary tumor. To get around this, we generated the mouse homolog of HLA-E, Qa-1b, knocked out tumor cells, and used them to generate GVAX without HLA-E/Qa-1b (QVAX). We found that QVAX was superior to GVAX at reducing tumor volumes in multiple mouse models.

## RESULTS

### NKG2A blockade synergizes with GVAX to reduce tumor volume

We have previously shown that NKG2A blockade synergizes with the E7 peptide vaccine to reduce tumor volume (374). We wanted to extend these findings to the whole cell vaccine GVAX, which is comprised of irradiated tumor cells and GM-CSF-producing B78h1-GM cells. Mice were inoculated with B16-mOVA or MOC2 on the flank and then administered GVAX on day five and NKG2A blockade two days later. GVAX plus NKG2A blockade significantly reduced tumor volume in B16-mOVA cells (**Fig.3-1 A**). Although not significant, we saw a similar trend with the MOC2 tumor model (**Fig.3-1 B**). We previously demonstrated that with a peptide vaccine, NKG2A blockade primarily works by blocking the interaction of CD8 T cells and the primary tumor. However, by using a whole cell vaccine instead of a peptide, NKG2A blockade might also work at the vaccination site since the tumor cells in GVAX also express HLA-E/Qa-1b.

Figure 3-1



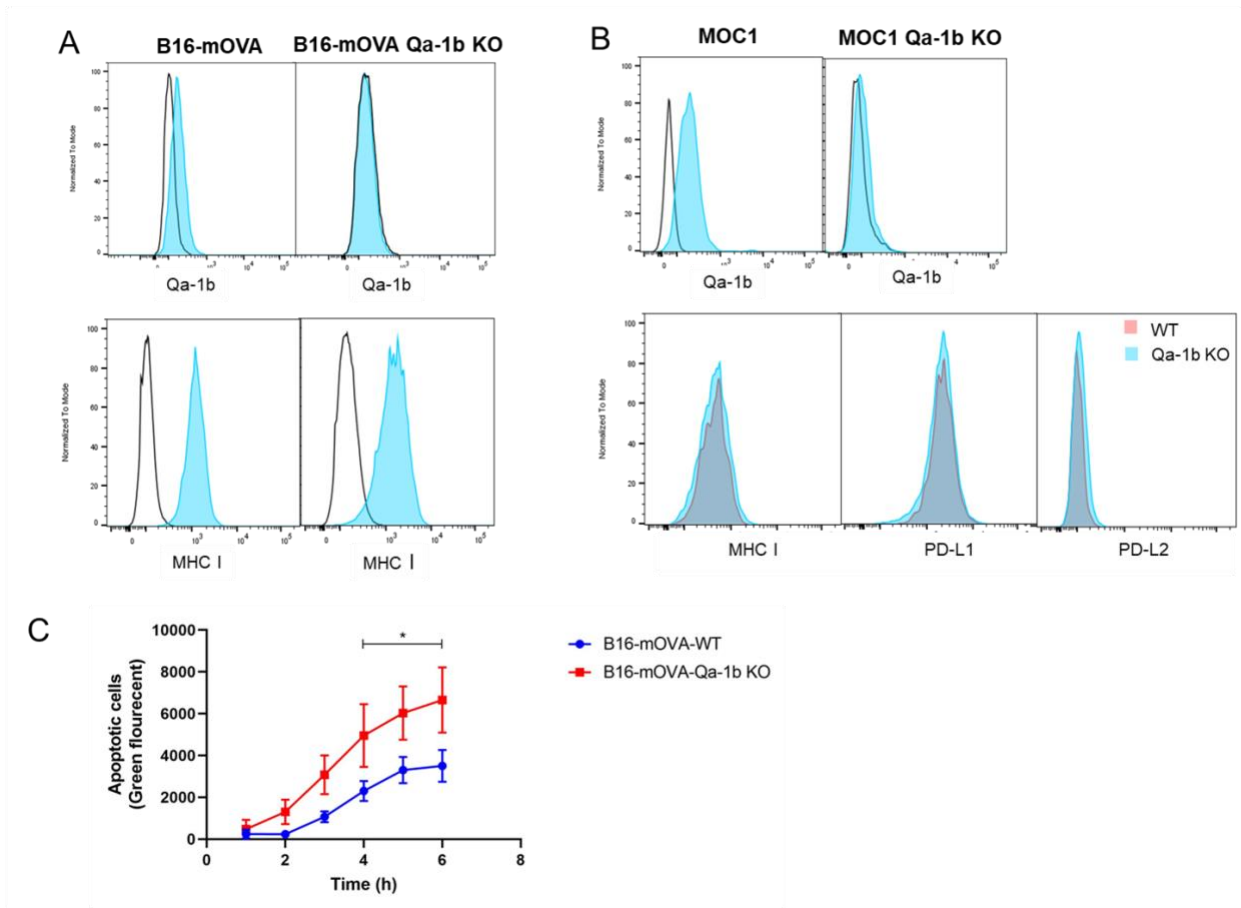
**Figure 3- 1: Therapeutic treatment of mice with NKG2A blockade and GVAX significantly reduces tumor**

Figure 3-1: Tumor volume of B16-mOVA tumors at endpoint administered GVAX or GVAX + anti-NKG2A. Mice were inoculated with B16-mOVA tumor s.c. in the flank and then administered **(A)** B16-mOVA GVAX or **(B)** MOC2 GVAX on day 5 on the opposite flank. Anti-NKG2A antibody was administered on day 7, 9 and 12. All data are given in mean  $\pm$  S.D. \*P < 0.05, \*\*P < 0.01, \*\*\*P < 0.001, \*\*\*\*P < 0.0001.

**Loss of Qa-1b does not alter expression of MHC I or PD-L1 on murine tumor cells**

To separate the effect of NKG2A blockade on the primary tumor and the vaccination site, we generated Qa-1b deficient B16-mOVA and MOC1 tumor cells to use as the vaccine source. We successfully knocked out Qa-1b on B16-mOVA Qa-1b cells (**Fig.3-2 A**) and MOC1 cells (**Fig.3-2 B**), while leaving MHC I, PD-L1, and PD-L2 expression unaffected. In addition, we performed an NK killing assay to determine if there was a functional loss of Qa-1b. NK cells express high levels of NKG2A, and NK cell-mediated killing was previously shown to be inhibited by the expression of HLA-E/Qa-1b (375). Furthermore, B16-mOVA Qa-1b KO cells were significantly more susceptible to NK cell-mediated killing than WT B16-mOVA cells (**Fig.3-2 C**), suggesting a functional loss of Qa-1b.

Figure 3-2



**Figure 3- 2:** MOC1 and B16-mOVA Qa-1b KO cells have a normal expression of MHC I, PD-L1, and increased susceptibility to NK cell-mediated killing.

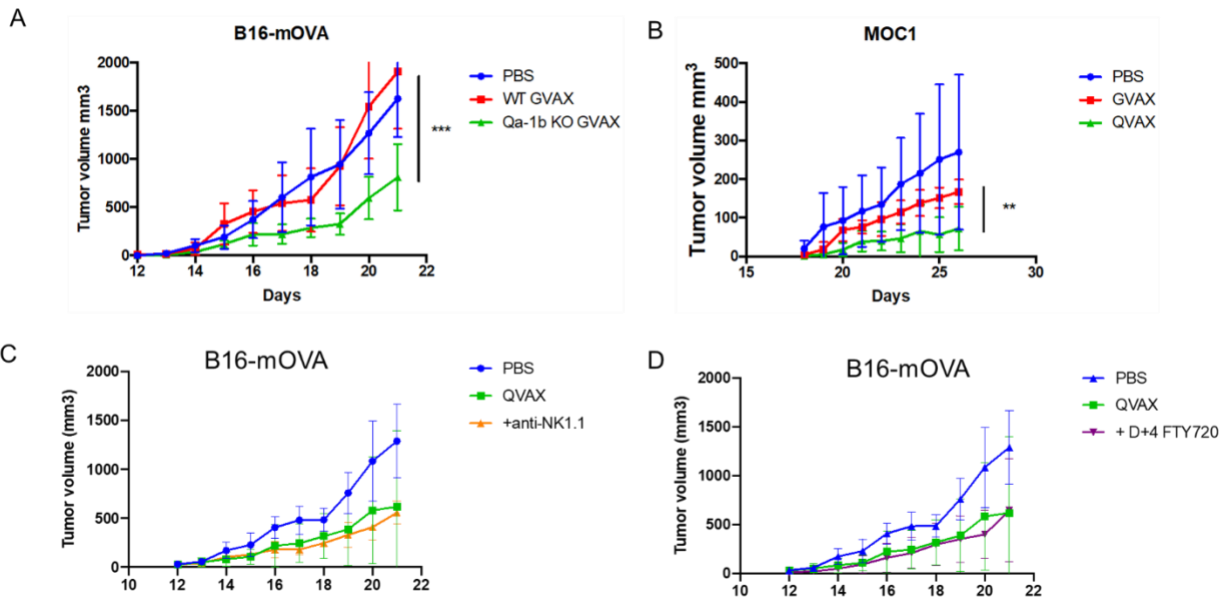
Figure 3-2: The phenotype of **(A)** B16-mOVA and B16-mOVA Qa-1bKO or **(B)** MOC1 and MOC1 Qa-1b KO shows MHC1, PD-L1, and PD-L2 unaffected by loss of Qa-1b. Cells were incubated with 100 IU/ml IFN $\gamma$  overnight. Black histogram unstained. **(C)** B16-mOVA-Qa-1b-KO cells have increased susceptibility to NK cell-mediated cytotoxicity. B16-mOVA-WT and B16-mOVA-Qa-1b-KO cells were co-cultured with IL-2 activated NK cells at an effector to target ratio of 25:1. Cell killing was determined by the cleavage of a caspase-3/7 sensitive dye and determined every hour by fluorescence microscopy. All data are given in mean  $\pm$  S.D. \*P < 0.05, \*\*P < 0.01, \*\*\*P < 0.001, \*\*\*\*P < 0.0001.

### **Knocking out HLA-E/Qa-1b on whole-cell vaccine significantly improves anti-tumor response**

We next determined if GVAX generated with tumor cells lacking Qa-1b (QVAX) is superior to GVAX at controlling WT tumor growth. Mice were inoculated with WT tumors on the flank and administered either GVAX or QVAX on the opposite side five days later. In both B16-mOVA and MOC1 tumor models, vaccination with QVAX provided significantly better tumor control than vaccination with GVAX (**Fig.3-3 A-B**). One possibility for the enhanced effect of QVAX over GVAX is the activation of NKG2A+ NK cells at the vaccination site. To determine if NK cells contribute to the increased tumor control of QVAX, we repeated our QVAX vaccination experiment with the addition of NK cell depletion starting one day before QVAX vaccination. We found no difference in tumor growth between QVAX vaccination and QVAX + NK cell depletion, suggesting that NK cells are unnecessary for QVAX-mediated tumor control (**Fig.3-3 C**). We next

determined if T cell ingress into the tumor was required using Fingolimod (FTY720). FTY720 is a drug that sequesters immune cells in lymphatic tissue through the downregulation of Sphingosine-1-phosphate receptor 1 (S1PR1). We started FTY720 treatment one day before QVAX vaccination and continued administering daily. Surprisingly, we found that QVAX + FTY720 treatment did not affect tumor growth following QVAX treatment (**Fig.3-3 D**). However, despite not altering tumor growth, FTY720 did significantly reduce immune cell infiltration in the tumor, reducing both CD4 and CD8 T cells to levels similar as PBS control tumors (not shown).

Figure 3-3



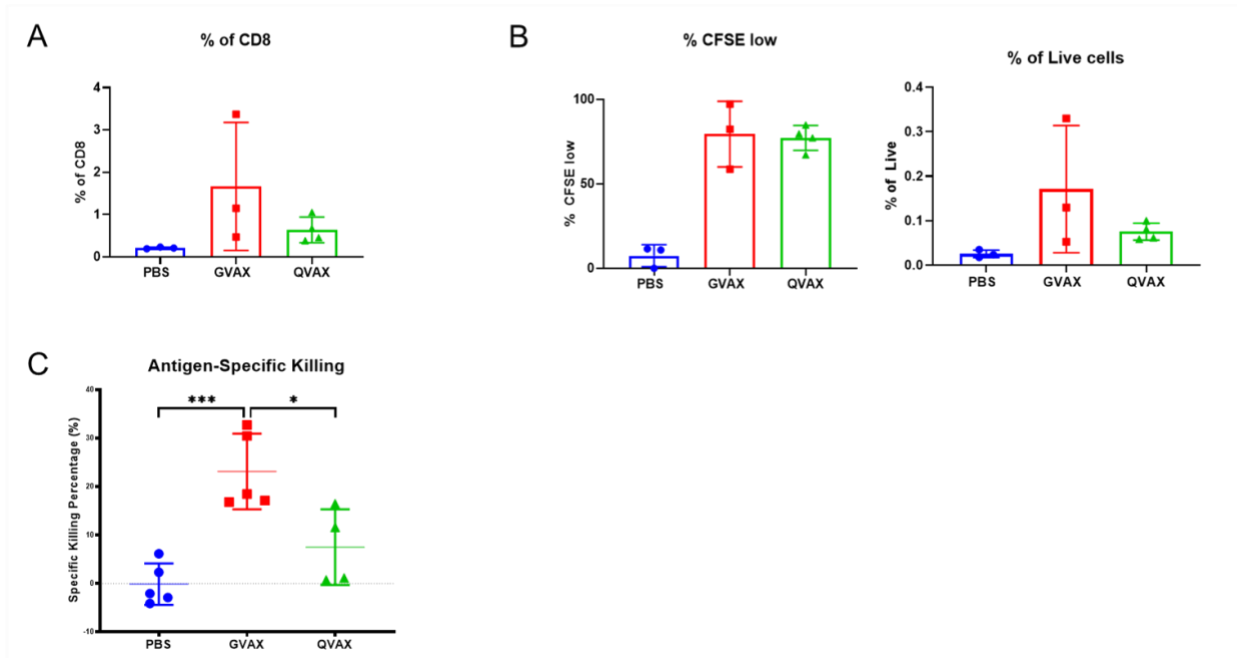
**Figure 3- 3: Whole-cell vaccine QVAX significantly reduces WT tumor volume**

Figure 3-3: **A)**  $1 \times 10^5$  WT B16-mOVA cells were implanted s.c. in the flank of B6 mice. Five days later, mice were administered  $1 \times 10^6$  GVAX cells or  $1 \times 10^6$  GVAX cells made with B16-mOVA-Qa-1b-KO cells (QVAX) in the opposite flank. **B)**  $1 \times 10^6$  MOC1 cells were implanted s.c. and administered MOC1 GVAX or QVAX on day 5. Tumor reduction by QVAX was not altered following **C)** NK cell depletion or the administration of **D)** FTY720. NK cell depletion and FTY720 administration were started 1 day prior to QVAX. All data are given in mean  $\pm$  S.D. \*P < 0.05, \*\*P < 0.01, \*\*\*P < 0.001, \*\*\*\*P < 0.0001. n=5 mice per

### **QVAX does not increase tumor-specific T cells or cytotoxic function compared to GVAX**

We compared GVAX and QVAX's ability to induce tumor-specific T cells using OT-1 CD8<sup>+</sup> T cells.  $1 \times 10^6$  CD45.1 CFSE labeled OT-1 CD8 T cells were adoptively transferred into B6 mice and then vaccinated with B16-mOVA GVAX or QVAX the next day. The mouse spleens were harvested and analyzed for OT-1 CD8<sup>+</sup> T cells five days later. We found no significant difference in the induction of OT-1 CD8<sup>+</sup> T cells between GVAX and QVAX (**Fig.3-4 A**) in the spleen. In addition, there was no difference in proliferation, as evidenced by CFSE low staining between the groups (**Fig.3-4 B**). Next, we performed *in vivo* CTL assays using SINFEKL pulsed splenocytes as targets. First, mice were vaccinated, and then the CTL assay was performed seven days later. We found that GVAX induced significantly more killing than QVAX (**Fig.3-4 C**). Together, these results suggest that QVAX does not generate a more robust anti-tumor T cell response than GVAX.

Figure 3-4



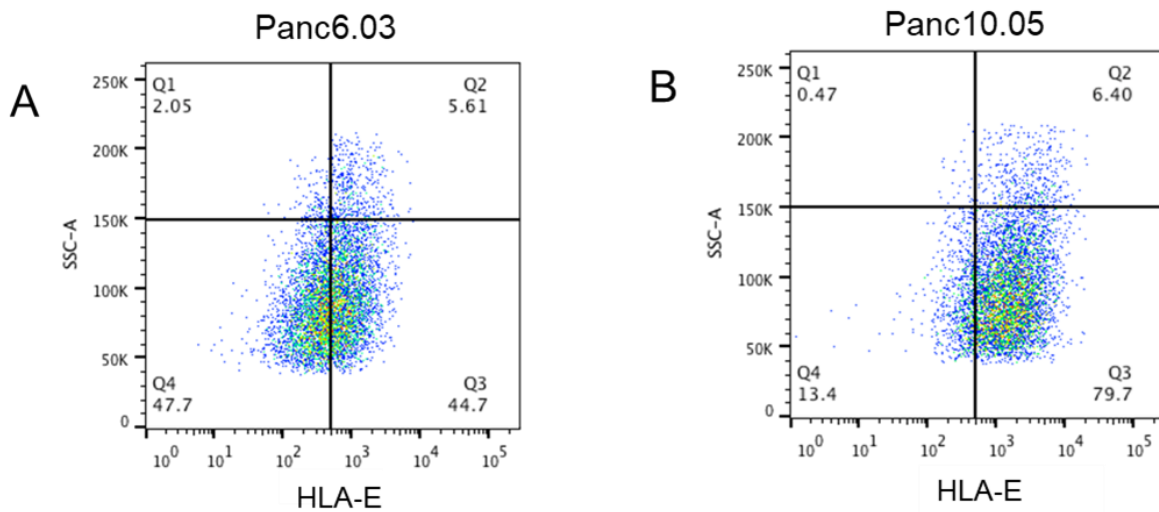
**Figure 3- 4:** QVAX induces similar levels of *in vivo* CD8 T cell proliferation as GVAX

Figure 3-4: **A)**  $1 \times 10^6$  CFSE labeled CD45.1 OT-1 CD8 T cells were adoptively transferred to B6 mice and then administered B16-mOVA GVAX or QVAX the next day. Five days post-vaccination, the number of OT-1 cells was enumerated from the spleen, and the percent of **B)** CFSE low OT-1 cells was calculated. **C)** In vivo CTL killing assay. B6 mice were vaccinated with B16-mOVA GVAX or QVAX and then administered SINFEKL pulsed target splenocytes seven days later. The specific killing was then determined. \*,  $p > .05$ ; \*\*\*,  $p < .001$ ; one-way ANOVA;  $n = 4-5$  mice per group; error bars = SD

## Human pancreatic cell lines used for clinical GVAX express HLA-E

Finally, we determined if the cell lines used in the clinical human GVAX expressed HLA-E. Panc6.03 and Panc10.05 cells were incubated overnight with IFN $\gamma$  and then checked for HLA-E. We found that both Panc6.03 and panc10.05 expressed HLA-E after IFN $\gamma$  stimulation (**Fig.3-5**).

Figure 3-5



**Figure 3- 5:** HLA-E is upregulated after IFN $\gamma$  stimulation on human Panc cell lines used in clinical GVAX treatment.

Figure 3-5: **A)** Human Panc6.03 and **B)** Panc 10.05 cells were stimulated overnight with 100 IU/mL IFN $\gamma$ , and flow cytometry was used to determine HLA-E expression and gated on live

## DISCUSSION

In this study, we demonstrated that the NKG2A ligand HLA-E/Qa-1b inhibits the anti-tumor immune response elicited by GVAX. We showed that murine and human tumor cells comprising clinical GVAX express HLA-E/Qa-1b following interferon-gamma stimulation. We reasoned that the expression of HLA-E/Qa-1b at the vaccination site would likely have the same immune dampening effects as we and others have observed in primary tumors (373, 374). To determine if HLA-E/Qa-1b was suppressing immune activation at the vaccination site, we generated tumor cells lacking Qa-1b, which had normal MHC I and PD-L1 expression. When Qa-1b deficient tumor cells were used in GVAX, which we termed QVAX, we observed a striking reduction in tumor volume compared to GVAX.

The mechanism by which QVAX but not GVAX reduces tumor volume remains unclear and requires further study. We demonstrated that QVAX did not require NK cells or the trafficking of T cells from lymph tissue to the tumor to reduce tumor volume. Paradoxically, QVAX does not increase antigen-specific T cells or T cell cytotoxicity compared to GVAX. These are similar to what we observed for TLR4 enhanced GVAX (TEGVAX), which also improved tumor control compared to GVAX but had significantly worse antigen-specific T cell induction (359). We also have found that QVAX is antigen-specific and that QVAX generated with B16-mOVA does not reduce the tumor volume of MOC1 tumors (data not shown). Together our data suggest that antigen-specific T cell generation is a requirement for GVAX but insufficient to reduce tumor

volume alone. We, therefore, hypothesize that QVAX is also modulating the tumor microenvironment, possibly through alterations in the myeloid compartment.

NK cells have a stable expression of NKG2A. Therefore, they would be expected to be present in the tissue at the vaccination site, making logical mediators of the improved immune response to QVAX. However, the depletion of NK cells did not affect the efficacy of QVAX. This is similar to what we observed in our prior studies with protein vaccination and NKG2A blockade, which also showed no role for NK cells in the primary tumor (374). However, one report found that NKG2A blockade worked through NKG2A+ CD8 T cells and NKG2A+ NK cells (373). Therefore, there is a possibility that our NK cell depletion was unable to deplete NK cells at the site of vaccination due to poor tissue penetration of the antibodies. Further studies in NK cell-deficient mice will need to confirm this finding.

GVAX in the clinical setting has not proven effective as a single agent but has excellent potential as an unbiased source of tumor antigens. GVAX has proven beneficial in combination with PD-1 blockade, Cyclophosphamide, and *listeria monocytogenes* vaccines (25, 367, 368). We believe that our data demonstrates that one of the problems with GVAX is that the human tumor cells used to generate it express the inhibitory receptor HLA-E. Our data suggest that deletion of HLA-E from GVAX has the potential to increase the anti-tumor immune response cost-effectively and straightforwardly significantly. Future studies must determine if the abrogation of other immune suppressive functions leads to further improvements in whole cell vaccines.

## **METHODS**

### **Mice**

Female C57BL/6 [strain #: 000664], female and male C57BL/6-Tg(TcraTcrb)1100Mjb/J (OT-1) [strain #: 003831], and female and male B6.SJL-Ptprca Pepcb/BoyJ (CD45.1) [strain #: 002014] mice were purchased from The Jackson Laboratory. OT-1 x CD45.1 and all other mice were housed according to the Vanderbilt University Medical Center Animal Care and Use Committee rules. All animal experiments were reviewed and approved by the Institutional Animal Care and Use Committee at Vanderbilt University Medical Center (M1900004-00). According to NIH guidelines, the Animal Welfare Act, and US Federal law, all experiments were performed.

### **Cell lines**

B16 m-OVA, Mouse Oral Squamous Cell Carcinoma (MOC1), and B78H1-GM cells were grown in complete RPMI (cRPMI) which consist of RPMI supplemented with 10% heat inactivated Fetal Bovine Serum (FBS), 5% Penicillin-Streptomycin, 5% HEPES, 5% GlutaMAX, and 0.5%  $\beta$ -Mercaptoethanol.

### **GVAX**

GVAX was generated by mixing  $1 \times 10^6$  tumor cells (B16-mOVA or MOC1) with  $1 \times 10^5$  B78H1-GM cells. The cells were irradiated with 10,000 rads using a Gammacell 1000 irradiator. B78H1-GM cells produce GM-CSF at  $3 \mu\text{g}$  per  $1 \times 10^6$  cells per twenty-four hours (CITE). GVAX was resuspended in  $100 \mu\text{L}$  of PBS and injected s.c. into the flank of mice five days after tumor induction.

## **Tumor studies**

Six-week-old female C57BL/6j mice were injected subcutaneously in the flank with  $1 \times 10^5$  B16-mOVA cells or  $1 \times 10^6$  MOC1 tumor cells in 100 $\mu$ L of PBS. GVAX or QVAX was administered five days post tumor induction on the opposite flank. 10 $\mu$ g of FTY720 was administered intraperitoneally one day before QVAX treatment (day four post tumor implantation) and once daily afterwards. 100 $\mu$ g of NK depletion was given day four, five and eight post tumor implantation then twice a week afterwards. Tumor measurements were initiated once palpable utilizing calipers. The following formula calculated tumor volume: Length (longer dimension) x Width (shorter dimension)<sup>2</sup>/2.

## ***In vivo* cytotoxic T-Cell killing assay**

Six- to twelve-week-old female C57BL/6 mice were vaccinated with PBS alone, GVAX, or QVAX. Seven days post-vaccination, splenocytes were extracted from non-vaccinated mice. Half of the splenocytes were given a high dose of 5 $\mu$ M CFSE with 1 $\mu$ g/mL SINFEKL peptide (specific splenocytes), and the other half was given a low dose of 0.5 $\mu$ M CFSE with no SINFEKL peptide (nonspecific splenocytes). The splenocytes were mixed 1:1, and then  $5 \times 10^6$  cells were injected intravenously into the vaccinated mice. Sixteen hours later, mice were euthanized, and spleens were extracted. Splenocytes were analyzed by flow cytometry and specific killing was calculated with the following equation: Ratio= Low Peak (non-specific) / High peak (ova-specific); Specific killing =  $(1 - (\text{PBS ratio average}) / (\text{Exp. ratio})) \times 100$ . No data points were excluded. No animals were excluded.

### ***In vivo* T-cell proliferation**

CD8<sup>+</sup> T-cells were isolated from six- to twelve-week-old female CD45.1 OT-1<sup>+</sup> mouse spleens. The CD45.1<sup>+</sup> OT-1<sup>+</sup> CD8<sup>+</sup> T-cells were 5 $\mu$ M CFSE stained. 2.5x10<sup>5</sup> CFSE stained CD8<sup>+</sup> T-cells were intravenously injected into naïve WT CD45.2 C57BL/6 mice. Twenty-four hours later, the CD45.2 C57BL/6 mice were vaccinated with PBS alone, GVAX, or QVAX. Five days post-vaccination, mice were euthanized, and spleens were extracted. Spleens were stained for CD45.1 and CD8 for flow cytometry. Percent proliferation and percentage of CD45.1<sup>+</sup> CD8<sup>+</sup> of total live splenocytes were calculated. No data points were excluded. No animals were excluded.

## **CHAPTER IV: CONCLUSION AND FUTURE PERSPECTIVES**

### **CONCLUSION**

Cancer remains the second leading cause of death worldwide. The host immune system's ability to recognize and attack transformed cells and generate durable clinical responses to immunotherapy has revolutionized oncology and cancer research. However, heterogeneity of the tumor cells and tumor-associated immune suppression produce substantial barriers. Fortunately, extensive research in the last decade has dramatically increased our understanding of tumor-immune cell interactions. These findings have resulted in breakthroughs in cancer immune therapy modalities, primarily immune checkpoint inhibitors (ICIs), which have shown clinical benefits in a fraction of patients. However, due to the lack of tumor-infiltrating lymphocytes (TILs), ICIs are ineffective in many cancer patients. Therefore, cancer therapeutic vaccines have emerged as an attractive treatment strategy, mainly because they increase TILs and elicit long-lasting memory against cancer antigens (376). Unfortunately, most therapeutic cancer vaccines have yielded unsatisfactory results in a clinical setting. This thesis section summarizes chapters II and III approaches to maximize antitumor responses for each cancer vaccine component and discusses the future recommendations for therapeutic cancer vaccines.

## FUTURE DIRECTIONS

### Combination of cancer vaccines with checkpoint inhibitors

Clinically, therapeutic cancer vaccines have failed to induce beneficial responses in cancer patients. Therefore, in chapters II and III, we demonstrated approaches to improve antitumor responses of the adjuvant platforms and tumor antigen source by combining adjuvants and modifying the antigen source, respectively. Specifically, in chapter II, we utilized the Multidimensional Synergy of Combinations (MuSyC) algorithm to optimize the combination of Stimulator of Interferon Gene (STING) agonist cyclic dinucleotide (CDN) and TLR7/8 agonist Resiquimod (R848). In chapter III, GM-CSF-secreting whole-cell vaccine (GVAX) was modified not to express HLA-E/Qa1b on the surface (QVAX). In both sections, the novel approaches significantly improved antitumor immunity.

Unfortunately, therapeutic cancer vaccines alone fail or have modest results based on previous preclinical and clinical datasets, suggesting additional agents are needed. For example, the chapter II study showed potential failure for the MuSyC-dose vaccine with the high expression of PD-1 on cytotoxic T-cells (**Fig.2-8 E**). Therefore, the expected next step for the MuSyC-dose vaccines is to combine with ICIs to prolong the antineoplastic response. Moreover, MuSyC-dose increased TILs compared to the vaccine alone (**Fig.2-8 E**), which positively correlates to clinical response to ICI treatment. We can do something similar for chapter III, where we further delete PD-L1 or other checkpoint proteins to improve the immunogenicity of QVAX or other forms of whole tumor cell vaccines.

Currently, clinical trials are testing the combination of therapeutic cancer vaccines plus ICIs and have shown increased benefits with the combination. For instance, a phase Ib/II clinical trial for cancer patients with late-stage melanoma studied the efficacy of CTLA-4 ICI Ipilimumab versus the combination oncoviral vaccine TVEC and Ipilimumab. The study saw a more than two times decrease in lesion size for the combination compared to Ipilimumab alone (173). In general, therapeutic cancer vaccines plus ICI have produced marginal improvements in response rates and some sporadic complete responses, but no one combination is effective in all tumor subtypes (377). Overall, our enhanced modifications for the whole cell tumor antigen source and algorithm-based optimization of adjuvant combinations can potentially improve the response associated with therapeutic cancer vaccines, thereby providing better combinatorial options for ICI treatment.

### **Multi-layered analyses on the effect of cancer vaccines on hematopoiesis and immune infiltrate**

Chapters II and III clearly showed that the generation and function of antigen-specific CD8<sup>+</sup> T cells is not the determining factor for antitumor immunity. For example, chapter II demonstrated that the MuSyC-dose adjuvanted peptide vaccine did not improve CD8<sup>+</sup> T cell proliferation and the killing of antigen-pulsed splenocytes (**Fig.2-7 D-E**) but significantly decreased the tumor volume compared to CDN alone and Max-dose (**Fig.2-8 B**). This paradox is more pronounced in Chapter III, where GVAX significantly increased antigen-specific CD8<sup>+</sup> T cell killing but had substantially less antitumor response than QVAX (**Fig.3-3 A-B**). Moreover, another study showed a similar finding:

GVAX caused more proliferation in the lymph node but had a less significant tumor size reduction than GVAX plus TLR4 agonist glucopyranosyl lipid adjuvant–stable emulsion (GLA-SE) (359). In chapter II, in addition to not causing further peripheral CD8+ T-cell activation and killing but drastically enhancing the antitumor response, the MuSyC-dose peptide vaccine did not significantly boost the TILs compared to CDN alone and Max-dose (**Fig.2-8 E**). However, we have new data showing that QVAX is CD8+ T cell-dependent (**Fig. 4-1**) and not natural killer (NK) cell-dependent (**Fig.3-3 C**). Therefore, other factors besides the number of TILs may be the key to identifying the proper TILs that induce or reduce antineoplastic effects.

Figure 4-1

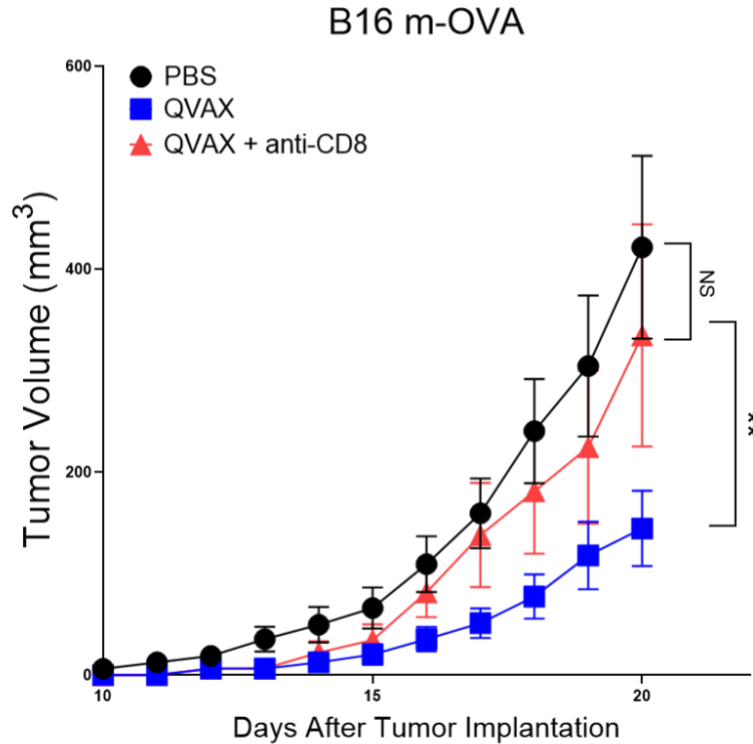


**Figure 4- 1:** QVAX-induced antitumor response is mediated by CD8+ T cells.

Figure 4-1:  $10^5$  B16 m-OVA tumor cells were subcutaneously injected on one flank of C57BL/6 mice (n=10). Four days post tumor implantation, the anti-CD8 group was depleted of CD8<sup>+</sup> T cells. Mice in this group were given depletion on days five, eight, and then two times a week afterward. QVAX was administered five days post tumor inoculation. Tumor volume was measured until day twenty utilizing the following equation: Length (longer dimension) x Width (shorter dimension)<sup>2</sup>/2. All data are given in mean  $\pm$  S.D. of biological replicates. \*P < 0.05, \*\*P < 0.01, \*\*\*P < 0.001, \*\*\*\*P < 0.0001, two-way analysis of variance for multiple comparisons.

One recent concept that addresses the reduction in the CD8<sup>+</sup> TILs' ability to enact their antitumor function in the tumor microenvironment is naïve versus progenitor exhausted (early dysfunctional) versus terminally exhausted (late dysfunctional) populations. These functionally heterogeneous cells occupy unique peripheral and intratumoral niches and are characterized by the transcriptional process that controls the transitional states of the cells. CD8<sup>+</sup> TILs' chronic exposure to antigen stimulation leads to a dysfunctional, hyporesponsive state called exhaustion (378). Naïve CD8<sup>+</sup> T cells develop in the bone marrow, mature in the thymus, and then home to secondary lymphoid organs, i.e., spleen and lymph node, by expressing the lymphoid homing receptors CC-chemokine receptor 7 (CCR7) and the cluster of differentiation 62 ligand (CD62L) (379). These naïve T cells have yet to be stimulated by antigen (antigen inexperienced) and are therefore not considered exhausted. Upon stimulation by major histocompatibility complex one (MHC I) bound to the processed peptide with the appropriate costimulation on cells in the periphery, naïve CD8<sup>+</sup> T cells become

activated, proliferate, and differentiate into cytolytic effector cells expressing the T cell receptor (TCR) specific for that MHC-antigen complex (380). When naïve CD8<sup>+</sup> T cells differentiate to the effector, memory, or other subtypes, distinct metabolic, epigenetic, and transcriptional programs are induced, which generates unique phenotypical and functional states for each cell type (381).

Since it is an arduous task to identify previous antigen recognition of T cells *in vivo*, surrogate markers are primarily used to classify different subtypes of CD8<sup>+</sup> T cells. For instance, in humans, naïve T cells express CD45RA and lack expression of memory-associated marker CD45RO (382). As stated earlier, naïve T cells express CCR7 and CD62L (379), which are more markers to distinguish between memory T cells that can start to reexpress CD45RA (383). Upon antigen stimulation, naïve T cells activate and differentiate into effector T cells when an acute infection occurs (384). At the peak of the acute infection T cell responses, these effector cells differentiate into short-lived effector T cells (SLECs) and memory precursor effector cells (MPECs) (384). SLECs express killer cell lectin-like receptor G1 (KLRG1), produce high amounts of inflammatory cytokines and cytolytic molecules and then undergo apoptosis (384). In contrast, MPECs further differentiate into central memory (T<sub>cm</sub>) or effector memory T cells (T<sub>em</sub>) and highly expresses Interleukin-7 receptor subunit alpha (IL-7R $\alpha$ ) for long-term protective immunity. However, these CD8 T cell subsets (SLECs and MPECs) are more prominent in acute infections. This thesis is cancer-focused which is more similar to chronic infections because T cells in late-stage, progressing tumors become hyporesponsive owing to continuous encounters with tumor antigens and share many

key features with T cells in chronic infection. Therefore, the section will focus only on these two disease models from this point.

The two critical subsets of exhausted CD8+ T cells associated with these two disease models are stem-like progenitor exhausted ( $T_{pex}$ ) and terminally exhausted ( $T_{ex}$ ) T cells, representing early dysfunctional and late dysfunctional programs, respectively. The first subset,  $T_{pex}$ , has a high expression T cell factor one (TCF1), a transcription factor that promotes self-renewal and persistence in mouse and human tumor models. In chronic infection and tumor disease models, various adoptive transfer experiments demonstrated that  $T_{pex}$  cells could repopulate and sustain T cell responses (385-388). In addition to expressing TCF1,  $T_{pex}$  has a high expression of PD1 and has been shown to improve T cell expansion, T cell sustainability, and response to anti-PD1/PDL1 checkpoint inhibitors, meaning these cells are still reprogrammable (387, 389, 390). For instance, in forty-eight tumor biopsies taken from thirty-two metastatic melanoma patients,  $T_{pex}$ , regardless of PD1 expression, positively correlated to the duration and efficacy of response to ICI (387, 391). Moreover, the combined expression of TCF1 and PD1 is significantly associated with overall survival in patients with melanoma (389). Therefore,  $T_{pex}$  may serve as a favorable biomarker for ICI treatment.

However, although  $T_{pex}$  initially is TCF1<sup>+</sup>, they subsequently downregulate that marker and differentiate into the second major subset of late dysfunctional terminally exhausted T cells ( $T_{ex}$ ). As a result,  $T_{ex}$  has a more direct cytolytic function ( $T_{pex}$  does not),

secretes low amounts of effector cytokines such as IFN $\gamma$  and TNF $\alpha$ , persists poorly, and does not proliferate or respond well to ICI (387, 389). Furthermore, T<sub>ex</sub> has a high expression of CD39, CD38, PD1, CTLA4, TIM3, and thymocyte selection-associated HMG BOX (TOX). Of these upregulated proteins, TOX plays an integral role in the function of T<sub>ex</sub> as it induces epigenetic changes and activates the transcription of genes that encode for both transcription factors (i.e., TCF1 and TOX) and checkpoint molecules (i.e., LAG3, PD1, and TIM3) (231). In addition, a recent study showed that knocking out TOX1 and TOX2 in CAR TILs enhanced the effector cytokine (IFN $\gamma$  and TNF $\alpha$ ) production and boosted the antitumor response (392). Another preclinical study demonstrated a similar finding where heterozygous deletion of TOX improved the T cell responses in the tumor (393). For these reasons, TOX is potentially necessary and sufficient for T<sub>ex</sub>; therefore, T<sub>ex</sub> needs to be minimized for maximum therapeutic response to ICI.

As stated earlier in the section, both QVAX and MuSyC vaccines did not significantly increase peripheral T cell proliferation, killing, and infiltration but increased the antitumor response substantially compared to other treatment groups in their respective study. Since the abundance of TILs was not boosted, did these modified vaccines (or therapeutic vaccines in general) have more T<sub>pex</sub> than T<sub>ex</sub> in the tumor microenvironment? There are monoclonal antibodies for TOX, TCF1, and other markers for T<sub>ex</sub> and T<sub>pex</sub>, so experiments can be conducted to test what T cell dysfunctional programs therapeutic vaccines induce. Thus, future studies of therapeutic cancer vaccines should include this distinction in their immunophenotyping because it

may better indicate how well the vaccine will work with ICI. After all, T<sub>pex</sub> has a significant positive correlation to ICI response.

Another hypothesis is that therapeutic vaccines generate T cells that are less susceptible to becoming T<sub>ex</sub> by reprogramming cells in the bone marrow, modifying hematopoiesis. Hematopoiesis is the process by which a small quantity (about one in ten thousand bone marrow cells) of self-renewing pluripotent hematopoietic stem cells that produce red blood cells, platelets, and all leukocytes (394, 395) (**Fig.4-2**). Multiple studies have demonstrated that established solid tumors secrete soluble factors (i.e., GM-CSF, G-CSF, IL-6, and IL-1) and exosomes to stimulate HSCs mobilization and alter normal hematopoiesis (396, 397). For example, myeloid-derived suppressor cells (MDSCs) in the bone marrow are generated from the chronic secretion of GM-CSF, G-CSF, VEGF, IL-6, IL-1 $\beta$ , adenosine, HIF1 $\alpha$  produced by the TME (398, 399). This reprogramming of immature myeloid cells into MDSCs in the bone marrow by the TME is accompanied by metabolic and epigenetic modifications that lead to the remodeling of MDSC characteristics. Activation of AMP-activated protein kinase (AMPK), an energy receptor, connects metabolism with epigenetics in MDSCs by increasing metabolite Acetyl-COA, a substrate for epigenetic modifying enzymes such as histone acetyltransferases (HATs) or lysine acetyltransferase (KATs) (400). The change in function of MDSC from modifications of epigenetics and metabolism was demonstrated in a study where NAD-dependent deacetylase sirtuin-1 (SIRT1) reduction decreased the inhibitory capabilities of MDSC, switching it to a more M1-like macrophage (401). More evidence of this functional switch was shown in multiple publications in which cancer

vaccine adjuvant Resiquimod (R848) significantly hindered MDSC function by differentiating them into dendritic cells and macrophages (358, 402). Moreover, chapter II clearly shows that the addition of adjuvants to full-length protein ovalbumin had significantly lower percentages of MDSCs twenty-one post tumor implantation than vaccine alone, demonstrating the potential durable effects **(Fig.2-8E)**. These cumulative data set a precedent that the TME can reprogram cells in the bone marrow and induce epigenetic and metabolic changes leading to functional variations but can be re-reprogrammed by therapeutic cancer vaccines. This phenomenon has been shown primarily in the myeloid department, but can something similar happen to T cell precursors in the bone marrow?

Figure 4-2

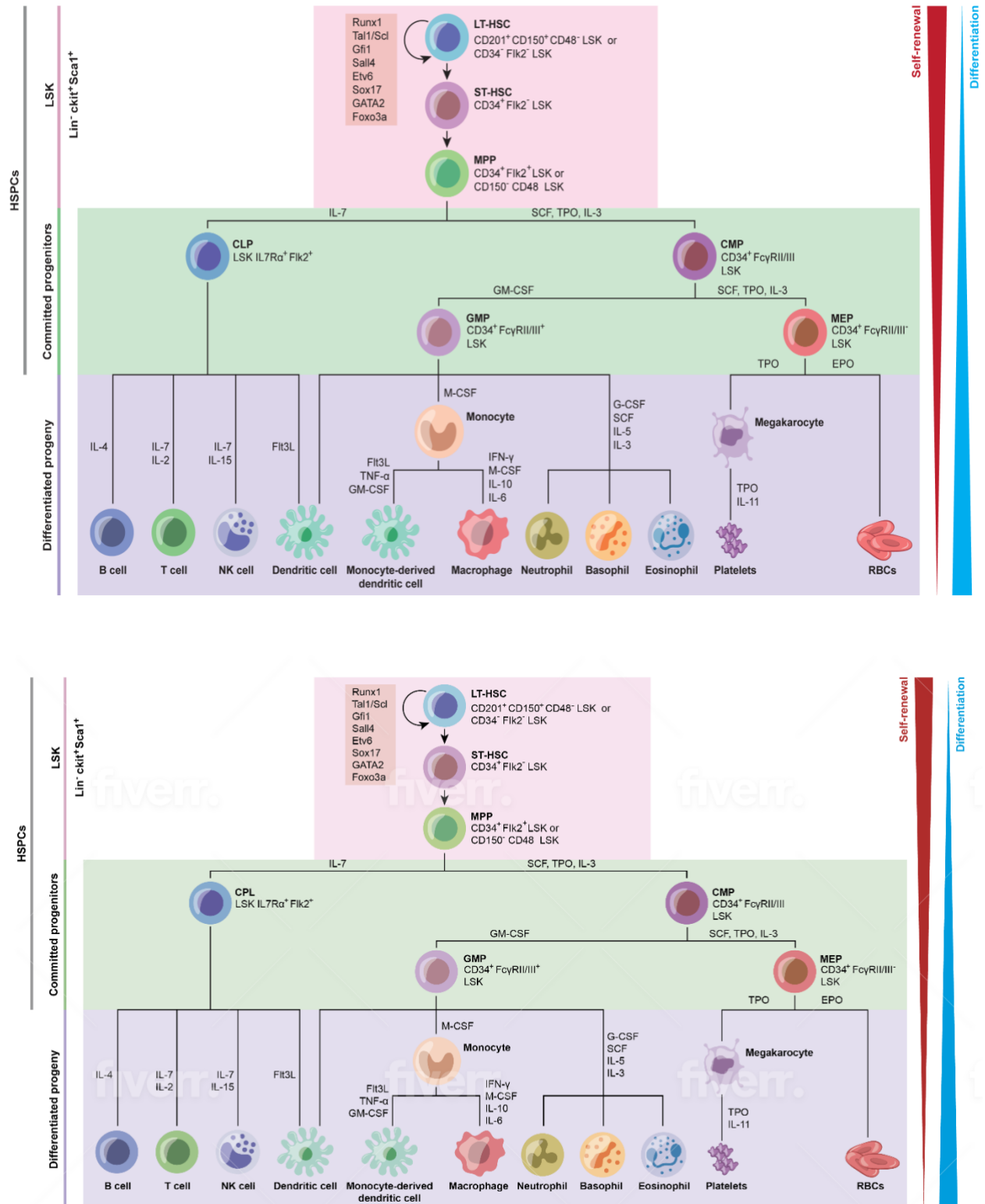


Figure 4- 2: The hierarchy of hematopoiesis

Figure 4-2: In the classical “stepwise” model of hematopoiesis, long-term hematopoietic stem cells (LT-HSCs) are at the top of the hierarchy. LT-HSCs can self-renew or differentiate into short-term HSCs (ST-HSCs), with the less self-renewing capability. ST-HSC subsequently differentiates into multi-potent progenitors (MPPs), which have an inferior self-renewing capacity to ST-HSC. These three groups of HSCs can generate all blood cells. The initial stage of lineage commitment occurs downstream of MPP, where there is a stringent division between common lymphoid progenitor (CLP) and common myeloid progenitor (CMPs) branches. CLPs differentiate into dendritic cells (DCs), natural killer cells (NK cells), T cells, and B cells. CMPs can give rise to granulocyte-macrophage progenitor (GMP) or megakaryocyte erythrocyte progenitor (MEP). GMP generates granulocytes, macrophages, and DCs. MEP produces platelets/megakaryocytes and red blood cells (RBCs). The stepwise hierarchy differentiation processes are controlled by various extrinsic cytokines and inherent transcription, metabolic, and epigenetic factors.

Our lab performed preliminary experiments on the therapeutic vaccine effect on the bone marrow in non-tumor-bearing mice. Mice were intraperitoneally vaccinated with PBS,  $\beta$ -glucan, GVAX, CDN, or CDN plus GVAX (STINGVAX). The bone marrow was extracted and analyzed twenty-four hours post-injection (**Fig.4-3**). Results showed that the LSK hematopoietic stem cell percentage ( $\text{Lin}^- \text{Sca}^1 + \text{ckit}^+$ ) of total live bone marrow cells was significantly higher with STINGVAX compared to PBS,  $\beta$ -glucan, GVAX, and CDN alone (**Fig.4-4 A-B**). This trend was similar to the absolute count for LSK (**Fig.4-4 B**). Next, we measured lymphopoiesis,  $\text{CD48}^+ \text{CD150}^- \text{Flt3}^+ \text{LSK}$  lymphoid-biased cells, and demonstrated that STINGVAX substantially enhanced lymphopoiesis compared to all the other treatment groups (**Fig.4-5**). Interestingly, this boost in the generation of

lymphoid committed cells requires both an antigen source and an adjuvant, as the individual components, GVAX or CDN alone) failed to induce lymphopoiesis. This substantial increase in the generation of lymphoid cells clearly indicates that STINGVAX caused significant changes to the bone marrow. Are these new lymphoid cells generated metabolically and epigenetically different from those produced in normal hematopoiesis? Are they functionally unique? Are they less susceptible to becoming terminally exhausted? Further studies have to be executed to answer these pertinent questions.

Figure 4-3

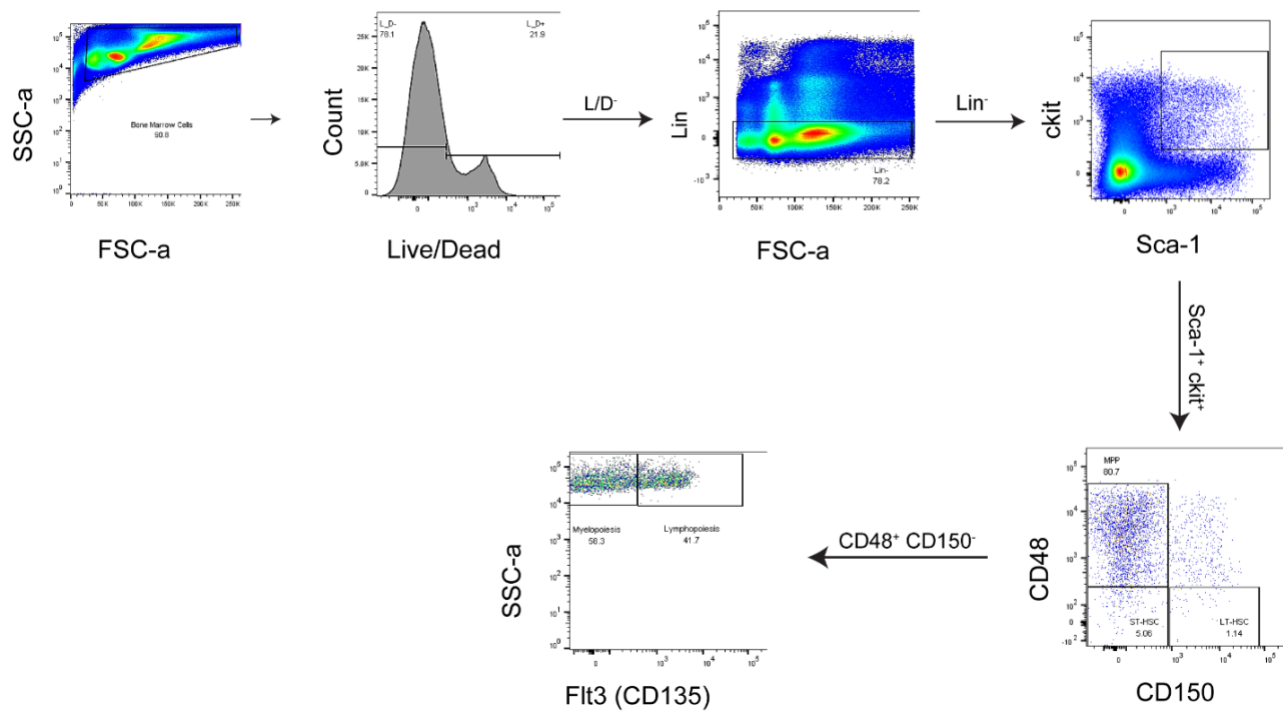


Figure 4- 3: Mouse hematopoietic stem cell (HSC) gating

Figure 4-3: Bone marrow cells were gated on live cells. Next, we gated on Lineage negative (Lin<sup>-</sup>) cells, excluding T cells, B cells, monocytes/macrophages, granulocytes, NK cells, and erythrocytes. Lin<sup>-</sup> cells were further gated on Sca1<sup>+</sup>ckit<sup>+</sup> (LSK) which are considered HSCs. The LSK HSCs were categorized into the following three groups: LT-HSC (CD48<sup>-</sup>CD150<sup>+</sup>LSK), ST-HSC (CD48<sup>+</sup>CD150<sup>-</sup>LSK), and MPP (CD48<sup>-</sup>CD150<sup>+</sup>LSK). The MPP was further divided into two groups Flt3<sup>+</sup>MPP (Lymphoid-biased) and Flt3<sup>-</sup>MPP (Myeloid-biased). Note- LT: long-term; ST: short-term; MPP: multi-potent progenitor.

Figure 4-4

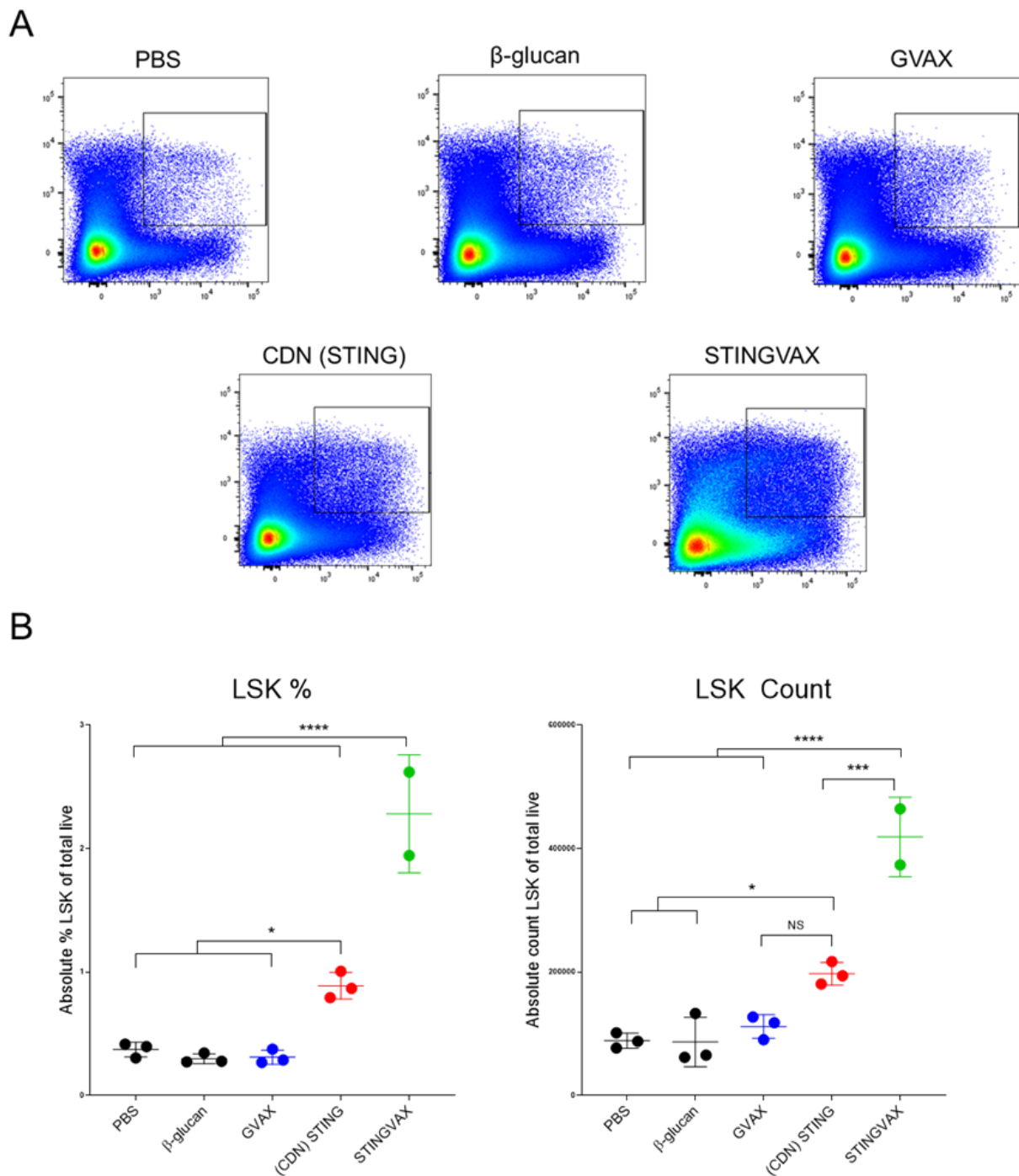


Figure 4- 4: STINGVAX significantly boosts LSK HSCs in the bone marrow

Figure 4-4: Non-tumor-bearing mice were intraperitoneally injected with PBS,  $\beta$ -glucan, GVAX, CDN (STING), and GVAX plus CDN (STINGVAX). Twenty-four hours post-injection, mice were euthanized, and the bone marrow was analyzed. **A)** Flow plots displaying the live Lin<sup>-</sup>Sca1<sup>+</sup>ckit<sup>+</sup> (LSK) HSCs populations. **B)** Cumulative LSK absolute percentage and count of total live. All data are given in mean  $\pm$  S.D. of biological replicates. \*P < 0.05, \*\*P < 0.01, \*\*\*P < 0.001, \*\*\*\*P < 0.0001, one-way analysis of variance for multiple comparisons.

Figure 4-5

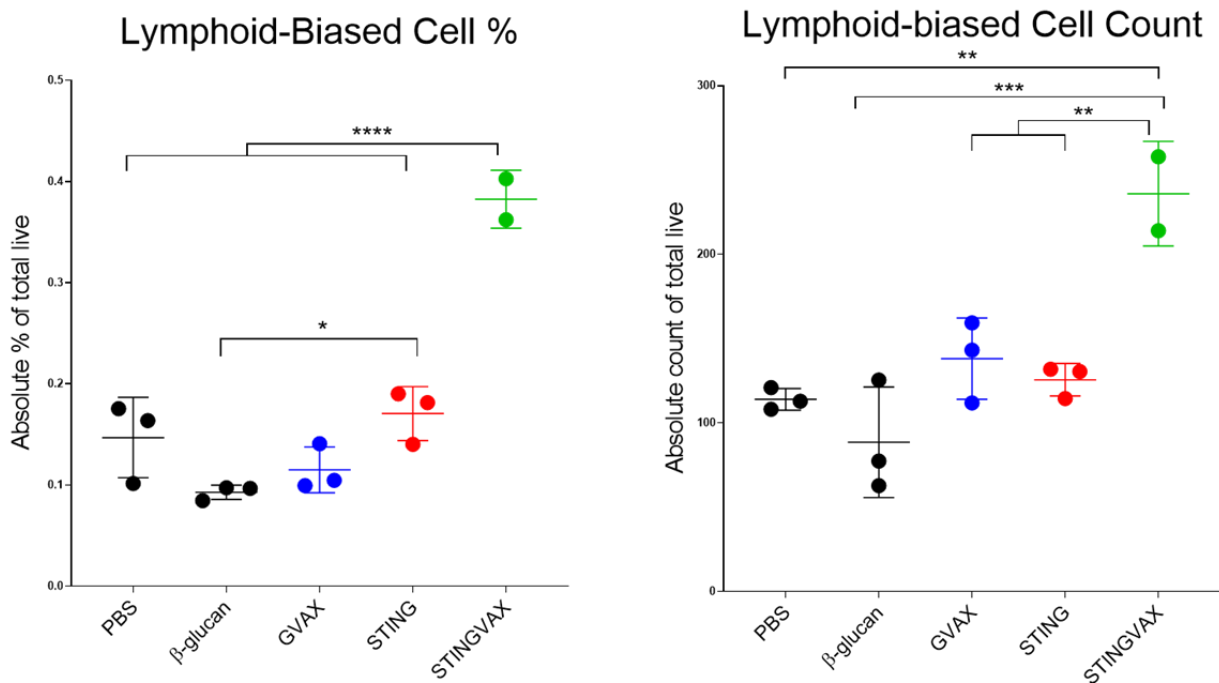


Figure 4- 5: STINGVAX significantly enhances lymphopoiesis

Figure 4-5: Non-tumor-bearing mice were intraperitoneally injected with PBS,  $\beta$ -glucan, GVAX, CDN (STING), and GVAX plus CDN (STINGVAX). Twenty-four hours post-injection, mice were euthanized, and the bone marrow was analyzed. Bone marrow cells were gate on lymphoid-biased cells (Lin<sup>-</sup>Sca-1<sup>+</sup>ckit<sup>+</sup>CD48<sup>-</sup>CD150<sup>+</sup>Flt3<sup>+</sup>). The absolute percentage and count of total live are shown. All data are given in mean  $\pm$  S.D. of biological replicates. \*P < 0.05, \*\*P < 0.01, \*\*\*P < 0.001, \*\*\*\*P < 0.0001, one-way analysis of variance for multiple

STINGVAX also significantly induces myelopoiesis (**Fig.4-6**) in the bone marrow, which has been demonstrated in multiple published articles to be an integral component in the process of trained immunity (403-405). Trained immunity refers to the the long-term functional reprogramming of innate immune cells (406) where pathogen-stimulated innate immune cells (i.e., macrophages and monocytes) have an augmented secondary challenge to the same or unrelated immunological stimuli (407, 408). This enhanced immune response, primarily boosted cytokine secretion, is associated with extensive intracellular epigenetic and metabolic reprogramming (409, 410). In contrast, some immunological stimuli, such as TLR4 agonist Lipopolysaccharide (LPS), have the opposite effect, where it leads tolerant innate immune cells (411). Therefore, more in-depth system biology analyses must be performed on the bone marrow and tumor microenvironment to identify epigenetic and metabolic programs that induce tolerance or superior functioning immune cells. In the future, we can discover therapeutics to counteract those resistant mechanisms and biomarkers for improved functioning of immune cells.

Figure 4-6

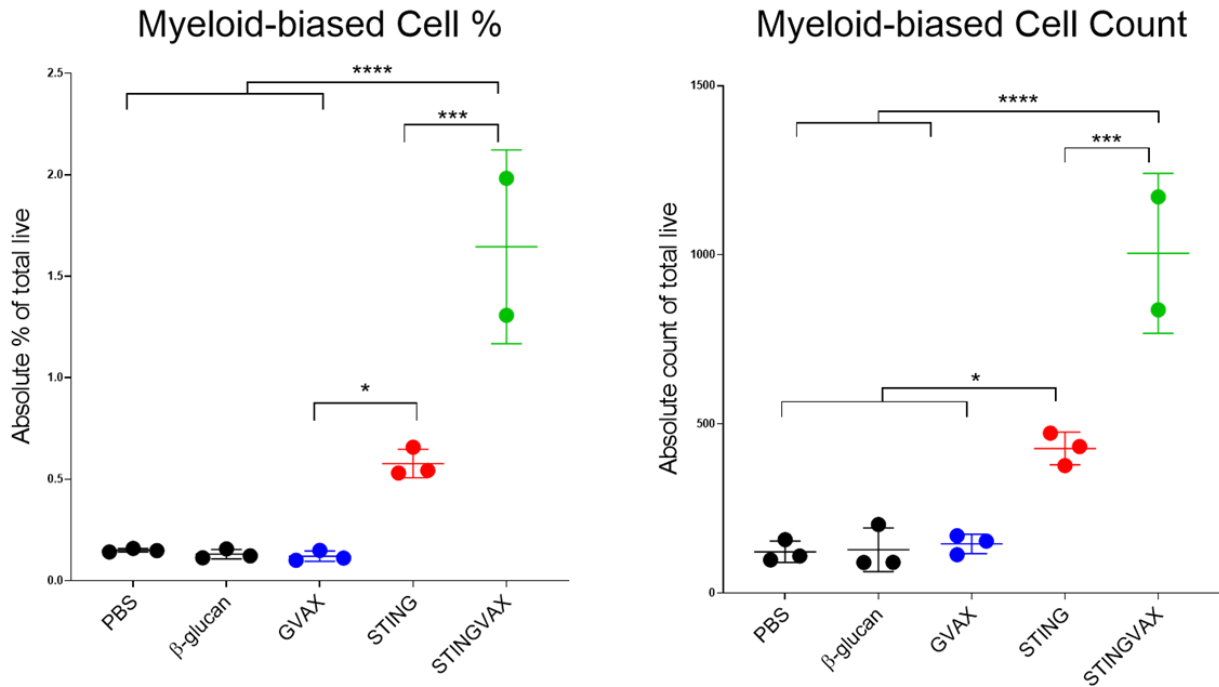


Figure 4- 6: STINGVAX significantly enhances myelopoiesis

Figure 4-6: Non-tumor-bearing mice were intraperitoneally injected with PBS,  $\beta$ -glucan, GVAX, CDN (STING), and GVAX plus CDN (STINGVAX). Twenty-four hours post-injection, mice were euthanized and the bone marrow was analyzed. Bone marrow cells were gate on myeloid-biased cells ( $\text{Lin}^- \text{Sca-1}^+ \text{ckit}^+ \text{CD48}^- \text{CD150}^+ \text{Flt3}^-$ ). The absolute percentage and count of total live are shown. All data are given in mean  $\pm$  S.D. of biological replicates. \*P < 0.05, \*\*P < 0.01, \*\*\*P < 0.001, \*\*\*\*P < 0.0001, one-way analysis of variance for multiple

### Combination with epigenetic modulators, metabolic modulators, and cytokine/chemokine blockers to improve antitumor responses

In chapters II and III, we introduced two novel immunotherapies, MuSyC-dose CDN(STING) plus R848 (TLR7/8). As stated earlier in this section, it is vital to discover

new epigenetic and metabolic targets to enhance the immunogenicity and anticancer effects of these novel and current immunotherapies. For instance, various tumor microenvironments are riddled with MDSCs that secrete immunosuppressive cytokines and express checkpoint proteins, inhibiting NK and effector T cell functions, thereby promoting tumor growth. Earlier, we stated that MDSCs are generated in the bone marrow through chronic secretion of proinflammatory cytokines derived from the TME or chronic infections causing emergency myelopoiesis (398, 399). One potential combinatorial strategy is blocking the cytokines generating MDSCs, such as GM-CSF and G-CSF. Multiple mouse pancreatic tumor models demonstrated that anti-GM-CSF or GM-CSF knockdown reduced the accumulation of tumor-infiltrating MDSCs in a CD8 T cell-dependent manner (412, 413). A phase I clinical trial for chronic myelomonocytic leukemia (CMML) testing an anti-GM-CSF monoclonal antibody (Lenzilumab) determined that the treatment was well tolerated without any grade 3-4 adverse events (NCT02546284) (414). However, this cytokine is involved in developing and recruiting other myeloid cells. It has yet to be determined if it's efficacious or a viable long-term treatment option.

Another strategy is to block MDSC trafficking to the tumor. Cancer cells recruit CCR2<sup>+</sup> MDSCs through a chemokine gradient cascade (415, 416). Therefore, blocking CCR2 can stop MDSC trafficking to the tumor, thereby not allowing it to induce its protumoral effects in the TME. Recent articles demonstrated that CCR2 deficient mice or CCR2 antagonism reduced MDSC tumor infiltration (417) and enhanced the response to anti-PD-1 therapy (417, 418). Based on these and other similar preclinical findings, two

prominent universities, Mount Sinai and John Hopkins, are conducting clinical trials of interest to this thesis because the trials are combining anti-CCR2 with anti-PD-1 (Nivolumab) (NCT04123379) or Nivolumab plus GVAX (NCT03767582). Unfortunately, these trials are ongoing, and no results or correlatives have been posted.

Previously in this thesis chapter, we specified that the functional characteristics of MDSCs can be modulated through fluctuations in epigenetics and metabolism (400). Epigenetically, the differentiation of immature myeloid cells to MDSCs required a decreased expression of histone deacetylase 11 (HDAC11), which indicates that it may be vital for MDSC development (419). Hence, therapies to enhance the production of HDAC11 may be a potent strategy for reducing MDSC expansion. Conversely, most epigenetic modulation of MDSCs focuses on inhibiting HDACs (HDACi). For instance, multiple preclinical mouse tumor studies have shown that the HDAC inhibitor, Entinostat, significantly reduces the MDSC expression of ARG-1, iNOS, and COX2, enhancing the effects of anti-PD-1 checkpoint blockade (420, 421). Clinically, the combination of anti-PD-1 (pembrolizumab) and Entinostat did not meet the primary endpoint but had an objective response rate of 9% with no new toxicities in anti-PD-L1-experienced metastatic non-small cell lung cancer (NSCLC) patients (NCT02437136) (422). Future correlative must be performed in this study to evaluate the association of the response to specific immune infiltrates. Although HDAC inhibitors have seen some clinical success, not all immune cells have the same beneficial effects depending on the particular HDACi (423). Further analyses are required to identify rational mechanisms for specific immunotherapy combinations.

Researchers have targeted the metabolism of MDSCs to alter their function. They've targeted fatty acids, glycolysis mediators, amino acid catabolism, and nucleic acids. In particular, enzymes involved in glycolysis are highly expressed in MDSCs, allowing the MDSCs to have a high rate of glycolysis, avoid ROS-mediated apoptosis, and expand in cancer patients (424). Moreover, HIF-1 $\alpha$  regulates glycolysis but can be inhibited by AMPK. Therefore, utilizing an agonist of AMPK can potentially reverse the beneficial glycolytic effects in MDSCs. In multiple preclinical mouse tumor models, Metformin, an AMPK agonist commonly used to treat diabetes, hindered the expansion and immunosuppressive effects of MDSCs (425, 426).

Interestingly, there is anecdotal evidence that AMPK activation can improve the metabolic fitness of other immune cells, including cytolytic CD8<sup>+</sup> T cells. For instance, in several published articles, anti-PD-1 therapy enhanced cytotoxic T cell fatty acid oxidation and mitochondrial biogenesis through the induction of peroxisome proliferator-activated receptors (PPAR) (427, 428). The mechanism by which this may occur is AMPK post-translationally regulates PPARG coactivator 1 alpha (PGC1 $\alpha$ ), which, when PGC1 $\alpha$ /PPAR is activated, can increase fatty acid oxidation and mitochondrial respiratory capacity. However, future studies have to be performed to determine the validity of this hypothesis. A more prominent example of improving the metabolic fitness of T cells is the use of glutaminase inhibitors. Unfortunately, glutaminase metabolizes glutamine, an amino acid required for T cell function, and depleting

glutamine can't be rescued by glutamine precursors (429). Multiple drugs have been developed to block glutamine and restore T cell function. For instance, various studies using pharmacological drugs (i.e. CB-839 or JHU083) demonstrated that inhibiting glutamine metabolism improved CTL killing activity by enhancing its metabolic fitness (i.e., up-regulating oxidative metabolism) (430, 431). Multiple ongoing trials are testing the clinical efficacy of these agents. Overall, this chapter indicates the importance of in-depth systems biology approaches to improve our understanding of immune activation and protumoral mechanisms and identify therapeutics to counteract those protumoral mechanisms (**Fig.4-7**).

Figure 4-7

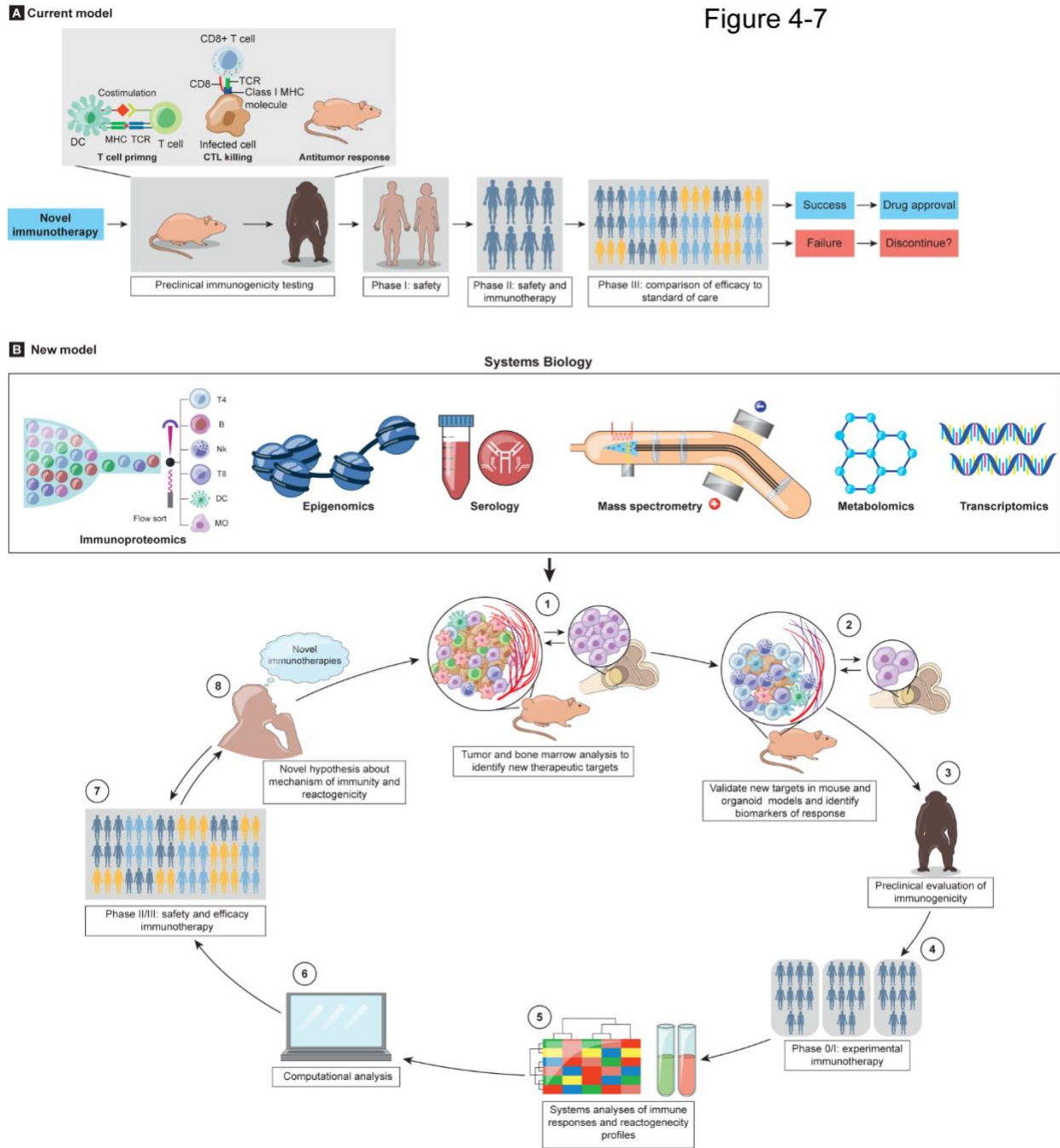


Figure 4- 7: New model for discovering and validating immunotherapies

Figure 4-7: **A)** Current model of developing novel immunotherapies, where standard experiments are used as the primary assays for determining immunogenicity in mice. This process leads to a linear progression ending in the clinic. **B)** The new model uses systems biology approaches at every process step. Also, the bone marrow is examined instead of the tumor alone being analyzed in the mouse models. This process leads to a cyclic cycle where clinical results produce new therapeutic ideas.

## REFERENCES

1. Kavanagh K, Pollock KG, Cuschieri K, Palmer T, Cameron RL, Watt C, et al. Changes in the prevalence of human papillomavirus following a national bivalent human papillomavirus vaccination programme in Scotland: a 7-year cross-sectional study. *Lancet Infect Dis.* 2017;17(12):1293-302.
2. Dehlendorff C, Baandrup L, Kjaer SK. Real-World Effectiveness of Human Papillomavirus Vaccination Against Vulvovaginal High-Grade Precancerous Lesions and Cancers. *J Natl Cancer Inst.* 2021;113(7):869-74.
3. Rosenberg SA, Yang JC, Restifo NP. Cancer immunotherapy: moving beyond current vaccines. *Nat Med.* 2004;10(9):909-15.
4. Guo C, Manjili MH, Subjeck JR, Sarkar D, Fisher PB, Wang XY. Therapeutic cancer vaccines: past, present, and future. *Adv Cancer Res.* 2013;119:421-75.
5. Pan RY, Chung WH, Chu MT, Chen SJ, Chen HC, Zheng L, et al. Recent Development and Clinical Application of Cancer Vaccine: Targeting Neoantigens. *J Immunol Res.* 2018;2018:4325874.
6. Melero I, Gaudernack G, Gerritsen W, Huber C, Parmiani G, Scholl S, et al. Therapeutic vaccines for cancer: an overview of clinical trials. *Nat Rev Clin Oncol.* 2014;11(9):509-24.
7. Hollingsworth RE, Jansen K. Turning the corner on therapeutic cancer vaccines. *NPJ Vaccines.* 2019;4:7.
8. Wei X, Chen F, Xin K, Wang Q, Yu L, Liu B, et al. Cancer-Testis Antigen Peptide Vaccine for Cancer Immunotherapy: Progress and Prospects. *Transl Oncol.* 2019;12(5):733-8.
9. Li F, Li C, Cai X, Xie Z, Zhou L, Cheng B, et al. The association between CD8+ tumor-infiltrating lymphocytes and the clinical outcome of cancer immunotherapy: A systematic review and meta-analysis. *EClinicalMedicine.* 2021;41:101134.
10. Dubensky TW, Jr., Reed SG. Adjuvants for cancer vaccines. *Semin Immunol.* 2010;22(3):155-61.
11. Rahman K, Iyer SS. Costimulatory molecules as vaccine adjuvants: to 4-1BB or not to 4-1BB? *Cell Mol Immunol.* 2015;12(4):508-9.
12. Chiang CL, Coukos G, Kandalaft LE. Whole Tumor Antigen Vaccines: Where Are We? *Vaccines (Basel).* 2015;3(2):344-72.
13. Chiang CL, Benencia F, Coukos G. Whole tumor antigen vaccines. *Semin Immunol.* 2010;22(3):132-43.
14. Buckwalter MR, Srivastava PK. "It is the antigen(s), stupid" and other lessons from over a decade of vaccitherapy of human cancer. *Semin Immunol.* 2008;20(5):296-300.
15. Dranoff G, Jaffee E, Lazenby A, Golumbek P, Levitsky H, Brose K, et al. Vaccination with irradiated tumor cells engineered to secrete murine granulocyte-macrophage colony-stimulating factor stimulates potent, specific, and long-lasting anti-tumor immunity. *Proc Natl Acad Sci U S A.* 1993;90(8):3539-43.
16. Armstrong CA, Botella R, Galloway TH, Murray N, Kramp JM, Song IS, et al. Antitumor effects of granulocyte-macrophage colony-stimulating factor production by melanoma cells. *Cancer Res.* 1996;56(9):2191-8.

17. Sanda MG, Ayyagari SR, Jaffee EM, Epstein JI, Clift SL, Cohen LK, et al. Demonstration of a rational strategy for human prostate cancer gene therapy. *J Urol*. 1994;151(3):622-8.
18. Dunussi-Joannopoulos K, Dranoff G, Weinstein HJ, Ferrara JL, Bierer BE, Croop JM. Gene immunotherapy in murine acute myeloid leukemia: granulocyte-macrophage colony-stimulating factor tumor cell vaccines elicit more potent antitumor immunity compared with B7 family and other cytokine vaccines. *Blood*. 1998;91(1):222-30.
19. Dranoff G. GM-CSF-based cancer vaccines. *Immunol Rev*. 2002;188:147-54.
20. Soiffer R, Hodi FS, Haluska F, Jung K, Gillessen S, Singer S, et al. Vaccination with irradiated, autologous melanoma cells engineered to secrete granulocyte-macrophage colony-stimulating factor by adenoviral-mediated gene transfer augments antitumor immunity in patients with metastatic melanoma. *J Clin Oncol*. 2003;21(17):3343-50.
21. Soiffer R, Lynch T, Mihm M, Jung K, Rhuda C, Schmollinger JC, et al. Vaccination with irradiated autologous melanoma cells engineered to secrete human granulocyte-macrophage colony-stimulating factor generates potent antitumor immunity in patients with metastatic melanoma. *Proc Natl Acad Sci U S A*. 1998;95(22):13141-6.
22. Thomas AM, Santarsiero LM, Lutz ER, Armstrong TD, Chen YC, Huang LQ, et al. Mesothelin-specific CD8(+) T cell responses provide evidence of in vivo cross-priming by antigen-presenting cells in vaccinated pancreatic cancer patients. *J Exp Med*. 2004;200(3):297-306.
23. Eager R, Nemunaitis J. GM-CSF gene-transduced tumor vaccines. *Mol Ther*. 2005;12(1):18-27.
24. Hege KM, Jooss K, Pardoll D. GM-CSF gene-modified cancer cell immunotherapies: of mice and men. *Int Rev Immunol*. 2006;25(5-6):321-52.
25. Laheru D, Lutz E, Burke J, Biedrzycki B, Solt S, Onners B, et al. Allogeneic granulocyte macrophage colony-stimulating factor-secreting tumor immunotherapy alone or in sequence with cyclophosphamide for metastatic pancreatic cancer: a pilot study of safety, feasibility, and immune activation. *Clin Cancer Res*. 2008;14(5):1455-63.
26. Lipson EJ, Sharfman WH, Chen S, McMiller TL, Pritchard TS, Salas JT, et al. Safety and immunologic correlates of Melanoma GVAX, a GM-CSF secreting allogeneic melanoma cell vaccine administered in the adjuvant setting. *J Transl Med*. 2015;13:214.
27. Small EJ, Sacks N, Nemunaitis J, Urba WJ, Dula E, Centeno AS, et al. Granulocyte macrophage colony-stimulating factor--secreting allogeneic cellular immunotherapy for hormone-refractory prostate cancer. *Clin Cancer Res*. 2007;13(13):3883-91.
28. Salgia R, Lynch T, Skarin A, Lucca J, Lynch C, Jung K, et al. Vaccination with irradiated autologous tumor cells engineered to secrete granulocyte-macrophage colony-stimulating factor augments antitumor immunity in some patients with metastatic non-small-cell lung carcinoma. *Journal of clinical oncology : official journal of the American Society of Clinical Oncology*. 2003;21(4):624-30.
29. Le DT, Picozzi VJ, Ko AH, Wainberg ZA, Kindler H, Wang-Gillam A, et al. Results from a Phase IIb, Randomized, Multicenter Study of GVAX Pancreas and CRS-207 Compared with Chemotherapy in Adults with Previously Treated Metastatic Pancreatic Adenocarcinoma (ECLIPSE Study). *Clin Cancer Res*. 2019.

30. Hoover HC, Jr., Surdyke MG, Dangel RB, Peters LC, Hanna MG, Jr. Prospectively randomized trial of adjuvant active-specific immunotherapy for human colorectal cancer. *Cancer*. 1985;55(6):1236-43.
31. Hoover HC, Jr., Brandhorst JS, Peters LC, Surdyke MG, Takeshita Y, Madariaga J, et al. Adjuvant active specific immunotherapy for human colorectal cancer: 6.5-year median follow-up of a phase III prospectively randomized trial. *Journal of clinical oncology : official journal of the American Society of Clinical Oncology*. 1993;11(3):390-9.
32. Vermorken JB, Claessen AM, van Tinteren H, Gall HE, Ezinga R, Meijer S, et al. Active specific immunotherapy for stage II and stage III human colon cancer: a randomised trial. *Lancet*. 1999;353(9150):345-50.
33. Van Poppel H, Joniau S, Van Gool SW. Vaccine therapy in patients with renal cell carcinoma. *Eur Urol*. 2009;55(6):1333-42.
34. May M, Kendel F, Hoschke B, Gilfrich C, Kiessig S, Pflanz S, et al. [Adjuvant autologous tumour cell vaccination in patients with renal cell carcinoma. Overall survival analysis with a follow-up period in excess of more than 10 years]. *Urologe A*. 2009;48(9):1075-83.
35. Simons JW, Jaffee EM, Weber CE, Levitsky HI, Nelson WG, Carducci MA, et al. Bioactivity of autologous irradiated renal cell carcinoma vaccines generated by ex vivo granulocyte-macrophage colony-stimulating factor gene transfer. *Cancer research*. 1997;57(8):1537-46.
36. Bol KF, Schreiber G, Gerritsen WR, de Vries IJ, Figdor CG. Dendritic Cell-Based Immunotherapy: State of the Art and Beyond. *Clin Cancer Res*. 2016;22(8):1897-906.
37. van Willigen WW, Bloemendal M, Gerritsen WR, Schreiber G, de Vries IJM, Bol KF. Dendritic Cell Cancer Therapy: Vaccinating the Right Patient at the Right Time. *Front Immunol*. 2018;9:2265.
38. Santos PM, Butterfield LH. Dendritic Cell-Based Cancer Vaccines. *J Immunol*. 2018;200(2):443-9.
39. Mastelic-Gavillet B, Balint K, Boudousquie C, Gannon PO, Kandalaft LE. Personalized Dendritic Cell Vaccines-Recent Breakthroughs and Encouraging Clinical Results. *Front Immunol*. 2019;10:766.
40. Huber A, Dammeijer F, Aerts J, Vroman H. Current State of Dendritic Cell-Based Immunotherapy: Opportunities for in vitro Antigen Loading of Different DC Subsets? *Front Immunol*. 2018;9:2804.
41. Saxena M, Bhardwaj N. Re-Emergence of Dendritic Cell Vaccines for Cancer Treatment. *Trends Cancer*. 2018;4(2):119-37.
42. Ahmed MS, Bae YS. Dendritic cell-based therapeutic cancer vaccines: past, present and future. *Clin Exp Vaccine Res*. 2014;3(2):113-6.
43. Dzionek A, Fuchs A, Schmidt P, Cremer S, Zysk M, Miltenyi S, et al. BDCA-2, BDCA-3, and BDCA-4: three markers for distinct subsets of dendritic cells in human peripheral blood. *J Immunol*. 2000;165(11):6037-46.
44. Lande R, Gregorio J, Facchinetti V, Chatterjee B, Wang YH, Homey B, et al. Plasmacytoid dendritic cells sense self-DNA coupled with antimicrobial peptide. *Nature*. 2007;449(7162):564-9.

45. Nizzoli G, Krietsch J, Weick A, Steinfeld S, Facciotti F, Gruarin P, et al. Human CD1c+ dendritic cells secrete high levels of IL-12 and potently prime cytotoxic T-cell responses. *Blood*. 2013;122(6):932-42.
46. Perussia B, Fanning V, Trinchieri G. A leukocyte subset bearing HLA-DR antigens is responsible for in vitro alpha interferon production in response to viruses. *Nat Immun Cell Growth Regul*. 1985;4(3):120-37.
47. Anguille S, Smits EL, Bryant C, Van Acker HH, Goossens H, Lion E, et al. Dendritic Cells as Pharmacological Tools for Cancer Immunotherapy. *Pharmacol Rev*. 2015;67(4):731-53.
48. Anguille S, Smits EL, Lion E, van Tendeloo VF, Berneman ZN. Clinical use of dendritic cells for cancer therapy. *The Lancet Oncology*. 2014;15(7):e257-67.
49. Koski GK, Cohen PA, Roses RE, Xu S, Czerniecki BJ. Reengineering dendritic cell-based anti-cancer vaccines. *Immunol Rev*. 2008;222:256-76.
50. Garg AD, Coulie PG, Van den Eynde BJ, Agostinis P. Integrating Next-Generation Dendritic Cell Vaccines into the Current Cancer Immunotherapy Landscape. *Trends Immunol*. 2017;38(8):577-93.
51. Butterfield LH. Dendritic cells in cancer immunotherapy clinical trials: are we making progress? *Front Immunol*. 2013;4:454.
52. Lim DS, Kim JH, Lee DS, Yoon CH, Bae YS. DC immunotherapy is highly effective for the inhibition of tumor metastasis or recurrence, although it is not efficient for the eradication of established solid tumors. *Cancer Immunol Immunother*. 2007;56(11):1817-29.
53. Germeau C, Ma W, Schiavetti F, Lurquin C, Henry E, Vigneron N, et al. High frequency of antitumor T cells in the blood of melanoma patients before and after vaccination with tumor antigens. *J Exp Med*. 2005;201(2):241-8.
54. Akasaki Y, Kikuchi T, Homma S, Koido S, Ohkusa T, Tasaki T, et al. Phase I/II trial of combination of temozolomide chemotherapy and immunotherapy with fusions of dendritic and glioma cells in patients with glioblastoma. *Cancer Immunol Immunother*. 2016;65(12):1499-509.
55. Rosenblatt J, Stone RM, Uhl L, Neuberg D, Joyce R, Levine JD, et al. Individualized vaccination of AML patients in remission is associated with induction of antileukemia immunity and prolonged remissions. *Sci Transl Med*. 2016;8(368):368ra171.
56. Crozat K, Guiton R, Williams M, Henri S, Baranek T, Schwartz-Cornil I, et al. Comparative genomics as a tool to reveal functional equivalences between human and mouse dendritic cell subsets. *Immunol Rev*. 2010;234(1):177-98.
57. Osugi Y, Vuckovic S, Hart DN. Myeloid blood CD11c(+) dendritic cells and monocyte-derived dendritic cells differ in their ability to stimulate T lymphocytes. *Blood*. 2002;100(8):2858-66.
58. Villani AC, Satija R, Reynolds G, Sarkizova S, Shekhar K, Fletcher J, et al. Single-cell RNA-seq reveals new types of human blood dendritic cells, monocytes, and progenitors. *Science*. 2017;356(6335).
59. Helft J, Bottcher J, Chakravarty P, Zelenay S, Huotari J, Schraml BU, et al. GM-CSF Mouse Bone Marrow Cultures Comprise a Heterogeneous Population of CD11c(+)MHCII(+) Macrophages and Dendritic Cells. *Immunity*. 2015;42(6):1197-211.

60. Balan S, Ollion V, Colletti N, Chelbi R, Montanana-Sanchis F, Liu H, et al. Human XCR1+ dendritic cells derived in vitro from CD34+ progenitors closely resemble blood dendritic cells, including their adjuvant responsiveness, contrary to monocyte-derived dendritic cells. *J Immunol.* 2014;193(4):1622-35.
61. Collin M, McGovern N, Haniffa M. Human dendritic cell subsets. *Immunology.* 2013;140(1):22-30.
62. Lundberg K, Albrekt AS, Nelissen I, Santegoets S, de Gruijl TD, Gibbs S, et al. Transcriptional profiling of human dendritic cell populations and models--unique profiles of in vitro dendritic cells and implications on functionality and applicability. *PLoS One.* 2013;8(1):e52875.
63. Jongbloed SL, Kassianos AJ, McDonald KJ, Clark GJ, Ju X, Angel CE, et al. Human CD141+ (BDCA-3)+ dendritic cells (DCs) represent a unique myeloid DC subset that cross-presents necrotic cell antigens. *J Exp Med.* 2010;207(6):1247-60.
64. Orsini E, Guarini A, Chiaretti S, Mauro FR, Foa R. The circulating dendritic cell compartment in patients with chronic lymphocytic leukemia is severely defective and unable to stimulate an effective T-cell response. *Cancer research.* 2003;63(15):4497-506.
65. Schreibelt G, Bol KF, Westdorp H, Wimmers F, Aarntzen EH, Duiveman-de Boer T, et al. Effective Clinical Responses in Metastatic Melanoma Patients after Vaccination with Primary Myeloid Dendritic Cells. *Clin Cancer Res.* 2016;22(9):2155-66.
66. Tel J, Aarntzen EH, Baba T, Schreibelt G, Schulte BM, Benitez-Ribas D, et al. Natural human plasmacytoid dendritic cells induce antigen-specific T-cell responses in melanoma patients. *Cancer research.* 2013;73(3):1063-75.
67. Di Nicola M, Carlo-Stella C, Mortarini R, Baldassari P, Guidetti A, Gallino GF, et al. Boosting T cell-mediated immunity to tyrosinase by vaccinia virus-transduced, CD34(+)-derived dendritic cell vaccination: a phase I trial in metastatic melanoma. *Clin Cancer Res.* 2004;10(16):5381-90.
68. Mackensen A, Herbst B, Chen JL, Kohler G, Noppen C, Herr W, et al. Phase I study in melanoma patients of a vaccine with peptide-pulsed dendritic cells generated in vitro from CD34(+) hematopoietic progenitor cells. *Int J Cancer.* 2000;86(3):385-92.
69. Balan S, Arnold-Schrauf C, Abbas A, Couespel N, Savoret J, Imperatore F, et al. Large-Scale Human Dendritic Cell Differentiation Revealing Notch-Dependent Lineage Bifurcation and Heterogeneity. *Cell Rep.* 2018;24(7):1902-15 e6.
70. Kirkling ME, Cytlak U, Lau CM, Lewis KL, Resteu A, Khodadadi-Jamayran A, et al. Notch Signaling Facilitates In Vitro Generation of Cross-Presenting Classical Dendritic Cells. *Cell Rep.* 2018;23(12):3658-72 e6.
71. Proietto AI, Mittag D, Roberts AW, Sprigg N, Wu L. The equivalents of human blood and spleen dendritic cell subtypes can be generated in vitro from human CD34(+) stem cells in the presence of fms-like tyrosine kinase 3 ligand and thrombopoietin. *Cell Mol Immunol.* 2012;9(6):446-54.
72. Lee AW, Truong T, Bickham K, Fonteneau JF, Larsson M, Da Silva I, et al. A clinical grade cocktail of cytokines and PGE2 results in uniform maturation of human monocyte-derived dendritic cells: implications for immunotherapy. *Vaccine.* 2002;20 Suppl 4:A8-A22.
73. Jongmans W, Tiemessen DM, van Vlodrop IJ, Mulders PF, Oosterwijk E. Th1-polarizing capacity of clinical-grade dendritic cells is triggered by Ribomunyl but is

- compromised by PGE2: the importance of maturation cocktails. *J Immunother.* 2005;28(5):480-7.
74. Krause P, Singer E, Darley PI, Klebensberger J, Groettrup M, Legler DF. Prostaglandin E2 is a key factor for monocyte-derived dendritic cell maturation: enhanced T cell stimulatory capacity despite IDO. *J Leukoc Biol.* 2007;82(5):1106-14.
75. Carreno BM, Becker-Hapak M, Huang A, Chan M, Alyasiry A, Lie WR, et al. IL-12p70-producing patient DC vaccine elicits Tc1-polarized immunity. *J Clin Invest.* 2013;123(8):3383-94.
76. Kolanowski ST, Sritharan L, Lissenberg-Thunnissen SN, Van Schijndel GM, Van Ham SM, ten Brinke A. Comparison of media and serum supplementation for generation of monophosphoryl lipid A/interferon-gamma-matured type I dendritic cells for immunotherapy. *Cytotherapy.* 2014;16(6):826-34.
77. Mailliard RB, Wankowicz-Kalinska A, Cai Q, Wesa A, Hilkens CM, Kapsenberg ML, et al. alpha-type-1 polarized dendritic cells: a novel immunization tool with optimized CTL-inducing activity. *Cancer research.* 2004;64(17):5934-7.
78. Wilgenhof S, Corthals J, Heirman C, van Baren N, Lucas S, Kvistborg P, et al. Phase II Study of Autologous Monocyte-Derived mRNA Electroporated Dendritic Cells (TriMixDC-MEL) Plus Ipilimumab in Patients With Pretreated Advanced Melanoma. *Journal of clinical oncology : official journal of the American Society of Clinical Oncology.* 2016;34(12):1330-8.
79. Wilgenhof S, Van Nuffel AM, Benteyn D, Corthals J, Aerts C, Heirman C, et al. A phase IB study on intravenous synthetic mRNA electroporated dendritic cell immunotherapy in pretreated advanced melanoma patients. *Ann Oncol.* 2013;24(10):2686-93.
80. Massa C, Thomas C, Wang E, Marincola F, Seliger B. Different maturation cocktails provide dendritic cells with different chemoattractive properties. *J Transl Med.* 2015;13:175.
81. Van Nuffel AM, Benteyn D, Wilgenhof S, Corthals J, Heirman C, Neyns B, et al. Intravenous and intradermal TriMix-dendritic cell therapy results in a broad T-cell response and durable tumor response in a chemorefractory stage IV-M1c melanoma patient. *Cancer Immunol Immunother.* 2012;61(7):1033-43.
82. Koido S. Dendritic-Tumor Fusion Cell-Based Cancer Vaccines. *Int J Mol Sci.* 2016;17(6).
83. Lee JM, Lee MH, Garon E, Goldman JW, Salehi-Rad R, Baratelli FE, et al. Phase I Trial of Intratumoral Injection of CCL21 Gene-Modified Dendritic Cells in Lung Cancer Elicits Tumor-Specific Immune Responses and CD8(+) T-cell Infiltration. *Clin Cancer Res.* 2017;23(16):4556-68.
84. Chiang CL, Kandalaft LE, Tanyi J, Hagemann AR, Motz GT, Svoronos N, et al. A dendritic cell vaccine pulsed with autologous hypochlorous acid-oxidized ovarian cancer lysate primes effective broad antitumor immunity: from bench to bedside. *Clin Cancer Res.* 2013;19(17):4801-15.
85. Zhao L, Niu C, Shi X, Xu D, Li M, Cui J, et al. Dendritic cells loaded with the lysate of tumor cells infected with Newcastle Disease Virus trigger potent anti-tumor immunity by promoting the secretion of IFN-gamma and IL-2 from T cells. *Oncol Lett.* 2018;16(1):1180-8.

86. Tanyi JL, Bobisse S, Ophir E, Tuyaeerts S, Roberti A, Genolet R, et al. Personalized cancer vaccine effectively mobilizes antitumor T cell immunity in ovarian cancer. *Sci Transl Med*. 2018;10(436).
87. Liao LM, Ashkan K, Tran DD, Campian JL, Trusheim JE, Cobbs CS, et al. First results on survival from a large Phase 3 clinical trial of an autologous dendritic cell vaccine in newly diagnosed glioblastoma. *J Transl Med*. 2018;16(1):142.
88. Overwijk WW, Wang E, Marincola FM, Rammensee HG, Restifo NP. Mining the mutanome: developing highly personalized Immunotherapies based on mutational analysis of tumors. *J Immunother Cancer*. 2013;1:11.
89. Carreno BM, Magrini V, Becker-Hapak M, Kaabinejadian S, Hundal J, Petti AA, et al. Cancer immunotherapy. A dendritic cell vaccine increases the breadth and diversity of melanoma neoantigen-specific T cells. *Science*. 2015;348(6236):803-8.
90. Ribas A, Comin-Anduix B, Chmielowski B, Jalil J, de la Rocha P, McCannel TA, et al. Dendritic cell vaccination combined with CTLA4 blockade in patients with metastatic melanoma. *Clin Cancer Res*. 2009;15(19):6267-76.
91. Bruggen Pvd, Traversari C, Chomez P, Lurquin C, Plaen ED, Eynde BVd, et al. A gene encoding an antigen recognized by cytolytic T lymphocytes on a human melanoma. *Science*. 1991;254(5038):1643-7.
92. Kallen K-J, Gnad-Vogt U, Scheel B, Rippin G, Stenzl A. A phase I/IIa study of the mRNA based cancer vaccine CV9103 prepared with the RNActive technology results in distinctly longer survival than predicted by the Halabi Nomogram which correlates with the induction of antigen-specific immune responses. *Journal for ImmunoTherapy of Cancer*. 2013;1(1):P219.
93. Shariat S, Badiee A, Jalali SA, Mansourian M, Yazdani M, Mortazavi SA, et al. P5 HER2/neu-derived peptide conjugated to liposomes containing MPL adjuvant as an effective prophylactic vaccine formulation for breast cancer. *Cancer Letters*. 2014;355(1):54-60.
94. Schmidt SM, Schag K, Müller MR, Weck MM, Appel S, Kanz L, et al. Survivin is a shared tumor-associated antigen expressed in a broad variety of malignancies and recognized by specific cytotoxic T cells. *Blood*. 2003;102(2):571-6.
95. Bakker AB, Schreurs MW, de Boer AJ, Kawakami Y, Rosenberg SA, Adema GJ, et al. Melanocyte lineage-specific antigen gp100 is recognized by melanoma-derived tumor-infiltrating lymphocytes. *J Exp Med*. 1994;179(3):1005-9.
96. Mikolajczyk SD, Rittenhouse HG. Tumor-associated forms of prostate specific antigen improve the discrimination of prostate cancer from benign disease. *Rinsho Byori The Japanese Journal of Clinical Pathology*. 2004;52(3):223-30.
97. Chi DD, Merchant RE, Rand R, Conrad AJ, Garrison D, Turner R, et al. Molecular detection of tumor-associated antigens shared by human cutaneous melanomas and gliomas. *The American Journal of Pathology*. 1997;150(6):2143-52.
98. Jungbluth AA, Busam KJ, Kolb D, Iversen K, Coplan K, Chen Y-T, et al. Expression of MAGE-antigens in normal tissues and cancer. *International Journal of Cancer*. 2000;85(4):460-5.
99. Schultz-Thater E, Noppen C, Gudat F, Dürmüller U, Zajac P, Kocher T, et al. NY-ESO-1 tumour associated antigen is a cytoplasmic protein detectable by specific monoclonal antibodies in cell lines and clinical specimens. *British Journal of Cancer*. 2000;83(2):204-8.

100. Williams RR, McIntire KR, Waldmann TA, Feinleib M, Go VLW, Kannel WB, et al. Tumor-Associated Antigen Levels (Carcinoembryonic Antigen, Human Chorionic Gonadotropin, and Alpha-Fetoprotein) Antedating the Diagnosis of Cancer in the Framingham Study 1. *JNCI: Journal of the National Cancer Institute*. 1977;58(6):1547-51.
101. Kelderman S, Heemskerk B, Fanchi L, Philips D, Toebes M, Kvistborg P, et al. Antigen-specific TIL therapy for melanoma: A flexible platform for personalized cancer immunotherapy. *Eur J Immunol*. 2016;46(6):1351-60.
102. Kelderman S, Kvistborg P. Tumor antigens in human cancer control. *Biochim Biophys Acta*. 2016;1865(1):83-9.
103. Pleasance ED, Cheetham RK, Stephens PJ, McBride DJ, Humphray SJ, Greenman CD, et al. A comprehensive catalogue of somatic mutations from a human cancer genome. *Nature*. 2010;463(7278):191-6.
104. Marchand M, Weynants P, Rankin E, Arienti F, Belli F, Parmiani G, et al. Tumor regression responses in melanoma patients treated with a peptide encoded by gene *MAGES-3*. *International Journal of Cancer*. 1995;63(6):883-5.
105. Parmiani G, Russo V, Maccalli C, Parolini D, Rizzo N, Maio M. Peptide-based vaccines for cancer therapy. *Human Vaccines & Immunotherapeutics*. 2014;10(11):3175-8.
106. Habjanec L, Halassy B, Tomašić J. Immunomodulatory activity of novel adjuvant formulations based on Montanide ISA oil-based adjuvants and peptidoglycan monomer. *International Immunopharmacology*. 2008;8(5):717-24.
107. Sabbatini P, Tsuji T, Ferran L, Ritter E, Sedrak C, Tuballes K, et al. Phase I trial of overlapping long peptides from a tumor self-antigen and poly-ICLC shows rapid induction of integrated immune response in ovarian cancer patients. *Clin Cancer Res*. 2012;18(23):6497-508.
108. Tsuji T, Sabbatini P, Jungbluth AA, Ritter E, Pan L, Ritter G, et al. Effect of Montanide and poly-ICLC adjuvant on human self/tumor antigen-specific CD4+ T cells in phase I overlapping long peptide vaccine trial. *Cancer Immunol Res*. 2013;1(5):340-50.
109. Chamani R, Ranji P, Hadji M, Nahvijou A, Esmati E, Alizadeh AM. Application of E75 peptide vaccine in breast cancer patients: A systematic review and meta-analysis. *European Journal of Pharmacology*. 2018;831:87-93.
110. Khleif SN, Abrams SI, Hamilton JM, Bergmann-Leitner E, Chen A, Bastian A, et al. A phase I vaccine trial with peptides reflecting ras oncogene mutations of solid tumors. *Journal of Immunotherapy (Hagerstown, Md: 1997)*. 1999;22(2):155-65.
111. Rahma OE, Hamilton JM, Wojtowicz M, Dakheel O, Bernstein S, Liewehr DJ, et al. The immunological and clinical effects of mutated ras peptide vaccine in combination with IL-2, GM-CSF, or both in patients with solid tumors. *Journal of Translational Medicine*. 2014;12(1):55.
112. Toubaji A, Achar M, Provenzano M, Herrin VE, Behrens R, Hamilton M, et al. Pilot study of mutant ras peptide-based vaccine as an adjuvant treatment in pancreatic and colorectal cancers. *Cancer Immunology, Immunotherapy*. 2008;57(9):1413-20.
113. Suzuki E, Kapoor V, Jassar AS, Kaiser LR, Albelda SM. Gemcitabine selectively eliminates splenic Gr-1+/CD11b+ myeloid suppressor cells in tumor-bearing animals and enhances antitumor immune activity. *Clin Cancer Res*. 2005;11(18):6713-21.

114. Wang Z, Till B, Gao Q. Chemotherapeutic agent-mediated elimination of myeloid-derived suppressor cells. *Oncoimmunology*. 2017;6(7):e1331807.
115. Lutsiak ME, Semnani RT, De Pascalis R, Kashmiri SV, Schlom J, Sabzevari H. Inhibition of CD4(+)25+ T regulatory cell function implicated in enhanced immune response by low-dose cyclophosphamide. *Blood*. 2005;105(7):2862-8.
116. Le HK, Graham L, Cha E, Morales JK, Manjili MH, Bear HD. Gemcitabine directly inhibits myeloid derived suppressor cells in BALB/c mice bearing 4T1 mammary carcinoma and augments expansion of T cells from tumor-bearing mice. *Int Immunopharmacol*. 2009;9(7-8):900-9.
117. Vincent J, Mignot G, Chalmin F, Ladoire S, Bruchard M, Chevriaux A, et al. 5-Fluorouracil selectively kills tumor-associated myeloid-derived suppressor cells resulting in enhanced T cell-dependent antitumor immunity. *Cancer research*. 2010;70(8):3052-61.
118. Qu X, Felder MA, Perez Horta Z, Sondel PM, Rakhmilevich AL. Antitumor effects of anti-CD40/CpG immunotherapy combined with gemcitabine or 5-fluorouracil chemotherapy in the B16 melanoma model. *Int Immunopharmacol*. 2013;17(4):1141-7.
119. Sawant A, Schafer CC, Jin TH, Zmijewski J, Tse HM, Roth J, et al. Enhancement of antitumor immunity in lung cancer by targeting myeloid-derived suppressor cell pathways. *Cancer research*. 2013;73(22):6609-20.
120. Otsubo D, Yamashita K, Fujita M, Nishi M, Kimura Y, Hasegawa H, et al. Early-phase Treatment by Low-dose 5-Fluorouracil or Primary Tumor Resection Inhibits MDSC-mediated Lung Metastasis Formation. *Anticancer Res*. 2015;35(8):4425-31.
121. Annels NE, Shaw VE, Gabitass RF, Billingham L, Corrie P, Eatock M, et al. The effects of gemcitabine and capecitabine combination chemotherapy and of low-dose adjuvant GM-CSF on the levels of myeloid-derived suppressor cells in patients with advanced pancreatic cancer. *Cancer Immunol Immunother*. 2014;63(2):175-83.
122. Chaudhary B, Elkord E. Regulatory T Cells in the Tumor Microenvironment and Cancer Progression: Role and Therapeutic Targeting. *Vaccines (Basel)*. 2016;4(3).
123. Ghiringhelli F, Larmonier N, Schmitt E, Parcellier A, Cathelin D, Garrido C, et al. CD4+CD25+ regulatory T cells suppress tumor immunity but are sensitive to cyclophosphamide which allows immunotherapy of established tumors to be curative. *Eur J Immunol*. 2004;34(2):336-44.
124. Li JY, Duan XF, Wang LP, Xu YJ, Huang L, Zhang TF, et al. Selective depletion of regulatory T cell subsets by docetaxel treatment in patients with nonsmall cell lung cancer. *J Immunol Res*. 2014;2014:286170.
125. Taniguchi H, Iwasa S, Yamazaki K, Yoshino T, Kiryu C, Naka Y, et al. Phase 1 study of OCV-C02, a peptide vaccine consisting of two peptide epitopes for refractory metastatic colorectal cancer. *Cancer Science*. 2017;108(5):1013-21.
126. Restifo NP, Ying H, Hwang L, Leitner WW. The promise of nucleic acid vaccines. *Gene Ther*. 2000;7(2):89-92.
127. Hobernik D, Bros M. DNA Vaccines-How Far From Clinical Use? *Int J Mol Sci*. 2018;19(11).
128. Pastor F, Berraondo P, Etxeberria I, Frederick J, Sahin U, Gilboa E, et al. An RNA toolbox for cancer immunotherapy. *Nat Rev Drug Discov*. 2018;17(10):751-67.
129. Rodriguez-Ruiz ME, Perez-Gracia JL, Rodriguez I, Alfaro C, Onate C, Perez G, et al. Combined immunotherapy encompassing intratumoral poly-ICLC, dendritic-cell

- vaccination and radiotherapy in advanced cancer patients. *Ann Oncol.* 2018;29(5):1312-9.
130. Pardi N, Muramatsu H, Weissman D, Kariko K. In vitro transcription of long RNA containing modified nucleosides. *Methods Mol Biol.* 2013;969:29-42.
131. Pardi N, Hogan MJ, Porter FW, Weissman D. mRNA vaccines - a new era in vaccinology. *Nat Rev Drug Discov.* 2018;17(4):261-79.
132. Conry RM, LoBuglio AF, Wright M, Sumerel L, Pike MJ, Johanning F, et al. Characterization of a messenger RNA polynucleotide vaccine vector. *Cancer research.* 1995;55(7):1397-400.
133. Dileo J, Miller TE, Jr., Chesnoy S, Huang L. Gene transfer to subdermal tissues via a new gene gun design. *Hum Gene Ther.* 2003;14(1):79-87.
134. Qiu P, Ziegelhoffer P, Sun J, Yang NS. Gene gun delivery of mRNA in situ results in efficient transgene expression and genetic immunization. *Gene Ther.* 1996;3(3):262-8.
135. Steitz J, Britten CM, Wolfel T, Tuting T. Effective induction of anti-melanoma immunity following genetic vaccination with synthetic mRNA coding for the fusion protein EGFP.TRP2. *Cancer Immunol Immunother.* 2006;55(3):246-53.
136. Weide B, Pascolo S, Scheel B, Derhovannessian E, Pflugfelder A, Eigentler TK, et al. Direct injection of protamine-protected mRNA: results of a phase 1/2 vaccination trial in metastatic melanoma patients. *J Immunother.* 2009;32(5):498-507.
137. Stenzl A, Feyerabend S, Syndikus I, Sarosiek T, Kübler H, Heidenreich A, et al. 1149P Results of the randomized, placebo-controlled phase I/IIb trial of CV9104, an mRNA based cancer immunotherapy, in patients with metastatic castration-resistant prostate cancer (mCRPC). *Annals of Oncology.* 2017;28(suppl\_5).
138. Sebastian M, Schroder A, Scheel B, Hong HS, Muth A, von Boehmer L, et al. A phase I/IIa study of the mRNA-based cancer immunotherapy CV9201 in patients with stage IIIB/IV non-small cell lung cancer. *Cancer Immunol Immunother.* 2019;68(5):799-812.
139. Hong HS, Koch SD, Scheel B, Gnad-Vogt U, Schroder A, Kallen KJ, et al. Distinct transcriptional changes in non-small cell lung cancer patients associated with multi-antigenic RActive(R) CV9201 immunotherapy. *Oncoimmunology.* 2016;5(12):e1249560.
140. Papachristofilou A, Hipp MM, Klinkhardt U, Fruh M, Sebastian M, Weiss C, et al. Phase Ib evaluation of a self-adjuvanted protamine formulated mRNA-based active cancer immunotherapy, BI1361849 (CV9202), combined with local radiation treatment in patients with stage IV non-small cell lung cancer. *J Immunother Cancer.* 2019;7(1):38.
141. Burris HA, Patel MR, Cho DC, Clarke JM, Gutierrez M, Zaks TZ, et al. A phase I multicenter study to assess the safety, tolerability, and immunogenicity of mRNA-4157 alone in patients with resected solid tumors and in combination with pembrolizumab in patients with unresectable solid tumors. *Journal of Clinical Oncology.* 2019;37(15\_suppl):2523-.
142. Bonehill A, Van Nuffel AM, Corthals J, Tuybaerts S, Heirman C, Francois V, et al. Single-step antigen loading and activation of dendritic cells by mRNA electroporation for the purpose of therapeutic vaccination in melanoma patients. *Clin Cancer Res.* 2009;15(10):3366-75.

143. Kyte JA, Kvalheim G, Aamdal S, Saeboe-Larssen S, Gaudernack G. Preclinical full-scale evaluation of dendritic cells transfected with autologous tumor-mRNA for melanoma vaccination. *Cancer gene therapy*. 2005;12(6):579-91.
144. McNamara MA, Nair SK, Holl EK. RNA-Based Vaccines in Cancer Immunotherapy. *J Immunol Res*. 2015;2015:794528.
145. Nair SK, Morse M, Boczkowski D, Cumming RI, Vasovic L, Gilboa E, et al. Induction of tumor-specific cytotoxic T lymphocytes in cancer patients by autologous tumor RNA-transfected dendritic cells. *Ann Surg*. 2002;235(4):540-9.
146. Su Z, Dannull J, Heiser A, Yancey D, Pruitt S, Madden J, et al. Immunological and clinical responses in metastatic renal cancer patients vaccinated with tumor RNA-transfected dendritic cells. *Cancer research*. 2003;63(9):2127-33.
147. Amin A, Dudek AZ, Logan TF, Lance RS, Holzbeierlein JM, Knox JJ, et al. Survival with AGS-003, an autologous dendritic cell-based immunotherapy, in combination with sunitinib in unfavorable risk patients with advanced renal cell carcinoma (RCC): Phase 2 study results. *J Immunother Cancer*. 2015;3:14.
148. Dorfel D, Appel S, Grunebach F, Weck MM, Muller MR, Heine A, et al. Processing and presentation of HLA class I and II epitopes by dendritic cells after transfection with in vitro-transcribed MUC1 RNA. *Blood*. 2005;105(8):3199-205.
149. Grunebach F, Kayser K, Weck MM, Muller MR, Appel S, Brossart P. Cotransfection of dendritic cells with RNA coding for HER-2/neu and 4-1BBL increases the induction of tumor antigen specific cytotoxic T lymphocytes. *Cancer gene therapy*. 2005;12(9):749-56.
150. Heiser A, Coleman D, Dannull J, Yancey D, Maurice MA, Lallas CD, et al. Autologous dendritic cells transfected with prostate-specific antigen RNA stimulate CTL responses against metastatic prostate tumors. *J Clin Invest*. 2002;109(3):409-17.
151. Morse MA, Nair SK, Boczkowski D, Tyler D, Hurwitz HI, Proia A, et al. The feasibility and safety of immunotherapy with dendritic cells loaded with CEA mRNA following neoadjuvant chemoradiotherapy and resection of pancreatic cancer. *Int J Gastrointest Cancer*. 2002;32(1):1-6.
152. Morse MA, Nair SK, Mosca PJ, Hobeika AC, Clay TM, Deng Y, et al. Immunotherapy with autologous, human dendritic cells transfected with carcinoembryonic antigen mRNA. *Cancer Invest*. 2003;21(3):341-9.
153. Van Lint S, Wilgenhof S, Heirman C, Corthals J, Breckpot K, Bonehill A, et al. Optimized dendritic cell-based immunotherapy for melanoma: the TriMix-formula. *Cancer Immunol Immunother*. 2014;63(9):959-67.
154. Wilgenhof S, Corthals J, Van Nuffel AM, Benteyn D, Heirman C, Bonehill A, et al. Long-term clinical outcome of melanoma patients treated with messenger RNA-electroporated dendritic cell therapy following complete resection of metastases. *Cancer Immunol Immunother*. 2015;64(3):381-8.
155. Lopes A, Vandermeulen G, Preat V. Cancer DNA vaccines: current preclinical and clinical developments and future perspectives. *J Exp Clin Cancer Res*. 2019;38(1):146.
156. Tiptiri-Kourpeti A, Spyridopoulou K, Pappa A, Chlichlia K. DNA vaccines to attack cancer: Strategies for improving immunogenicity and efficacy. *Pharmacol Ther*. 2016;165:32-49.

157. Aghi M, Visted T, Depinho RA, Chiocca EA. Oncolytic herpes virus with defective ICP6 specifically replicates in quiescent cells with homozygous genetic mutations in p16. *Oncogene*. 2008;27(30):4249-54.
158. Howells A, Marelli G, Lemoine NR, Wang Y. Oncolytic Viruses-Interaction of Virus and Tumor Cells in the Battle to Eliminate Cancer. *Front Oncol*. 2017;7:195.
159. Russell SJ, Barber GN. Oncolytic Viruses as Antigen-Agnostic Cancer Vaccines. *Cancer Cell*. 2018;33(4):599-605.
160. Twumasi-Boateng K, Pettigrew JL, Kwok YYE, Bell JC, Nelson BH. Oncolytic viruses as engineering platforms for combination immunotherapy. *Nature Reviews Cancer*. 2018;18(7):419-32.
161. Bommareddy PK, Shettigar M, Kaufman HL. Integrating oncolytic viruses in combination cancer immunotherapy. *Nature Reviews Immunology*. 2018;18(8):498-513.
162. Coffey MC, Strong JE, Forsyth PA, Lee PW. Reovirus therapy of tumors with activated Ras pathway. *Science*. 1998;282(5392):1332-4.
163. Roy S, Bag AK, Dutta S, Polavaram NS, Islam R, Schellenburg S, et al. Macrophage-Derived Neuropilin-2 Exhibits Novel Tumor-Promoting Functions. *Cancer research*. 2018;78(19):5600-17.
164. Barber GN. Cytoplasmic DNA innate immune pathways. *Immunol Rev*. 2011;243(1):99-108.
165. Barber GN. Innate immune DNA sensing pathways: STING, AIMII and the regulation of interferon production and inflammatory responses. *Curr Opin Immunol*. 2011;23(1):10-20.
166. Franz KM, Kagan JC. Innate Immune Receptors as Competitive Determinants of Cell Fate. *Mol Cell*. 2017;66(6):750-60.
167. Takeuchi O, Akira S. Innate immunity to virus infection. *Immunol Rev*. 2009;227(1):75-86.
168. Kaminsky V, Zhivotovsky B. To kill or be killed: how viruses interact with the cell death machinery. *J Intern Med*. 2010;267(5):473-82.
169. Schock SN, Chandra NV, Sun Y, Irie T, Kitagawa Y, Gotoh B, et al. Induction of necroptotic cell death by viral activation of the RIG-I or STING pathway. *Cell Death Differ*. 2017;24(4):615-25.
170. Raja J, Ludwig JM, Gettinger SN, Schalper KA, Kim HS. Oncolytic virus immunotherapy: future prospects for oncology. *J Immunother Cancer*. 2018;6(1):140.
171. Lundstrom K. New frontiers in oncolytic viruses: optimizing and selecting for virus strains with improved efficacy. *Biologics*. 2018;12:43-60.
172. Andtbacka RH, Kaufman HL, Collichio F, Amatruda T, Senzer N, Chesney J, et al. Talimogene Laherparepvec Improves Durable Response Rate in Patients With Advanced Melanoma. *Journal of clinical oncology : official journal of the American Society of Clinical Oncology*. 2015;33(25):2780-8.
173. Chesney J, Puzanov I, Collichio F, Singh P, Milhem MM, Glaspy J, et al. Randomized, Open-Label Phase II Study Evaluating the Efficacy and Safety of Talimogene Laherparepvec in Combination With Ipilimumab Versus Ipilimumab Alone in Patients With Advanced, Unresectable Melanoma. *J Clin Oncol*. 2018;36(17):1658-67.
174. Ribas A, Dummer R, Puzanov I, VanderWalde A, Andtbacka RHI, Michielin O, et al. Oncolytic Virotherapy Promotes Intratumoral T Cell Infiltration and Improves Anti-PD-1 Immunotherapy. *Cell*. 2017;170(6):1109-19 e10.

175. Desjardins A, Gromeier M, Herndon JE, 2nd, Beaubier N, Bolognesi DP, Friedman AH, et al. Recurrent Glioblastoma Treated with Recombinant Poliovirus. *N Engl J Med*. 2018;379(2):150-61.
176. Brown MC, Holl EK, Boczkowski D, Dobrikova E, Mosaheb M, Chandramohan V, et al. Cancer immunotherapy with recombinant poliovirus induces IFN-dominant activation of dendritic cells and tumor antigen-specific CTLs. *Sci Transl Med*. 2017;9(408).
177. Samson A, Scott KJ, Taggart D, West EJ, Wilson E, Nuovo GJ, et al. Intravenous delivery of oncolytic reovirus to brain tumor patients immunologically primes for subsequent checkpoint blockade. *Sci Transl Med*. 2018;10(422).
178. Bourgeois-Daigneault MC, Roy DG, Aitken AS, El Sayes N, Martin NT, Varette O, et al. Neoadjuvant oncolytic virotherapy before surgery sensitizes triple-negative breast cancer to immune checkpoint therapy. *Sci Transl Med*. 2018;10(422).
179. Lawler SE, Speranza MC, Cho CF, Chiocca EA. Oncolytic Viruses in Cancer Treatment: A Review. *JAMA Oncol*. 2017;3(6):841-9.
180. Pol J, Bloy N, Obrist F, Eggermont A, Galon J, Cremer I, et al. Trial Watch:: Oncolytic viruses for cancer therapy. *Oncoimmunology*. 2014;3:e28694.
181. Hoption Cann SA, van Netten JP, van Netten C. Dr William Coley and tumour regression: a place in history or in the future. *Postgrad Med J*. 2003;79(938):672-80.
182. Richardson MA, Ramirez T, Russell NC, Moye LA. Coley toxins immunotherapy: a retrospective review. *Altern Ther Health Med*. 1999;5(3):42-7.
183. Felgner S, Pawar V, Kocijancic D, Erhardt M, Weiss S. Tumour-targeting bacteria-based cancer therapies for increased specificity and improved outcome. *Microb Biotechnol*. 2017;10(5):1074-8.
184. Theys J, Lambin P. Clostridium to treat cancer: dream or reality? *Ann Transl Med*. 2015;3(Suppl 1):S21.
185. Zhang YL, Lu R, Chang ZS, Zhang WQ, Wang QB, Ding SY, et al. Clostridium sporogenes delivers interleukin-12 to hypoxic tumours, producing antitumour activity without significant toxicity. *Lett Appl Microbiol*. 2014;59(6):580-6.
186. Chowdhury S, Castro S, Coker C, Hinchliffe TE, Arpaia N, Danino T. Programmable bacteria induce durable tumor regression and systemic antitumor immunity. *Nat Med*. 2019;25(7):1057-63.
187. Le DT, Brockstedt DG, Nir-Paz R, Hampl J, Mathur S, Nemunaitis J, et al. A live-attenuated Listeria vaccine (ANZ-100) and a live-attenuated Listeria vaccine expressing mesothelin (CRS-207) for advanced cancers: phase I studies of safety and immune induction. *Clin Cancer Res*. 2012;18(3):858-68.
188. Goyvaerts C, Breckpot K. Towards a personalized iPSC-based vaccine. *Nature Biomedical Engineering*. 2018;2(5):277-8.
189. Brewer BG, Mitchell RA, Harandi A, Eaton JW. Embryonic vaccines against cancer: an early history. *Exp Mol Pathol*. 2009;86(3):192-7.
190. Ben-Porath I, Thomson MW, Carey VJ, Ge R, Bell GW, Regev A, et al. An embryonic stem cell-like gene expression signature in poorly differentiated aggressive human tumors. *Nat Genet*. 2008;40(5):499-507.
191. Ghosh Z, Huang M, Hu S, Wilson KD, Dey D, Wu JC. Dissecting the oncogenic and tumorigenic potential of differentiated human induced pluripotent stem cells and human embryonic stem cells. *Cancer research*. 2011;71(14):5030-9.

192. de Almeida PE, Meyer EH, Kooreman NG, Diecke S, Dey D, Sanchez-Freire V, et al. Transplanted terminally differentiated induced pluripotent stem cells are accepted by immune mechanisms similar to self-tolerance. *Nat Commun.* 2014;5:3903.
193. Cao J, Li X, Lu X, Zhang C, Yu H, Zhao T. Cells derived from iPSC can be immunogenic - yes or no? *Protein Cell.* 2014;5(1):1-3.
194. Zhao T, Zhang ZN, Rong Z, Xu Y. Immunogenicity of induced pluripotent stem cells. *Nature.* 2011;474(7350):212-5.
195. Bock C, Kiskinis E, Verstappen G, Gu H, Boulting G, Smith ZD, et al. Reference Maps of human ES and iPS cell variation enable high-throughput characterization of pluripotent cell lines. *Cell.* 2011;144(3):439-52.
196. Mallon BS, Chenoweth JG, Johnson KR, Hamilton RS, Tesar PJ, Yavatkar AS, et al. StemCellDB: the human pluripotent stem cell database at the National Institutes of Health. *Stem Cell Res.* 2013;10(1):57-66.
197. Mallon BS, Hamilton RS, Kozhich OA, Johnson KR, Fann YC, Rao MS, et al. Comparison of the molecular profiles of human embryonic and induced pluripotent stem cells of isogenic origin. *Stem Cell Res.* 2014;12(2):376-86.
198. Soldner F, Hockemeyer D, Beard C, Gao Q, Bell GW, Cook EG, et al. Parkinson's disease patient-derived induced pluripotent stem cells free of viral reprogramming factors. *Cell.* 2009;136(5):964-77.
199. Kooreman NG, Kim Y, de Almeida PE, Termglinchan V, Diecke S, Shao NY, et al. Autologous iPSC-Based Vaccines Elicit Anti-tumor Responses In Vivo. *Cell Stem Cell.* 2018;22(4):501-13 e7.
200. Klebanoff CA, Wolchok JD. Shared cancer neoantigens: Making private matters public. *J Exp Med.* 2018;215(1):5-7.
201. Castle JC, Kreiter S, Diekmann J, Lower M, van de Roemer N, de Graaf J, et al. Exploiting the mutanome for tumor vaccination. *Cancer research.* 2012;72(5):1081-91.
202. Kreiter S, Vormehr M, van de Roemer N, Diken M, Lower M, Diekmann J, et al. Mutant MHC class II epitopes drive therapeutic immune responses to cancer. *Nature.* 2015;520(7549):692-6.
203. Matsushita H, Vesely MD, Koboldt DC, Rickert CG, Uppaluri R, Magrini VJ, et al. Cancer exome analysis reveals a T-cell-dependent mechanism of cancer immunoediting. *Nature.* 2012;482(7385):400-4.
204. Gubin MM, Zhang X, Schuster H, Caron E, Ward JP, Noguchi T, et al. Checkpoint blockade cancer immunotherapy targets tumour-specific mutant antigens. *Nature.* 2014;515(7528):577-81.
205. Yadav M, Jhunjhunwala S, Phung QT, Lupardus P, Tanguay J, Bumbaca S, et al. Predicting immunogenic tumour mutations by combining mass spectrometry and exome sequencing. *Nature.* 2014;515(7528):572-6.
206. Duan F, Duitama J, Al Seesi S, Ayres CM, Corcelli SA, Pawashe AP, et al. Genomic and bioinformatic profiling of mutational neoepitopes reveals new rules to predict anticancer immunogenicity. *J Exp Med.* 2014;211(11):2231-48.
207. Li L, Goedegebuure SP, Gillanders WE. Preclinical and clinical development of neoantigen vaccines. *Ann Oncol.* 2017;28(suppl\_12):xii11-xii7.
208. Tran E, Robbins PF, Rosenberg SA. 'Final common pathway' of human cancer immunotherapy: targeting random somatic mutations. *Nature immunology.* 2017;18(3):255-62.

209. van der Burg SH, Arens R, Ossendorp F, van Hall T, Melief CJ. Vaccines for established cancer: overcoming the challenges posed by immune evasion. *Nature reviews Cancer*. 2016;16(4):219-33.
210. Fifis T, Gamvrellis A, Crimeen-Irwin B, Pietersz GA, Li J, Mottram PL, et al. Size-dependent immunogenicity: therapeutic and protective properties of nano-vaccines against tumors. *J Immunol*. 2004;173(5):3148-54.
211. Liu H, Moynihan KD, Zheng Y, Szeto GL, Li AV, Huang B, et al. Structure-based programming of lymph-node targeting in molecular vaccines. *Nature*. 2014;507(7493):519-22.
212. Manolova V, Flace A, Bauer M, Schwarz K, Saudan P, Bachmann MF. Nanoparticles target distinct dendritic cell populations according to their size. *Eur J Immunol*. 2008;38(5):1404-13.
213. Hanson MC, Crespo MP, Abraham W, Moynihan KD, Szeto GL, Chen SH, et al. Nanoparticulate STING agonists are potent lymph node-targeted vaccine adjuvants. *J Clin Invest*. 2015;125(6):2532-46.
214. Nuhn L, Vanparijs N, De Beuckelaer A, Lybaert L, Verstraete G, Deswarte K, et al. pH-degradable imidazoquinoline-ligated nanogels for lymph node-focused immune activation. *Proc Natl Acad Sci U S A*. 2016;113(29):8098-103.
215. Ott PA, Hu Z, Keskin DB, Shukla SA, Sun J, Bozym DJ, et al. An immunogenic personal neoantigen vaccine for patients with melanoma. *Nature*. 2017;547(7662):217-21.
216. Guo Y, Lei K, Tang L. Neoantigen Vaccine Delivery for Personalized Anticancer Immunotherapy. *Front Immunol*. 2018;9:1499.
217. Luo M, Wang H, Wang Z, Cai H, Lu Z, Li Y, et al. A STING-activating nanovaccine for cancer immunotherapy. *Nat Nanotechnol*. 2017;12(7):648-54.
218. Li AW, Sobral MC, Badrinath S, Choi Y, Graveline A, Stafford AG, et al. A facile approach to enhance antigen response for personalized cancer vaccination. *Nat Mater*. 2018;17(6):528-34.
219. Sahin U, Derhovanessian E, Miller M, Kloke BP, Simon P, Lower M, et al. Personalized RNA mutanome vaccines mobilize poly-specific therapeutic immunity against cancer. *Nature*. 2017;547(7662):222-6.
220. Rammensee HG, Singh-Jasuja H. HLA ligandome tumor antigen discovery for personalized vaccine approach. *Expert Rev Vaccines*. 2013;12(10):1211-7.
221. Singh-Jasuja H, Emmerich NP, Rammensee HG. The Tübingen approach: identification, selection, and validation of tumor-associated HLA peptides for cancer therapy. *Cancer Immunol Immunother*. 2004;53(3):187-95.
222. Walter S, Weinschenk T, Stenzl A, Zdrojowy R, Pluzanska A, Szczylik C, et al. Multi-peptide immune response to cancer vaccine IMA901 after single-dose cyclophosphamide associates with longer patient survival. *Nat Med*. 2012;18(8):1254-61.
223. Bentzen AK, Marquard AM, Lyngaa R, Saini SK, Ramskov S, Donia M, et al. Large-scale detection of antigen-specific T cells using peptide-MHC-I multimers labeled with DNA barcodes. *Nat Biotechnol*. 2016;34(10):1037-45.
224. Bentzen AK, Such L, Jensen KK, Marquard AM, Jessen LE, Miller NJ, et al. T cell receptor fingerprinting enables in-depth characterization of the interactions governing recognition of peptide-MHC complexes. *Nat Biotechnol*. 2018.

225. Zugazagoitia J, Guedes C, Ponce S, Ferrer I, Molina-Pinelo S, Paz-Ares L. Current Challenges in Cancer Treatment. *Clin Ther*. 2016;38(7):1551-66.
226. Zaretsky JM, Garcia-Diaz A, Shin DS, Escuin-Ordinas H, Hugo W, Hu-Lieskovan S, et al. Mutations Associated with Acquired Resistance to PD-1 Blockade in Melanoma. *N Engl J Med*. 2016;375(9):819-29.
227. Anderson KG, Stromnes IM, Greenberg PD. Obstacles Posed by the Tumor Microenvironment to T cell Activity: A Case for Synergistic Therapies. *Cancer Cell*. 2017;31(3):311-25.
228. Blank CU, Haining WN, Held W, Hogan PG, Kallies A, Lugli E, et al. Defining 'T cell exhaustion'. *Nat Rev Immunol*. 2019;19(11):665-74.
229. Philip M, Schietinger A. Heterogeneity and fate choice: T cell exhaustion in cancer and chronic infections. *Curr Opin Immunol*. 2019;58:98-103.
230. Wei SC, Duffy CR, Allison JP. Fundamental Mechanisms of Immune Checkpoint Blockade Therapy. *Cancer Discov*. 2018;8(9):1069-86.
231. Alfei F, Kanev K, Hofmann M, Wu M, Ghoneim HE, Roelli P, et al. TOX reinforces the phenotype and longevity of exhausted T cells in chronic viral infection. *Nature*. 2019;571(7764):265-9.
232. Jiang Y, Li Y, Zhu B. T-cell exhaustion in the tumor microenvironment. *Cell Death Dis*. 2015;6:e1792.
233. Wang JC, Xu Y, Huang ZM, Lu XJ. T cell exhaustion in cancer: Mechanisms and clinical implications. *J Cell Biochem*. 2018;119(6):4279-86.
234. Quiox E, Lena H, Losonczy G, Forget F, Chouaid C, Papai Z, et al. TG4010 immunotherapy and first-line chemotherapy for advanced non-small-cell lung cancer (TIME): results from the phase 2b part of a randomised, double-blind, placebo-controlled, phase 2b/3 trial. *The Lancet Oncology*. 2016;17(2):212-23.
235. Vermaelen K. Vaccine Strategies to Improve Anti-cancer Cellular Immune Responses. *Front Immunol*. 2019;10:8.
236. Cuadros C, Dominguez AL, Lollini PL, Croft M, Mittler RS, Borgstrom P, et al. Vaccination with dendritic cells pulsed with apoptotic tumors in combination with anti-OX40 and anti-4-1BB monoclonal antibodies induces T cell-mediated protective immunity in Her-2/neu transgenic mice. *Int J Cancer*. 2005;116(6):934-43.
237. Ito F, Li Q, Shreiner AB, Okuyama R, Jure-Kunkel MN, Teitz-Tennenbaum S, et al. Anti-CD137 monoclonal antibody administration augments the antitumor efficacy of dendritic cell-based vaccines. *Cancer research*. 2004;64(22):8411-9.
238. Becker JC, Andersen MH, Schrama D, Thor Straten P. Immune-suppressive properties of the tumor microenvironment. *Cancer Immunol Immunother*. 2013;62(7):1137-48.
239. Hanahan D, Coussens LM. Accessories to the crime: functions of cells recruited to the tumor microenvironment. *Cancer Cell*. 2012;21(3):309-22.
240. Kumar V, Patel S, Tcyganov E, Gabrilovich DI. The Nature of Myeloid-Derived Suppressor Cells in the Tumor Microenvironment. *Trends Immunol*. 2016;37(3):208-20.
241. Stromnes IM, Brockenbrough JS, Izeradjene K, Carlson MA, Cuevas C, Simmons RM, et al. Targeted depletion of an MDSC subset unmasks pancreatic ductal adenocarcinoma to adaptive immunity. *Gut*. 2014;63(11):1769-81.
242. Stromnes IM, DelGiorno KE, Greenberg PD, Hingorani SR. Stromal reengineering to treat pancreas cancer. *Carcinogenesis*. 2014;35(7):1451-60.

243. Stromnes IM, Greenberg PD, Hingorani SR. Molecular pathways: myeloid complicity in cancer. *Clin Cancer Res.* 2014;20(20):5157-70.
244. Whiteside TL. The tumor microenvironment and its role in promoting tumor growth. *Oncogene.* 2008;27(45):5904-12.
245. Gunderson AJ, Kaneda MM, Tsujikawa T, Nguyen AV, Affara NI, Ruffell B, et al. Bruton Tyrosine Kinase-Dependent Immune Cell Cross-talk Drives Pancreas Cancer. *Cancer Discov.* 2016;6(3):270-85.
246. Lee KE, Spata M, Bayne LJ, Buza EL, Durham AC, Allman D, et al. Hif1a Deletion Reveals Pro-Neoplastic Function of B Cells in Pancreatic Neoplasia. *Cancer Discov.* 2016;6(3):256-69.
247. Schwartz M, Zhang Y, Rosenblatt JD. B cell regulation of the anti-tumor response and role in carcinogenesis. *J Immunother Cancer.* 2016;4:40.
248. Pylayeva-Gupta Y, Das S, Handler JS, Hajdu CH, Coffre M, Koralov SB, et al. IL35-Producing B Cells Promote the Development of Pancreatic Neoplasia. *Cancer Discov.* 2016;6(3):247-55.
249. Oberg HH, Kellner C, Peipp M, Sebens S, Adam-Klages S, Gramatzki M, et al. Monitoring Circulating gammadelta T Cells in Cancer Patients to Optimize gammadelta T Cell-Based Immunotherapy. *Front Immunol.* 2014;5:643.
250. Wesch D, Peters C, Siegers GM. Human gamma delta T regulatory cells in cancer: fact or fiction? *Front Immunol.* 2014;5:598.
251. Stanford JC, Young C, Hicks D, Owens P, Williams A, Vaught DB, et al. Efferocytosis produces a prometastatic landscape during postpartum mammary gland involution. *J Clin Invest.* 2014;124(11):4737-52.
252. Vaught DB, Cook RS. Clearance of dying cells accelerates malignancy. *Oncotarget.* 2015;6(28):24590-1.
253. Wesolowski R, Duggan MC, Stiff A, Markowitz J, Trikha P, Levine KM, et al. Circulating myeloid-derived suppressor cells increase in patients undergoing neo-adjuvant chemotherapy for breast cancer. *Cancer Immunol Immunother.* 2017;66(11):1437-47.
254. Chandra D, Quispe-Tintaya W, Jahangir A, Asafu-Adjei D, Ramos I, Sintim HO, et al. STING ligand c-di-GMP improves cancer vaccination against metastatic breast cancer. *Cancer Immunol Res.* 2014;2(9):901-10.
255. Nicholaou T, Ebert LM, Davis ID, McArthur GA, Jackson H, Dimopoulos N, et al. Regulatory T-cell-mediated attenuation of T-cell responses to the NY-ESO-1 ISCOMATRIX vaccine in patients with advanced malignant melanoma. *Clin Cancer Res.* 2009;15(6):2166-73.
256. Jacobs C, Duewell P, Heckelsmiller K, Wei J, Bauernfeind F, Ellermeier J, et al. An ISCOM vaccine combined with a TLR9 agonist breaks immune evasion mediated by regulatory T cells in an orthotopic model of pancreatic carcinoma. *Int J Cancer.* 2011;128(4):897-907.
257. Ghiringhelli F, Menard C, Puig PE, Ladoire S, Roux S, Martin F, et al. Metronomic cyclophosphamide regimen selectively depletes CD4+CD25+ regulatory T cells and restores T and NK effector functions in end stage cancer patients. *Cancer Immunol Immunother.* 2007;56(5):641-8.
258. O'Sullivan D, Sanin DE, Pearce EJ, Pearce EL. Metabolic interventions in the immune response to cancer. *Nat Rev Immunol.* 2019;19(5):324-35.

259. Porporato PE, Filigheddu N, Pedro JMB, Kroemer G, Galluzzi L. Mitochondrial metabolism and cancer. *Cell Res.* 2018;28(3):265-80.
260. Gardiner CM. NK cell metabolism. *J Leukoc Biol.* 2019;105(6):1235-42.
261. Terren I, Orrantia A, Vitalle J, Zenarruzabeitia O, Borrego F. NK Cell Metabolism and Tumor Microenvironment. *Front Immunol.* 2019;10:2278.
262. Gabrilovich DI. Myeloid-Derived Suppressor Cells. *Cancer Immunol Res.* 2017;5(1):3-8.
263. Kishton RJ, Sukumar M, Restifo NP. Metabolic Regulation of T Cell Longevity and Function in Tumor Immunotherapy. *Cell Metab.* 2017;26(1):94-109.
264. O'Neill LA, Pearce EJ. Immunometabolism governs dendritic cell and macrophage function. *J Exp Med.* 2016;213(1):15-23.
265. Hanahan D, Weinberg RA. Hallmarks of cancer: the next generation. *Cell.* 2011;144(5):646-74.
266. Cascone T, McKenzie JA, Mbofung RM, Punt S, Wang Z, Xu C, et al. Increased Tumor Glycolysis Characterizes Immune Resistance to Adoptive T Cell Therapy. *Cell Metab.* 2018;27(5):977-87 e4.
267. Cao Y, Rathmell JC, Macintyre AN. Metabolic reprogramming towards aerobic glycolysis correlates with greater proliferative ability and resistance to metabolic inhibition in CD8 versus CD4 T cells. *PLoS One.* 2014;9(8):e104104.
268. Chang CH, Pearce EL. Emerging concepts of T cell metabolism as a target of immunotherapy. *Nature immunology.* 2016;17(4):364-8.
269. Chang CH, Qiu J, O'Sullivan D, Buck MD, Noguchi T, Curtis JD, et al. Metabolic Competition in the Tumor Microenvironment Is a Driver of Cancer Progression. *Cell.* 2015;162(6):1229-41.
270. Ho PC, Bihuniak JD, Macintyre AN, Staron M, Liu X, Amezcua R, et al. Phosphoenolpyruvate Is a Metabolic Checkpoint of Anti-tumor T Cell Responses. *Cell.* 2015;162(6):1217-28.
271. Jacobs SR, Herman CE, Maciver NJ, Wofford JA, Wieman HL, Hammen JJ, et al. Glucose uptake is limiting in T cell activation and requires CD28-mediated Akt-dependent and independent pathways. *J Immunol.* 2008;180(7):4476-86.
272. Renner K, Geiselhoringer AL, Fante M, Bruss C, Farber S, Schonhammer G, et al. Metabolic plasticity of human T cells: Preserved cytokine production under glucose deprivation or mitochondrial restriction, but 2-deoxy-glucose affects effector functions. *Eur J Immunol.* 2015;45(9):2504-16.
273. Ota Y, Ishihara S, Otani K, Yasuda K, Nishikawa T, Tanaka T, et al. Effect of nutrient starvation on proliferation and cytokine secretion of peripheral blood lymphocytes. *Mol Clin Oncol.* 2016;4(4):607-10.
274. Scharping NE, Delgoffe GM. Tumor Microenvironment Metabolism: A New Checkpoint for Anti-Tumor Immunity. *Vaccines (Basel).* 2016;4(4).
275. Pearce EL, Walsh MC, Cejas PJ, Harms GM, Shen H, Wang LS, et al. Enhancing CD8 T-cell memory by modulating fatty acid metabolism. *Nature.* 2009;460(7251):103-7.
276. Fennemann FL, de Vries IJM, Figdor CG, Verdoes M. Attacking Tumors From All Sides: Personalized Multiplex Vaccines to Tackle Intratumor Heterogeneity. *Front Immunol.* 2019;10:824.

277. Heemskerk B, Kvistborg P, Schumacher TN. The cancer antigenome. *EMBO J*. 2013;32(2):194-203.
278. Yarchoan M, Johnson BA, 3rd, Lutz ER, Laheru DA, Jaffee EM. Targeting neoantigens to augment antitumor immunity. *Nat Rev Cancer*. 2017;17(9):569.
279. Lim YW, Chen-Harris H, Mayba O, Lianoglou S, Wuster A, Bhangale T, et al. Germline genetic polymorphisms influence tumor gene expression and immune cell infiltration. *Proc Natl Acad Sci U S A*. 2018;115(50):E11701-E10.
280. Tran E, Robbins PF, Lu YC, Prickett TD, Gartner JJ, Jia L, et al. T-Cell Transfer Therapy Targeting Mutant KRAS in Cancer. *N Engl J Med*. 2016;375(23):2255-62.
281. Juric D, Castel P, Griffith M, Griffith OL, Won HH, Ellis H, et al. Convergent loss of PTEN leads to clinical resistance to a PI(3)K inhibitor. *Nature*. 2015;518(7538):240-4.
282. Niederst MJ, Sequist LV, Poirier JT, Mermel CH, Lockerman EL, Garcia AR, et al. RB loss in resistant EGFR mutant lung adenocarcinomas that transform to small-cell lung cancer. *Nat Commun*. 2015;6:6377.
283. Zhao J, Chen AX, Gartrell RD, Silverman AM, Aparicio L, Chu T, et al. Immune and genomic correlates of response to anti-PD-1 immunotherapy in glioblastoma. *Nat Med*. 2019;25(3):462-9.
284. Stanta G, Bonin S. Overview on Clinical Relevance of Intra-Tumor Heterogeneity. *Front Med (Lausanne)*. 2018;5:85.
285. Meacham CE, Morrison SJ. Tumour heterogeneity and cancer cell plasticity. *Nature*. 2013;501(7467):328-37.
286. Reiter JG, Baretta M, Gerold JM, Makohon-Moore AP, Daud A, Iacobuzio-Donahue CA, et al. An analysis of genetic heterogeneity in untreated cancers. *Nature reviews Cancer*. 2019;19(11):639-50.
287. Jamal-Hanjani M, Quezada SA, Larkin J, Swanton C. Translational implications of tumor heterogeneity. *Clin Cancer Res*. 2015;21(6):1258-66.
288. Cusnir M, Cavalcante L. Inter-tumor heterogeneity. *Hum Vaccin Immunother*. 2012;8(8):1143-5.
289. de Sousa VML, Carvalho L. Heterogeneity in Lung Cancer. *Pathobiology*. 2018;85(1-2):96-107.
290. Liu J, Dang H, Wang XW. The significance of intertumor and intratumor heterogeneity in liver cancer. *Exp Mol Med*. 2018;50(1):e416.
291. Finotello F, Eduati F. Multi-Omics Profiling of the Tumor Microenvironment: Paving the Way to Precision Immuno-Oncology. *Front Oncol*. 2018;8:430.
292. Janiszewska M. The microcosmos of intratumor heterogeneity: the space-time of cancer evolution. *Oncogene*. 2019.
293. Losic B, Craig AJ, Villacorta-Martin C, Martins-Filho SN, Akers N, Chen X, et al. Intratumoral heterogeneity and clonal evolution in liver cancer. *Nat Commun*. 2020;11(1):291.
294. Kemper K, Krijgsman O, Cornelissen-Steijger P, Shahrabi A, Weeber F, Song JY, et al. Intra- and inter-tumor heterogeneity in a vemurafenib-resistant melanoma patient and derived xenografts. *EMBO Mol Med*. 2015;7(9):1104-18.
295. Charoentong P, Finotello F, Angelova M, Mayer C, Efremova M, Rieder D, et al. Pan-cancer Immunogenomic Analyses Reveal Genotype-Immunophenotype

- Relationships and Predictors of Response to Checkpoint Blockade. *Cell Rep.* 2017;18(1):248-62.
296. Chowell D, Morris LGT, Grigg CM, Weber JK, Samstein RM, Makarov V, et al. Patient HLA class I genotype influences cancer response to checkpoint blockade immunotherapy. *Science.* 2018;359(6375):582-7.
297. Hopkins AC, Yarchoan M, Durham JN, Yusko EC, Rytlewski JA, Robins HS, et al. T cell receptor repertoire features associated with survival in immunotherapy-treated pancreatic ductal adenocarcinoma. *JCI Insight.* 2018;3(13).
298. Thorsson V, Gibbs DL, Brown SD, Wolf D, Bortone DS, Ou Yang TH, et al. The Immune Landscape of Cancer. *Immunity.* 2018;48(4):812-30 e14.
299. Wellenstein MD, de Visser KE. Cancer-Cell-Intrinsic Mechanisms Shaping the Tumor Immune Landscape. *Immunity.* 2018;48(3):399-416.
300. Wada S, Jackson CM, Yoshimura K, Yen HR, Getnet D, Harris TJ, et al. Sequencing CTLA-4 blockade with cell-based immunotherapy for prostate cancer. *J Transl Med.* 2013;11:89.
301. Remy-Ziller C, Thioudellet C, Hortelano J, Gantzer M, Nourtier V, Claudepierre MC, et al. Sequential administration of MVA-based vaccines and PD-1/PD-L1-blocking antibodies confers measurable benefits on tumor growth and survival: Preclinical studies with MVA-betaGal and MVA-MUC1 (TG4010) in a murine tumor model. *Hum Vaccin Immunother.* 2018;14(1):140-5.
302. McNeel DG, Eickhoff JC, Wargowski E, Zahm C, Staab MJ, Straus J, et al. Concurrent, but not sequential, PD-1 blockade with a DNA vaccine elicits anti-tumor responses in patients with metastatic, castration-resistant prostate cancer. *Oncotarget.* 2018;9(39):25586-96.
303. Helminck BA, Khan MAW, Hermann A, Gopalakrishnan V, Wargo JA. The microbiome, cancer, and cancer therapy. *Nat Med.* 2019;25(3):377-88.
304. Gopalakrishnan V, Spencer CN, Nezi L, Reuben A, Andrews MC, Karpinets TV, et al. Gut microbiome modulates response to anti-PD-1 immunotherapy in melanoma patients. *Science.* 2018;359(6371):97-103.
305. Routy B, Le Chatelier E, Derosa L, Duong CPM, Alou MT, Daillere R, et al. Gut microbiome influences efficacy of PD-1-based immunotherapy against epithelial tumors. *Science.* 2018;359(6371):91-7.
306. Farkona S, Diamandis EP, Blasutig IM. Cancer immunotherapy: the beginning of the end of cancer? *BMC Med.* 2016;14:73.
307. Mogensen TH. Pathogen recognition and inflammatory signaling in innate immune defenses. *Clin Microbiol Rev.* 2009;22(2):240-73, Table of Contents.
308. Chon HJ, Kim H, Noh JH, Yang H, Lee WS, Kong SJ, et al. STING signaling is a potential immunotherapeutic target in colorectal cancer. *J Cancer.* 2019;10(20):4932-8.
309. Fu J, Kanne DB, Leong M, Glickman LH, McWhirter SM, Lemmens E, et al. STING agonist formulated cancer vaccines can cure established tumors resistant to PD-1 blockade. *Sci Transl Med.* 2015;7(283):283ra52.
310. Nemunaitis J. Vaccines in cancer: GVAX, a GM-CSF gene vaccine. *Expert Rev Vaccines.* 2005;4(3):259-74.
311. Fu J, Kanne DB, Leong M, Glickman LH, McWhirter SM, Lemmens E, et al. STING agonist formulated cancer vaccines can cure established tumors resistant to PD-1 blockade. *Science Translational Medicine.* 2015;7(283):283ra52-ra52.

312. Kadam P, Singh RP, Davoodi M, Lee JM, John MS, Sharma S. Immune Checkpoint Blockade Enhances Immune Activity of Therapeutic Lung Cancer Vaccine. *Vaccines (Basel)*. 2020;8(4).
313. Messenheimer DJ, Jensen SM, Afentoulis ME, Wegmann KW, Feng Z, Friedman DJ, et al. Timing of PD-1 Blockade Is Critical to Effective Combination Immunotherapy with Anti-OX40. *Clin Cancer Res*. 2017;23(20):6165-77.
314. Sharma N, Vacher J, Allison JP. TLR1/2 ligand enhances antitumor efficacy of CTLA-4 blockade by increasing intratumoral Treg depletion. *Proc Natl Acad Sci U S A*. 2019;116(21):10453-62.
315. Tumeh PC, Harview CL, Yearley JH, Shintaku IP, Taylor EJ, Robert L, et al. PD-1 blockade induces responses by inhibiting adaptive immune resistance. *Nature*. 2014;515(7528):568-71.
316. Uryvaev A, Passhak M, Hershkovits D, Sabo E, Bar-Sela G. The role of tumor-infiltrating lymphocytes (TILs) as a predictive biomarker of response to anti-PD1 therapy in patients with metastatic non-small cell lung cancer or metastatic melanoma. *Med Oncol*. 2018;35(3):25.
317. Farsaci B, Donahue RN, Coplin MA, Grenga I, Lepone LM, Molinolo AA, et al. Immune consequences of decreasing tumor vasculature with antiangiogenic tyrosine kinase inhibitors in combination with therapeutic vaccines. *Cancer Immunol Res*. 2014;2(11):1090-102.
318. Fu J, Malm IJ, Kadayakkara DK, Levitsky H, Pardoll D, Kim YJ. Preclinical evidence that PD1 blockade cooperates with cancer vaccine TEGVAX to elicit regression of established tumors. *Cancer Res*. 2014;74(15):4042-52.
319. Ho VT, Kim HT, Brock J, Galinsky I, Daley H, Reynolds CG, et al. GM-CSF secreting leukemia cell vaccination for MDS/AML after allogeneic HSCT: a randomized double blinded phase 2 trial. *Blood Adv*. 2021.
320. Rowe J, Cen P. TroVax in colorectal cancer. *Hum Vaccin Immunother*. 2014;10(11):3196-200.
321. Testori A, Richards J, Whitman E, Mann GB, Lutzky J, Camacho L, et al. Phase III comparison of vitespen, an autologous tumor-derived heat shock protein gp96 peptide complex vaccine, with physician's choice of treatment for stage IV melanoma: the C-100-21 Study Group. *J Clin Oncol*. 2008;26(6):955-62.
322. Gutjahr A, Papagno L, Nicoli F, Kanuma T, Kuse N, Cabral-Piccin MP, et al. The STING ligand cGAMP potentiates the efficacy of vaccine-induced CD8+ T cells. *JCI Insight*. 2019;4(7).
323. Heidegger S, Kreppel D, Bscheider M, Stritzke F, Nedelko T, Wintges A, et al. RIG-I activating immunostimulatory RNA boosts the efficacy of anticancer vaccines and synergizes with immune checkpoint blockade. *EBioMedicine*. 2019;41:146-55.
324. Pufnock JS, Cigal M, Rolczynski LS, Andersen-Nissen E, Wolf M, McElrath MJ, et al. Priming CD8+ T cells with dendritic cells matured using TLR4 and TLR7/8 ligands together enhances generation of CD8+ T cells retaining CD28. *Blood*. 2011;117(24):6542-51.
325. Selvanantham T, Escalante NK, Cruz Tleugabulova M, Fieve S, Girardin SE, Philpott DJ, et al. Nod1 and Nod2 enhance TLR-mediated invariant NKT cell activation during bacterial infection. *J Immunol*. 2013;191(11):5646-54.

326. Donin NM, Chamie K, Lenis AT, Pantuck AJ, Reddy M, Kivlin D, et al. A phase 2 study of TMX-101, intravesical imiquimod, for the treatment of carcinoma in situ bladder cancer. *Urol Oncol*. 2017;35(2):39 e1- e7.
327. Kyi C, Roudko V, Sabado R, Saenger Y, Loging W, Mandeli J, et al. Therapeutic Immune Modulation against Solid Cancers with Intratumoral Poly-ICLC: A Pilot Trial. *Clin Cancer Res*. 2018;24(20):4937-48.
328. Mahipal A, Ejadi S, Gnjatic S, Kim-Schulze S, Lu H, Ter Meulen JH, et al. First-in-human phase 1 dose-escalating trial of G305 in patients with advanced solid tumors expressing NY-ESO-1. *Cancer Immunol Immunother*. 2019;68(7):1211-22.
329. Weihrauch MR, Richly H, von Bergwelt-Baildon MS, Becker HJ, Schmidt M, Hacker UT, et al. Phase I clinical study of the toll-like receptor 9 agonist MGN1703 in patients with metastatic solid tumours. *Eur J Cancer*. 2015;51(2):146-56.
330. Caisova V, Vieru A, Kumzakova Z, Glaserova S, Husnikova H, Vacova N, et al. Innate immunity based cancer immunotherapy: B16-F10 murine melanoma model. *BMC Cancer*. 2016;16(1):940.
331. Pandey S, Gruenbaum A, Kanashova T, Mertins P, Cluzel P, Chevrier N. Pairwise Stimulations of Pathogen-Sensing Pathways Predict Immune Responses to Multi-adjutant Combinations. *Cell Syst*. 2020;11(5):495-508 e10.
332. Stier S, Maletzki C, Klier U, Linnebacher M. Combinations of TLR ligands: a promising approach in cancer immunotherapy. *Clin Dev Immunol*. 2013;2013:271246.
333. Temizoz B, Kuroda E, Ohata K, Jounai N, Ozasa K, Kobiyama K, et al. TLR9 and STING agonists synergistically induce innate and adaptive type-II IFN. *Eur J Immunol*. 2015;45(4):1159-69.
334. Bagchi A, Herrup EA, Warren HS, Trigilio J, Shin HS, Valentine C, et al. MyD88-dependent and MyD88-independent pathways in synergy, priming, and tolerance between TLR agonists. *J Immunol*. 2007;178(2):1164-71.
335. Moreno Ayala MA, Gottardo MF, Gori MS, Nicola Candia AJ, Caruso C, De Laurentiis A, et al. Dual activation of Toll-like receptors 7 and 9 impairs the efficacy of antitumor vaccines in murine models of metastatic breast cancer. *J Cancer Res Clin Oncol*. 2017;143(9):1713-32.
336. Dhodapkar MV, Sznol M, Zhao B, Wang D, Carvajal RD, Keohan ML, et al. Induction of antigen-specific immunity with a vaccine targeting NY-ESO-1 to the dendritic cell receptor DEC-205. *Sci Transl Med*. 2014;6(232):232ra51.
337. Goldinger SM, Dummer R, Baumgaertner P, Mihic-Probst D, Schwarz K, Hammann-Haenni A, et al. Nano-particle vaccination combined with TLR-7 and -9 ligands triggers memory and effector CD8(+) T-cell responses in melanoma patients. *Eur J Immunol*. 2012;42(11):3049-61.
338. Grimmig T, Matthes N, Hoeland K, Tripathi S, Chandraker A, Grimm M, et al. TLR7 and TLR8 expression increases tumor cell proliferation and promotes chemoresistance in human pancreatic cancer. *Int J Oncol*. 2015;47(3):857-66.
339. Hsiao CC, Chen PH, Cheng CI, Tsai MS, Chang CY, Lu SC, et al. Toll-like receptor-4 is a target for suppression of proliferation and chemoresistance in HepG2 hepatoblastoma cells. *Cancer Lett*. 2015;368(1):144-52.
340. Larkin B, Ilyukha V, Sorokin M, Buzdin A, Vannier E, Poltorak A. Cutting Edge: Activation of STING in T Cells Induces Type I IFN Responses and Cell Death. *J Immunol*. 2017;199(2):397-402.

341. Liang D, Xiao-Feng H, Guan-Jun D, Er-Ling H, Sheng C, Ting-Ting W, et al. Activated STING enhances Tregs infiltration in the HPV-related carcinogenesis of tongue squamous cells via the c-jun/CCL22 signal. *Biochim Biophys Acta*. 2015;1852(11):2494-503.
342. Zhang Y, Wang Q, Ma A, Li Y, Li R, Wang Y. Functional expression of TLR9 in esophageal cancer. *Oncol Rep*. 2014;31(5):2298-304.
343. Fajgenbaum DC, June CH. Cytokine Storm. *N Engl J Med*. 2020;383(23):2255-73.
344. Meyer CT, Wooten DJ, Lopez CF, Quaranta V. Charting the Fragmented Landscape of Drug Synergy. *Trends Pharmacol Sci*. 2020;41(4):266-80.
345. Meyer CT, Wooten DJ, Paudel BB, Bauer J, Hardeman KN, Westover D, et al. Quantifying Drug Combination Synergy along Potency and Efficacy Axes. *Cell Syst*. 2019;8(2):97-108 e16.
346. Wooten DJ, Meyer CT, Lubbock ALR, Quaranta V, Lopez CF. MuSyC is a consensus framework that unifies multi-drug synergy metrics for combinatorial drug discovery. *Nat Commun*. 2021;12(1):4607.
347. Blaauboer SM, Gabrielle VD, Jin L. MPYS/STING-mediated TNF-alpha, not type I IFN, is essential for the mucosal adjuvant activity of (3'-5')-cyclic-di-guanosine-monophosphate in vivo. *J Immunol*. 2014;192(1):492-502.
348. Dearman RJ, Cumberbatch M, Maxwell G, Basketter DA, Kimber I. Toll-like receptor ligand activation of murine bone marrow-derived dendritic cells. *Immunology*. 2009;126(4):475-84.
349. Ilyinskii PO, Kovalev GI, O'Neil CP, Roy CJ, Michaud AM, Drefs NM, et al. Synthetic vaccine particles for durable cytolytic T lymphocyte responses and anti-tumor immunotherapy. *PLoS One*. 2018;13(6):e0197694.
350. Ilyinskii PO, Roy CJ, O'Neil CP, Browning EA, Pittet LA, Altreuter DH, et al. Adjuvant-carrying synthetic vaccine particles augment the immune response to encapsulated antigen and exhibit strong local immune activation without inducing systemic cytokine release. *Vaccine*. 2014;32(24):2882-95.
351. Desch AN, Gibbings SL, Clambey ET, Janssen WJ, Slansky JE, Kiedl RM, et al. Dendritic cell subsets require cis-activation for cytotoxic CD8 T-cell induction. *Nat Commun*. 2014;5:4674.
352. Reuter S, Dehzad N, Martin H, Bohm L, Becker M, Buhl R, et al. TLR3 but not TLR7/8 ligand induces allergic sensitization to inhaled allergen. *J Immunol*. 2012;188(10):5123-31.
353. van Aalst S, Jansen MAA, Ludwig IS, van der Zee R, van Eden W, Broere F. Routing dependent immune responses after experimental R848-adjuvanted vaccination. *Vaccine*. 2018;36(11):1405-13.
354. Desbien AL, Reed SJ, Bailor HR, Dubois Cauwelaert N, Laurance JD, Orr MT, et al. Squalene emulsion potentiates the adjuvant activity of the TLR4 agonist, GLA, via inflammatory caspases, IL-18, and IFN-gamma. *Eur J Immunol*. 2015;45(2):407-17.
355. Seydoux E, Liang H, Dubois Cauwelaert N, Archer M, Rintala ND, Kramer R, et al. Effective Combination Adjuvants Engage Both TLR and Inflammasome Pathways To Promote Potent Adaptive Immune Responses. *J Immunol*. 2018;201(1):98-112.

356. Shae D, Becker KW, Christov P, Yun DS, Lytton-Jean AKR, Sevimli S, et al. Endosomolytic polymersomes increase the activity of cyclic dinucleotide STING agonists to enhance cancer immunotherapy. *Nat Nanotechnol.* 2019;14(3):269-78.
357. Rossi M, Carboni S, Di Berardino-Besson W, Riva E, Santiago-Raber ML, Belnoue E, et al. STING Agonist Combined to a Protein-Based Cancer Vaccine Potentiates Peripheral and Intra-Tumoral T Cell Immunity. *Front Immunol.* 2021;12:695056.
358. Spinetti T, Spagnuolo L, Mottas I, Secondini C, Treinies M, Ruegg C, et al. TLR7-based cancer immunotherapy decreases intratumoral myeloid-derived suppressor cells and blocks their immunosuppressive function. *Oncoimmunology.* 2016;5(11):e1230578.
359. Kadayakkara DK, Korrer MJ, Bulte JW, Levitsky HI. Paradoxical decrease in the capture and lymph node delivery of cancer vaccine antigen induced by a TLR4 agonist as visualized by dual-mode imaging. *Cancer Res.* 2015;75(1):51-61.
360. Abdulrahman Z, de Miranda N, van Esch EMG, de Vos van Steenwijk PJ, Nijman HW, M JPW, et al. Pre-existing inflammatory immune microenvironment predicts the clinical response of vulvar high-grade squamous intraepithelial lesions to therapeutic HPV16 vaccination. *J Immunother Cancer.* 2020;8(1).
361. Melief CJM, Welters MJP, Vergote I, Kroep JR, Kenter GG, Ottevanger PB, et al. Strong vaccine responses during chemotherapy are associated with prolonged cancer survival. *Sci Transl Med.* 2020;12(535).
362. van Poelgeest MI, Welters MJ, Vermeij R, Stynenbosch LF, Loof NM, Berends-van der Meer DM, et al. Vaccination against Oncoproteins of HPV16 for Noninvasive Vulvar/Vaginal Lesions: Lesion Clearance Is Related to the Strength of the T-Cell Response. *Clin Cancer Res.* 2016;22(10):2342-50.
363. Meric-Bernstam F, Sweis RF, Hodi FS, Messersmith WA, Andtbacka RHI, Ingham M, et al. Phase I Dose-Escalation Trial of MIW815 (ADU-S100), an Intratumoral STING Agonist, in Patients With Advanced/Metastatic Solid Tumors or Lymphomas. *Clin Cancer Res.* 2021.
364. Meyer T, Surber C, French LE, Stockfleth E. Resiquimod, a topical drug for viral skin lesions and skin cancer. *Expert Opin Investig Drugs.* 2013;22(1):149-59.
365. Block MS, Nevala WK, Pang YP, Allred JB, Strand C, Markovic SN. A pilot clinical trial testing topical resiquimod and a xenopeptide as immune adjuvants for a melanoma vaccine targeting MART-1. *Melanoma Res.* 2019;29(4):420-7.
366. Jaffee EM, Hruban RH, Biedrzycki B, Laheru D, Schepers K, Sauter PR, et al. Novel allogeneic granulocyte-macrophage colony-stimulating factor-secreting tumor vaccine for pancreatic cancer: a phase I trial of safety and immune activation. *J Clin Oncol.* 2001;19(1):145-56.
367. Le DT, Picozzi VJ, Ko AH, Wainberg ZA, Kindler H, Wang-Gillam A, et al. Results from a Phase IIb, Randomized, Multicenter Study of GVAX Pancreas and CRS-207 Compared with Chemotherapy in Adults with Previously Treated Metastatic Pancreatic Adenocarcinoma (ECLIPSE Study). *Clin Cancer Res.* 2019;25(18):5493-502.
368. Brahmer JR, Tykodi SS, Chow LQ, Hwu WJ, Topalian SL, Hwu P, et al. Safety and activity of anti-PD-L1 antibody in patients with advanced cancer. *N Engl J Med.* 2012;366(26):2455-65.

369. Le DT, Wang-Gillam A, Picozzi V, Greten TF, Crocenzi T, Springett G, et al. Safety and survival with GVAX pancreas prime and *Listeria Monocytogenes*-expressing mesothelin (CRS-207) boost vaccines for metastatic pancreatic cancer. *J Clin Oncol*. 2015;33(12):1325-33.
370. Gooden M, Lampen M, Jordanova ES, Leffers N, Trimbos JB, van der Burg SH, et al. HLA-E expression by gynecological cancers restrains tumor-infiltrating CD8(+) T lymphocytes. *Proc Natl Acad Sci U S A*. 2011;108(26):10656-61.
371. Gustafson KS, Ginder GD. Interferon-gamma induction of the human leukocyte antigen-E gene is mediated through binding of a complex containing STAT1alpha to a distinct interferon-gamma-responsive element. *J Biol Chem*. 1996;271(33):20035-46.
372. Kaiser BK, Pizarro JC, Kerns J, Strong RK. Structural basis for NKG2A/CD94 recognition of HLA-E. *Proc Natl Acad Sci U S A*. 2008;105(18):6696-701.
373. Andre P, Denis C, Soulas C, Bourbon-Caillet C, Lopez J, Arnoux T, et al. Anti-NKG2A mAb Is a Checkpoint Inhibitor that Promotes Anti-tumor Immunity by Unleashing Both T and NK Cells. *Cell*. 2018;175(7):1731-43 e13.
374. van Montfoort N, Borst L, Korner MJ, Sluiter M, Marijt KA, Santegoets SJ, et al. NKG2A Blockade Potentiates CD8 T Cell Immunity Induced by Cancer Vaccines. *Cell*. 2018;175(7):1744-55 e15.
375. Masilamani M, Nguyen C, Kabat J, Borrego F, Coligan JE. CD94/NKG2A inhibits NK cell activation by disrupting the actin network at the immunological synapse. *J Immunol*. 2006;177(6):3590-6.
376. Lin MJ, Svensson-Arvelund J, Lubitz GS, Marabelle A, Melero I, Brown BD, et al. Cancer vaccines: the next immunotherapy frontier. *Nat Cancer*. 2022;3(8):911-26.
377. Collins JM, Redman JM, Gulley JL. Combining vaccines and immune checkpoint inhibitors to prime, expand, and facilitate effective tumor immunotherapy. *Expert Rev Vaccines*. 2018;17(8):697-705.
378. Schietinger A, Philip M, Krisnawan VE, Chiu EY, Delrow JJ, Basom RS, et al. Tumor-Specific T Cell Dysfunction Is a Dynamic Antigen-Driven Differentiation Program Initiated Early during Tumorigenesis. *Immunity*. 2016;45(2):389-401.
379. Bjorkdahl O, Barber KA, Brett SJ, Daly MG, Plumpton C, Elshourbagy NA, et al. Characterization of CC-chemokine receptor 7 expression on murine T cells in lymphoid tissues. *Immunology*. 2003;110(2):170-9.
380. Pennock ND, White JT, Cross EW, Cheney EE, Tamburini BA, Kedl RM. T cell responses: naive to memory and everything in between. *Adv Physiol Educ*. 2013;37(4):273-83.
381. Verdon DJ, Mulazzani M, Jenkins MR. Cellular and Molecular Mechanisms of CD8(+) T Cell Differentiation, Dysfunction and Exhaustion. *Int J Mol Sci*. 2020;21(19).
382. Caccamo N, Joosten SA, Ottenhoff THM, Dieli F. Atypical Human Effector/Memory CD4(+) T Cells With a Naive-Like Phenotype. *Front Immunol*. 2018;9:2832.
383. Sallusto F, Lenig D, Forster R, Lipp M, Lanzavecchia A. Two subsets of memory T lymphocytes with distinct homing potentials and effector functions. *Nature*. 1999;401(6754):708-12.
384. Joshi NS, Cui W, Chandele A, Lee HK, Urso DR, Hagman J, et al. Inflammation directs memory precursor and short-lived effector CD8(+) T cell fates via the graded expression of T-bet transcription factor. *Immunity*. 2007;27(2):281-95.

385. Im SJ, Hashimoto M, Gerner MY, Lee J, Kissick HT, Burger MC, et al. Defining CD8+ T cells that provide the proliferative burst after PD-1 therapy. *Nature*. 2016;537(7620):417-21.
386. He R, Hou S, Liu C, Zhang A, Bai Q, Han M, et al. Follicular CXCR5- expressing CD8(+) T cells curtail chronic viral infection. *Nature*. 2016;537(7620):412-28.
387. Miller BC, Sen DR, Al Aboosy R, Bi K, Virkud YV, LaFleur MW, et al. Subsets of exhausted CD8(+) T cells differentially mediate tumor control and respond to checkpoint blockade. *Nat Immunol*. 2019;20(3):326-36.
388. Utzschneider DT, Charmoy M, Chennupati V, Pousse L, Ferreira DP, Calderon-Copete S, et al. T Cell Factor 1-Expressing Memory-like CD8(+) T Cells Sustain the Immune Response to Chronic Viral Infections. *Immunity*. 2016;45(2):415-27.
389. Siddiqui I, Schaeuble K, Chennupati V, Fuertes Marraco SA, Calderon-Copete S, Pais Ferreira D, et al. Intratumoral Tcf1(+)/PD-1(+)/CD8(+) T Cells with Stem-like Properties Promote Tumor Control in Response to Vaccination and Checkpoint Blockade Immunotherapy. *Immunity*. 2019;50(1):195-211 e10.
390. Blackburn SD, Shin H, Freeman GJ, Wherry EJ. Selective expansion of a subset of exhausted CD8 T cells by alphaPD-L1 blockade. *Proc Natl Acad Sci U S A*. 2008;105(39):15016-21.
391. Sade-Feldman M, Yizhak K, Bjorgaard SL, Ray JP, de Boer CG, Jenkins RW, et al. Defining T Cell States Associated with Response to Checkpoint Immunotherapy in Melanoma. *Cell*. 2018;175(4):998-1013 e20.
392. Seo H, Chen J, Gonzalez-Avalos E, Samaniego-Castruita D, Das A, Wang YH, et al. TOX and TOX2 transcription factors cooperate with NR4A transcription factors to impose CD8(+) T cell exhaustion. *Proc Natl Acad Sci U S A*. 2019;116(25):12410-5.
393. Khan O, Giles JR, McDonald S, Manne S, Ngiow SF, Patel KP, et al. TOX transcriptionally and epigenetically programs CD8(+) T cell exhaustion. *Nature*. 2019;571(7764):211-8.
394. Till JE, Mc CE. A direct measurement of the radiation sensitivity of normal mouse bone marrow cells. *Radiat Res*. 1961;14:213-22.
395. Spangrude GJ, Heimfeld S, Weissman IL. Purification and characterization of mouse hematopoietic stem cells. *Science*. 1988;241(4861):58-62.
396. Casbon AJ, Reynaud D, Park C, Khuc E, Gan DD, Schepers K, et al. Invasive breast cancer reprograms early myeloid differentiation in the bone marrow to generate immunosuppressive neutrophils. *Proc Natl Acad Sci U S A*. 2015;112(6):E566-75.
397. Hong IS. Stimulatory versus suppressive effects of GM-CSF on tumor progression in multiple cancer types. *Exp Mol Med*. 2016;48(7):e242.
398. Solito S, Falisi E, Diaz-Montero CM, Doni A, Pinton L, Rosato A, et al. A human promyelocytic-like population is responsible for the immune suppression mediated by myeloid-derived suppressor cells. *Blood*. 2011;118(8):2254-65.
399. Marigo I, Bosio E, Solito S, Mesa C, Fernandez A, Dolcetti L, et al. Tumor-induced tolerance and immune suppression depend on the C/EBPbeta transcription factor. *Immunity*. 2010;32(6):790-802.
400. De Veirman K, Menu E, Maes K, De Beule N, De Smedt E, Maes A, et al. Myeloid-derived suppressor cells induce multiple myeloma cell survival by activating the AMPK pathway. *Cancer Lett*. 2019;442:233-41.

401. Liu G, Bi Y, Shen B, Yang H, Zhang Y, Wang X, et al. SIRT1 limits the function and fate of myeloid-derived suppressor cells in tumors by orchestrating HIF-1 $\alpha$ -dependent glycolysis. *Cancer Res.* 2014;74(3):727-37.
402. Lee M, Park CS, Lee YR, Im SA, Song S, Lee CK. Resiquimod, a TLR7/8 agonist, promotes differentiation of myeloid-derived suppressor cells into macrophages and dendritic cells. *Arch Pharm Res.* 2014;37(9):1234-40.
403. Chavakis T, Mitroulis I, Hajishengallis G. Hematopoietic progenitor cells as integrative hubs for adaptation to and fine-tuning of inflammation. *Nat Immunol.* 2019;20(7):802-11.
404. Mitroulis I, Ruppova K, Wang B, Chen LS, Grzybek M, Grinenko T, et al. Modulation of Myelopoiesis Progenitors Is an Integral Component of Trained Immunity. *Cell.* 2018;172(1-2):147-61 e12.
405. Bomans K, Schenz J, Sztwiertnia I, Schaack D, Weigand MA, Uhle F. Sepsis Induces a Long-Lasting State of Trained Immunity in Bone Marrow Monocytes. *Front Immunol.* 2018;9:2685.
406. Netea MG, Quintin J, van der Meer JW. Trained immunity: a memory for innate host defense. *Cell Host Microbe.* 2011;9(5):355-61.
407. Kleinnijenhuis J, Quintin J, Preijers F, Joosten LA, Ifrim DC, Saeed S, et al. Bacille Calmette-Guerin induces NOD2-dependent nonspecific protection from reinfection via epigenetic reprogramming of monocytes. *Proc Natl Acad Sci U S A.* 2012;109(43):17537-42.
408. Quintin J, Saeed S, Martens JHA, Giamarellos-Bourboulis EJ, Ifrim DC, Logie C, et al. *Candida albicans* infection affords protection against reinfection via functional reprogramming of monocytes. *Cell Host Microbe.* 2012;12(2):223-32.
409. Saeed S, Quintin J, Kerstens HH, Rao NA, Aghajani-refah A, Matarese F, et al. Epigenetic programming of monocyte-to-macrophage differentiation and trained innate immunity. *Science.* 2014;345(6204):1251086.
410. Arts RJW, Carvalho A, La Rocca C, Palma C, Rodrigues F, Silvestre R, et al. Immunometabolic Pathways in BCG-Induced Trained Immunity. *Cell Rep.* 2016;17(10):2562-71.
411. Butcher SK, O'Carroll CE, Wells CA, Carmody RJ. Toll-Like Receptors Drive Specific Patterns of Tolerance and Training on Restimulation of Macrophages. *Front Immunol.* 2018;9:933.
412. Pylayeva-Gupta Y, Lee KE, Hajdu CH, Miller G, Bar-Sagi D. Oncogenic Kras-induced GM-CSF production promotes the development of pancreatic neoplasia. *Cancer Cell.* 2012;21(6):836-47.
413. Bayne LJ, Beatty GL, Jhala N, Clark CE, Rhim AD, Stanger BZ, et al. Tumor-derived granulocyte-macrophage colony-stimulating factor regulates myeloid inflammation and T cell immunity in pancreatic cancer. *Cancer Cell.* 2012;21(6):822-35.
414. Patnaik MM, Sallman DA, Mangaonkar AA, Heuer R, Hirvela J, Zblewski D, et al. Phase 1 study of lenzilumab, a recombinant anti-human GM-CSF antibody, for chronic myelomonocytic leukemia. *Blood.* 2020;136(7):909-13.
415. Qian BZ, Li J, Zhang H, Kitamura T, Zhang J, Campion LR, et al. CCL2 recruits inflammatory monocytes to facilitate breast-tumour metastasis. *Nature.* 2011;475(7355):222-5.

416. Kitamura T, Qian BZ, Soong D, Cassetta L, Noy R, Sugano G, et al. CCL2-induced chemokine cascade promotes breast cancer metastasis by enhancing retention of metastasis-associated macrophages. *J Exp Med*. 2015;212(7):1043-59.
417. Flores-Toro JA, Luo D, Gopinath A, Sarkisian MR, Campbell JJ, Charo IF, et al. CCR2 inhibition reduces tumor myeloid cells and unmasks a checkpoint inhibitor effect to slow progression of resistant murine gliomas. *Proc Natl Acad Sci U S A*. 2020;117(2):1129-38.
418. Tu MM, Abdel-Hafiz HA, Jones RT, Jean A, Hoff KJ, Duex JE, et al. Inhibition of the CCL2 receptor, CCR2, enhances tumor response to immune checkpoint therapy. *Commun Biol*. 2020;3(1):720.
419. Sahakian E, Powers JJ, Chen J, Deng SL, Cheng F, Distler A, et al. Histone deacetylase 11: A novel epigenetic regulator of myeloid derived suppressor cell expansion and function. *Mol Immunol*. 2015;63(2):579-85.
420. Christmas BJ, Rafie CI, Hopkins AC, Scott BA, Ma HS, Cruz KA, et al. Entinostat Converts Immune-Resistant Breast and Pancreatic Cancers into Checkpoint-Responsive Tumors by Reprogramming Tumor-Infiltrating MDSCs. *Cancer Immunol Res*. 2018;6(12):1561-77.
421. Orillion A, Hashimoto A, Damayanti N, Shen L, Adelaiye-Ogala R, Arisa S, et al. Entinostat Neutralizes Myeloid-Derived Suppressor Cells and Enhances the Antitumor Effect of PD-1 Inhibition in Murine Models of Lung and Renal Cell Carcinoma. *Clin Cancer Res*. 2017;23(17):5187-201.
422. Hellmann MD, Janne PA, Opyrchal M, Hafez N, Raez LE, Gabrilovich DI, et al. Entinostat plus Pembrolizumab in Patients with Metastatic NSCLC Previously Treated with Anti-PD-(L)1 Therapy. *Clin Cancer Res*. 2021;27(4):1019-28.
423. Li G, Tian Y, Zhu WG. The Roles of Histone Deacetylases and Their Inhibitors in Cancer Therapy. *Front Cell Dev Biol*. 2020;8:576946.
424. Jian SL, Chen WW, Su YC, Su YW, Chuang TH, Hsu SC, et al. Glycolysis regulates the expansion of myeloid-derived suppressor cells in tumor-bearing hosts through prevention of ROS-mediated apoptosis. *Cell Death Dis*. 2017;8(5):e2779.
425. Qin G, Lian J, Huang L, Zhao Q, Liu S, Zhang Z, et al. Metformin blocks myeloid-derived suppressor cell accumulation through AMPK-DACH1-CXCL1 axis. *Oncoimmunology*. 2018;7(7):e1442167.
426. Xu P, Yin K, Tang X, Tian J, Zhang Y, Ma J, et al. Metformin inhibits the function of granulocytic myeloid-derived suppressor cells in tumor-bearing mice. *Biomed Pharmacother*. 2019;120:109458.
427. Patsoukis N, Bardhan K, Chatterjee P, Sari D, Liu B, Bell LN, et al. PD-1 alters T-cell metabolic reprogramming by inhibiting glycolysis and promoting lipolysis and fatty acid oxidation. *Nat Commun*. 2015;6:6692.
428. Chowdhury PS, Chamoto K, Kumar A, Honjo T. PPAR-Induced Fatty Acid Oxidation in T Cells Increases the Number of Tumor-Reactive CD8(+) T Cells and Facilitates Anti-PD-1 Therapy. *Cancer Immunol Res*. 2018;6(11):1375-87.
429. Carr EL, Kelman A, Wu GS, Gopaul R, Senkevitch E, Aghvanyan A, et al. Glutamine uptake and metabolism are coordinately regulated by ERK/MAPK during T lymphocyte activation. *J Immunol*. 2010;185(2):1037-44.

430. Varghese S, Pramanik S, Williams LJ, Hodges HR, Hudgens CW, Fischer GM, et al. The Glutaminase Inhibitor CB-839 (Telaglenastat) Enhances the Antimelanoma Activity of T-Cell-Mediated Immunotherapies. *Mol Cancer Ther.* 2021;20(3):500-11.
431. Leone RD, Zhao L, Englert JM, Sun IM, Oh MH, Sun IH, et al. Glutamine blockade induces divergent metabolic programs to overcome tumor immune evasion. *Science.* 2019;366(6468):1013-21.